RESEARCH & REVIEWS IN SCIENCE AND MATHEMATICS

MAY 2021

VOLUME 2

EDITORS

PROF. DR. HASAN AKGÜL
PROF. DR. HASAN HÜSEYİN DOĞAN
ASSOC. PROF. DR. MEHMET YÜKSEL
DR. ONUR KARAMAN

AUTHORS

SEVİNÇ AYDIN
DOĞUKAN TAŞER
MELİS ULU DOĞRU
GULSAH CONGUR
NERGİZ SOYUPAK
ÇAĞIN KANDEMİR-ÇAVAŞ
ELİF NAZ ALVER
KAAN KALTALİOGLU,
SULE COSKUN-CEVHER
ERHAN USTAOĞLU
NİHAL ERCAN
HASAN AKGÜL
CELAL BAL
EMRE CEM ERASLAN
ALİ İMRAN KORKMAZ

gece kitaplığı

İmtiyaz Sahibi / Publisher • Yaşar Hız
Genel Yayın Yönetmeni / Editor in Chief • Eda Altunel
Kapak & İç Tasarım / Cover & Interior Design • Gece Kitaplığı
Editörler/ Edıtors • PROF. DR. HASAN AKGÜL
PROF. DR. HASAN HÜSEYİN DOĞAN
ASSOC. PROF. DR. MEHMET YÜKSEL
DR. ONUR KARAMAN
Birinci Basım / First Edition • © May 2021
ISBN • 978-625-7411-76-9

Gece Kitaplığı / Gece Publishing
Türkiye Adres / Turkey Address: Kızılay Mah. Fevzi Çakmak 1. Sokak Ümit Apt. No: 22/A Çankaya / Ankara / TR
Telefon / Phone: +90 312 384 80 40
web: www.gecekitapligi.com
e-mail: gecekitapligi@gmail.com

Baskı & Cilt / Printing & Volume
Sertifika / Certificate No: 47083

Research & Reviews in Science and Mathematics

May 2021

Volume 2

EDITORS

PROF. DR. HASAN AKGÜL

PROF. DR. HASAN HÜSEYİN DOĞAN

ASSOC. PROF. DR. MEHMET YÜKSEL

DR. ONUR KARAMAN

gece kitaplığı

CONTENTS

CHAPTER 8

USAGE OF GRAPES (VITIS VINIFERA L.)
WHICH ARE SOURCE OF ANTIOXIDANT AND THEIR WASTES

Sevinç AYDIN 1

CHAPTER 9

$\mathfrak{f}(\mathfrak{R},\mathfrak{T})$GRAVITY AND NON-STATIC PLANE SYMMETRIC DOMAIN WALLS

Doğukan TAŞER , Melis ULU DOĞRU 19

CHAPTER 10

DEVELOPMENT OF DIAGNOSTICS FOR HUMAN-PATHOGENIC VIRUSES: ELECTROCHEMICAL BIOSENSOR APPLICATIONS

Gulsah CONGUR 37

CHAPTER 11

IN SILICO ANALYSIS OF BIOSEQUENCE SIMILARITIES

Nergiz SOYUPAK, Çağın KANDEMİR-ÇAVAŞ 53

CHAPTER 12

REACTIVE OXYGEN SPECIES AND WOUND HEALING

Elif Naz ALVER, Kaan KALTALIOGLU, Sule COSKUN-CEVHER 65

CHAPTER 13

INTERVAL ESTIMATION FOR ORDER STATISTICS BY CHEBYSHEV INEQUALITY

Erhan USTAOĞLU 79

CHAPTER 14

BLACK HOLES

Nihal ERCAN 95

CHAPTER 15

THE STATUS OF MYCETOZOA STUDIES OF THE WORLD AND TURKEY

Hasan AKGÜL, Celal BAL, Emre Cem ERASLAN, Ali İmran KORKMAZ 109

Chapter 8

USAGE OF GRAPES (*Vitis Vinifera L.*) WHICH ARE SOURCE OF ANTIOXIDANT AND THEIR WASTES

Sevinç AYDIN [1]

1 Assistant professor Sevinç Aydın, Çemizgezek Vocational School/ Munzur University
sevincaydin2380@gmail.com ORCID ID: https://orcid.org/0000-0001-8597-8064

INTRODUCTION

Antioxidants are substances that end or reduce the effects of free radicals. Due to the toxic and arcinogenic effects of synthetically created antioxidants and their damage on enzymes (1), interest particularly in herbal and naturally sourced antioxidants has increased. Natural antioxidants may protect against free radicals that can induce some chronic and fatal diseases (2). Although synthetic phenolic antioxidants like BHT (butyl hydroxy toluene) and BHA (butyl hydroxy quinone) are known to inhibit lipid oxidation, studies on the benefits of natural antioxidants have increased due to consumer concerns about such additives (3).

The main compounds of natural antioxidants are flavonoids and phenolic acids that exist in free or complex structure. The amounts of these compounds in various fruits and vegetables were determined and their relationship with their antioxidant activities was shown (4). Phenolic compounds are organic compounds with a benzene ring and the family they belong to is quite large. These compounds are known to be associated with certain quality properties of fruits and vegetables, like color, taste, and smell, and have antiradical and antioxidant effects. The antioxidant efficiencies of phenolics were associated with their molecular structure, especially ring form (5).

ANTIOXIDANT CONTENT IN GRAPES AND GRAPE PRODUCTS

Polyphenolic compounds have a significant impact on the quality of grapes and wines. And these organic substances can be grouped into non-flavonoids (hydroxybenzoic and hydroxycinnamic acids and stilbens) and flavonoid compounds (anthocyanins, flavan-3-ols and flavonols) (6). Anthocyanins are the polyphenols responsible for color of grapes and young wines. Anthocyanins are considered potential ingredients of synthetic colorants due to their bright, attractive color and water solubility and are thus incorporated into various food systems (7). There is a positive charge on anthocyanins, which provides it to suck light and acquire color. It also has an anthocyanin esterified carbohydrate (sugar, usually glucose) at the 3 position (Figure 1.)

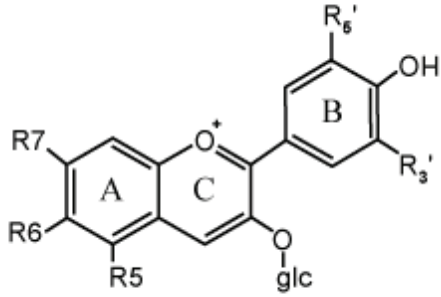

Figure 1. *General formula of anthocyanins (8).*

All naturally occurring anthocyanins are in equilibrium between the colored flavylium cation and the colorless hydrated structure. This balance moves to the left as the pH of the wine decreases and to the right as the pH increases. At pH above 4,5, destabilizing and undesirable reactions such as opening of the ring C begin (Figure 2). Also, Véronique Cheynier proposed that the hydrated form is actually the reactive form of anthocyanin (9).

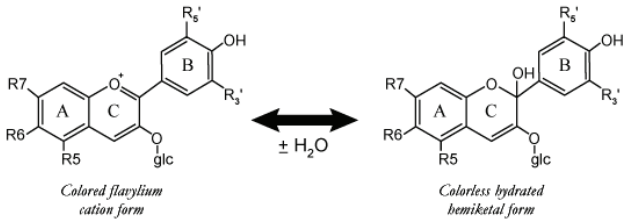

Figure 2. *Anthocyanin forms occurring at the pH of wine (9).*

Flavan-3-ols (monomeric catechins and proanthocyanidins) group is another large family of polyphenolic compounds liable for the consistency, bitterness and texture of wines (10, 11). Another group of flavonoids are quercetin, myricetin, kaempferol, isorhamnetin and flavonols that are their glycosides, which are known to conduce to piquancy in wine (Figure 3).

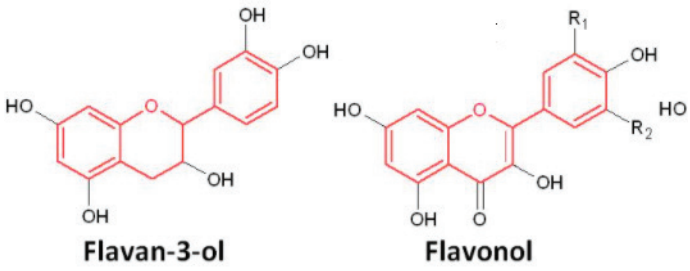

Figure 3. *General formula of Flavan-3-ol and Flavonols (12).*

Phenolics are usually found in grape skins and seeds. On the other hand, flavonols are more abundant in grape skins and flavan-3-ol in grape seeds (13). The phenolic compound density in grapes depends on the variety of the vine, and environmental factors such as viticulture, fruit size, ripeness and climate (14-16). Another factor is the number of seeds contained in each fruit. This factor is a variable that affects the quantity of polyphenols that the all grape contributes (16). Besides these, polyphenols, especially certain phenolic acids and flavonols, join in the structure of copigmentation. Therefore, anthocyanins show much more color than would be expected from their concentrations. If there is not a good balance between anthocyanin and other polyphenol concentrations in any of the grapes, its use by co-fermentation of red grapes of different varieties is recommended (17). This is also applicable for the fermentation of red grape varieties and white grapes that conduce to such polyphenolic compounds (18).

Along with the fact that the phenolics in the red grape fruit is known to be richer, it was shown that the peels and seeds of the white grape varieties are qualitatively and quantitatively similar to the red grape varieties in point of non-anthocyanic polyphenols (16). While Rockenbach et al. observed the highest value of resveratrol in Merlot grape variety (6,40 mg/100 g) in their study, they reported the existence of resveratrol in pulp in three of the other four grape varieties in this study. In another study, t-resveratrol, a phytoalexin, was identified in grapes and red wine (16). In particular, it was shown that grape skin is a good source of resveratrol, that fresh skin include approximately 50-100 µg/g resveratrol, while in red wine this

quantity varies between 1,5 and 3,0 mg/L (19). Researchers reported that resveratrol is a potent antimutagenic, antioxidant, anti-inflammatory and antiproliferative agent, besides being an inhibitor of cyclooxygenase and hydroperoxidase (20, 21).

As a qualitative difference between red and white grapes, it was reported that the myricetin glycosides found in the skin of red grape varieties are not found in the skin of white grape varieties. For this reason, white grape varieties should be considered as a good non-anthocyanic phenol source when used in fermentation with red grape must or should be considered as a resource of natural antioxidant compounds of increasing industrial significance. In other words, since the must obtained from white grapes cannot be fermented with the grape skins, the phenolic composition of the grapes from the white varieties was the subject of less studies than the red grape varieties, which have a great impact on the quality of the grape skin (16).

In other studies, gallic acid (a non-flavonoid phenolic acid) was observed in Vitis grape varieties (6, 16, 22). In addition to the known phenolics, it was emphasized that the compounds that could not be quantified because of the lack of some other phenolic standards in the grape press may be oligomers and polymers of polyhydroxy flavan-3-ols like (+) catechin and (-) - epicatechin, most of which are in the structure of gallate esters or glycosides (23). In a study carried to observe the antioxidant impacts of grape contents, researchers stated that the phenolic content of fruits was significantly related to the antioxidant capacity of wines in their study on the investigation of the polyphenols and total antioxidant activities of four-wine grapes and four table grapes (24). In a similar study, scientists reported that grape seeds have the best antioxidant activity regardless of the analysis method and that grapes with darker skins have higher antioxidant activity than grapes with lighter skins. They showed that pulp fractions have low antioxidant activity regardless of whether the grape is red or white (25).

There are many studies reporting that *Vitis vinifera* L. extracts have anti-inflammatory, antimicrobial, antioxidant, anti-atherosclerotic, and antitumor or cytoprotective properties (26, 27). Moreover, components from grapes were reported to have many properties such as sweeteners, skin care agents, antioxidants, anti-irritants, depigmentation agents, emollients, antimicrobial and oral care agents (28, 29).

Researchers continue to work on modifying these factors to produce varieties with higher antioxidant content (30). In addition, information on total phenolic content and antioxidant activity obtained from hybrid or less used grape varieties can be used to increase the nutritional attributes of grape varieties (31).

BIOCHEMICAL CONTENTS AND USAGE OF GRAPE WASTES

Almost 75 million tons of grapes are breeded every year in the world and almost 80% of this amount is used for wine production (32). During wine production, many of the health-beneficial compounds obtained from grape grains are converted into juice or wine, but still a significant part remains in the pulp (skins and seeds). Lately, there has been an increasing interest in recycling wine by-products. In the studies held as a result of this interest, grape pulp containing abundant active compounds was recommended for enrichment of food, pharmaceutical and even cosmetic products (33). Studies on wine waste and by-products mostly focused on antioxidant bioactive compounds. The quantity of these compounds can chance according as on the matrix of the plant, extraction technology methods and parameters. And among these methods, traditional extraction methods using aqueous or ethanolic solvents with or without temperature effect are more preferred because of their affordability and ease of usage (34).

Especially recently, this part was subjected to intense research as it is known that more than 70% of polyphenols are left in pulp from winemaking by-products. Also, these by-products are often used for the preparation of soil fertilizers and livestock feeds, however, the active ingredients (polyphenols, stilbene, etc.) derived from by-products have a high potential for human health (29, 35, 36). Phenolic compounds found in wine attracted great attention because of their antioxidant attributes and potential benefits for human health (37). Also, the total polyphenol contents of grape seed and peel were examined, taking into account the knowledge that there are active compounds remaining in the grape pulp, which supports previous studies on the significance of profitable and sustainable usage of wine by-products (27).

Wastes from grapes are usually solid by-products like stem, pulp and liquid permeate. The resulting pulp total may comprise 13,5% to 14,5% of the grape capacity and can reach 20% (38, 39). These pulps consist of water, proteins, lipids, carbohydrates, vitamins, minerals and compounds like fiber, vitamin C and phenolics changeable connected on the type of grape, climate and growing conditions (38- 41).

By-products such as seeds or pulps from wine production used for the extraction of antioxidant flavonoids provide a convenient source for food supplements and the production of phytochemicals (42). Studies conducted in recent years aimed to prevent environmental pollution and to reuse harvest wastes or many fabrication wastes, whose raw material is agricultural product, in different areas. Grape is one of the agricultural industrial products used for this purpose. If these wastes are not used properly, it is known that they cause many pollution, from surface and groundwater pollution to bad

odor. Due to compounds such as tannins in grape pulp, these wastes use and consume oxygen when mixed into the soil (43).

Fresh grape production in Turkey is around 4 million tons annually. And about 3% of it is used for wine production. The pulp left over from the processing of the grape consists of 50% skin, 25% seed and 25% grape stem. As a result of insufficient utilization of this pulp that comes out after the process, it causes significant amounts of accumulation, thus causing environmental pollution (44). With many studies today, it was shown that these wastes can be a source of organic matter for plants by direct addition to the soil or can be used as a growing medium in the form of a mixture (45-47).

In addition to the production of pharmaceutical and cosmetic products from these wastes, various analysis techniques were developed with other researches (48). Research on the reuse of wastes started to be supported in many pioneering countries in wine production (49). These wastes are an effective source of energy, activated carbon and chemicals production, and problems such as proper disposal of these wastes and low-cost raw material production can be easily solved (48,50,51).

Characteristics and Usage Methods of Grape Pulp

In a study, the first analysis of grape pulp grown in Piaui state was made. The results obtained showed that grape pulp is an significant resource of nutrients and has functional compounds. It was stated that the grape pulp flour obtained with this study showed low and below neutral pH, and this feature could help prevent the growth of pathogenic microorganisms. It was shown that the total amount of dietary fiber of grape pump is quantitatively higher than carbohydrates, proteins and lipids, and this pulp can be included in the daily diet as a fiber source and nutritional supplement. The results obtained with the functional compounds in the studies showed that grape pulp is a potential resource of bioactive compounds, particularly the indissoluble fibers have higher concentrations compared to the soluble compounds, and the quantities of vitamin C and anthocyanins may be in significant amounts. In terms of minerals, iron, potassium, zinc, calcium and manganese were detected in significant amounts. Moreover, as a result of toxicity bioassays, it was observed that grape pulp was not contaminated and therefore it was taken into consideration microbiologically (52).

Grape pulp, whose biochemical content was shown by studies, is used as a growing medium, as a silage additive (animal feed), in poultry feed, as a coloring agent and in other fields (ethyl alcohol, potassium bitartrate and tartaric acid production). Furthermore, grape pulp can be used in biscuit production after it is dried and milled with appropriate methods (53), as well as adding to foods such as yoghurt and salad dressing as it increases the phenolic content, and it became important to use it as a food additive (54).

Characteristics and Usage Methods of Grape Seed

Grape seed is a rich source of phenolic compounds, phytosterols, vitamins and fatty acids (55,56). Grape seed oil is particularly rich in linoleic and oleic acids (unsaturated fatty acids), which are responsible for the oil's nutritional value and contribute to the antioxidant effect. In particular, linoleic acid (66-78 g/100 g) is the predominant fatty acid in the total fat ratio and this ratio depends on the grape variety (55, 57). Apart from these fatty acids, grape seed oil contains tannin and this value is higher than other seed oils. Furthermore, it was stated that there are 0,8-1,5% non-saponifiable lipids, sitosterol, campesterol and stigmasterol in grape seed oil, which increase antioxidant activity by providing resistance to peroxidation (58). It was reported that catechin, epicatechin, procyanidins and anthocyanins as flavonoid ingredients and gallic acid from phenolic acids are also an important source of resveratrol (59).

Due to all these ingredients, grape seed, which is produced as waste, found a wide usage area as a nutritional supplement. In particular, obtaining antioxidants and flavonoids by cheap extraction methods was seen as an economic advantage (60). Today, grape seed is also sold in powder form and is used in the production of bread, cake, etc. Grape seed is also used in the production of laccase enzyme and (61) to obtain oil. Moreover, obtaining biodiesel production from grape seed oil is another alternative (62). Grape seed oil also has an important place in the cosmetic industry. Especially sunscreen gel and protective day care creams contain grape seed oil (63). Another usage area is aromatherapy, an adjunct treatment method that has become increasingly important in recent years. In this area, it is used both as a carrier oil and for treatment purposes (64).

Characteristics and Usage Methods of Vine Leaves

Many studies reported that grape leaves are a resource of phenolic compounds that exhibit antioxidant activity (65-71). In a study, catechin (3,84-14,02 mg/g-1) and tannic acid (0,34-1,84 mg/g-1) were reported as the total amount of phenolic substance in grape leaves. Furthermore, the existence of phenolic compounds like gallic acid, protocatechic acid, catechin, caffeic acid, chlorogenic acid, vanillin, p-coumaric acid, ferulic acid, o-coumaric acid, rutin, hesperidin, quarcetin, luteolin and campherol were shown in leaf samples (72).

In another study, gallic, caffeic and p-coumaric acid contents were determined in grape leaf extracts. Also, in the analyzed sample, caffeic acid was found free, esterified and in the form of its glycoside component, while gallic and p-coumaric acids were identified as compounds released only from esters and glycosides. Moreover, the presence of substances such as Quercetin, Quercitrin and Karotin, which are anthraquinone group, were shown in the vine leaves (73).

Thanks to its antioxidant content, vine leaves can be used for treatment in traditional medicine. Especially red grape leaves have anti-inflammatory and astringent properties. Leaf decoction is used for mouth ulcers and for the treatment of vaginal discharge. Red grape leaves are also beneficial in the treatment of varicose veins, hemorrhoids and capillary fragility (74). In addition to various pharmacological characteristics like antioxidant, antidiabetic (75), hepatoprotective (leaf extract) (76), anti-atherosclerotic, anti-tumor, antioxidant, collagen stabilization, cytoprotective, hair growth, anti-ischemic (seed extract) were showned in animal studies (77-79). Apart from its medicinal properties, vine leaves are used to obtain yellow, yellow-green colors in natural dyeing thanks to its components. Moreover, since vine leaves contain phenolic compounds, they are used as food protectives and in the production of nutritional support tablets. The grape leaves that fall off in autumn can be collected and used in organic fertilizer production (80). Besides these uses, it is well known that *Vitis vinifera* leaves can be eaten and used for cooking. Fresh leaves cooked by wrapping them around other foods add a pleasant flavor and taste to the dish (81).

In the light of all these data, we see that the wastes generated by the processing of grapes have been used and utilized in different ways since ancient times. Of course, as waste technology develops, the value of these wastes will increase day by day. In order to bring these wastes to the national economy, establishing facilities where these wastes can be processed is important both in terms of health, environmental cleanliness and new business opportunities.

REFERENCES

1) Ito, N., Hiroze, M., Fukushima, G., Tauda, H., Shira, T., Tatematsu, M. (1986). Studies on antioxidant; their carcinogenic and modifying effects on chemical carcinogenesis. *Food Chemistry Toxicology* 24, 1071-1081.

2) Kinsella, J. E., Frankel, E., German, B., Kanner, J. (1993). Possible mechanisms for the protective role of antioxidants in wine and plant foods. *Food Technology* 47, 85-89

3) Formanek, Z., Kerry, J. P., Higgins, F. M., Buckley, D. J., Morrissey, P. A., Farkas, J. (2001). Addition of synthetic and natural antioxidants tocopheryl acetate supplemented beef patties: Effects of antioxidants and packaging on lipid oxidation. *Meat Science*, 58, 337–341.

4) Einbond, L.S., Reynertson, K.A., Luo, X.D, Basile, M.J., Kennelly, E.J. (2004). Anthocyanin antioxidants from edible fruits. *Food Chemistry*, 84, 23–28.

5) Gadow, A., Joubert, E., Hansmann, C.F. (1997). Comparasion of the antioxidant activity of aspalathin with that of other plant phenols of rooibos tea (*Aspalathus linearis*), α- tocopherol, BHT, and BHA. *Journal of Agricultural Food Chemistry* 45, 632-63.

6) Montealegre, R.R., Peces, R.R., Vozmediano, J.C., Gascueña, J.M., Romero, E.G. (2006). Phenolic compounds in skins and seeds of ten grape Vitis vinifera varieties grown in a warm climate. *Journal of Food Composition and Analysis*, 19, 687–693.

7) Bordignon-Luiz, M.T., Gauche, C., Gris, E.F., Falcão, L.D. (2007). Colour stability of anthocyanins from Isabel grapes (Vitis labrusca L.) in model systems. *LWT – Food Science and Technology*, 40(4), 594–599.

8) http://www.micro-ox.com/chem_antho.htm, 18.04.2021.

9) http://www.micro-ox.com/chem_antho.htm, 18.04.2021.

10) Singleton, V.L., Essau, P. (1969). Phenolic Substances in grapes and wine, and their significance. Academic Press, New York, 1-261.

11) Gawel, R. (1998). Red wine astringency: a review. *Australian Journal of Grape and Wine Research* 4, 74–95.

12) https://enoviti-hanumangirl.blogspot.com/2013/01/, 18.04.2021.

13) Cheynier, V., Rigaud, J. (1986). HPLC separation and characterization of flavonols in the skins of Vitis vinifera var. Cinsault. *American Journal of Enology and Viticulture* 37, 248–252.

14) Broussaud, F., Cheynier, V., Asselin, C., Moutounet, M. (1999). Flavonoid compositional differences of grapes among site test plantings of Cabernet franc. *American Journal of Enology and Viticulture* 50, 277–284.

15) Cheynier, V., Moutounet, M., Sarni-Manchado, P. (1998). Les compose´s phe´noliques. In: Flanzy, C. (Ed.), Oenologie, fondements scientifiques et tecnologiques. Lavoisier Tec&Doc, Paris, 124.

16) Rockenbach, I.I., Rodrigues, E., Gonzaga, L.M., Caliari, V., Genovese, M.I., Gonçalves, S.S., Fett, R. (2011). Phenolic compounds content and antioxidant activity in pomace from selected red grapes (Vitis vinifera L. and Vitis labrusca L.) widely produced in Brazil. *Food Chemistry* 127, 174–179

17) Boulton, R. (2001). The copigmentation of anthocyanins and its role in the color of red wine: a critical review. *American Journal of Enology and Viticulture*, 52, 67–87.

18) Gigliotti, A., Bucelli, P.L., Faviere, V. (1985). Influenza delle uve bianche Trebbiano e Malvasia sul colore del vino Chianti. *Vignevini,* 11, 39–46.

19) Baliga, M.S., Katiyar, S.K. (2006). Chemoprevention of photocarcinogenesis by selected dietary botanicals. *Photochemical and Photobiological Sciences*, 5, 243–253.

20) Aziz, M. H., Kumar, R., Ahmad, N. (2003). Cancer chemoprevention by resveratrol: In vitro and in vivo studies and the underlying mechanisms (Review). *International Journal of Oncology*, 23, 17–28.

21) Jang, M., Cai, L., Udeani, G. O., Slowing, K. V., Thomas, C. F., Beecher, C. W., Fong, H.H., Farnsworth, N.R., Kinghorn,A.D., Mehta R.G., Moon, R.C., Pezzuto, J.M. (1997). Cancer chemopreventive activity of resveratrol, a natural product derived from grapes. *Science*, 275, 218–220.

22) Yilmaz, Y., Toledo, R. T. (2004). Major flavonoids in grape seeds and skins: Antioxidant capacity of catechin, epicatechin, and gallic acid. *Journal of Agricultural and Food Chemistry*, 52, 255-260.

23) Brannan, R.G. (2008). Effect of grape seed extract on physicochemical properties of ground, salted, chicken thigh meat during refrigerated storage at different relative humidity levels. *Journal of Food Science*, 73, C36–C40.

24) Du, B., He, B.J., Shi, P.B., Li, F.Y., Li, J., Zhu, F.M. (2012). Phenolic content and antioxidant activity of wine grapes and table grapes. *Journal Medicinal Plant Research*, *6*, 3381–3387.

25) Anastasiadi, M., Pratsinis, H., Kletsas, D., Skaltsounis, A., Haroutounian, S.A. (2010). Bioactive non-coloured polyphenols content of grapes, wines and vinification by-products: Evaluation of the antioxidant activities of their extracts. *Food Research International, 43*, 805–813.

26) Katalinic, V., Generalic, I., Skroza, D., Ljubenkov, I., Teskera, A., Konta, I., Boban, M. (2009). Insight in the phenolic composition and antioxidative properties of *Vitis vinifera* leaves extracts Croat. *Journal of Food Science Technology,* 1(2), 7-15.

27) Ky, I., Lorrain, B., Kolbas, N., Crozier, A., Teissedre, P.L. (2014). Wine by-products: phenolic characterization and antioxidant activity evaluation of grapes and grape pomaces from six different French grape varieties. *Molecules*, 19(1), 482-506.

28) Sales, N.F.F., Silva da Costa, L., Carneiro, T.I.A., Minuzzo, D.A., Oliveira, F.L., Cabral, L.MC, Torres, A.G., El-Bacha, T. (2018). Anthocyanin-rich grape pomace extract (*Vitis vinifera* L.) from wine industry affects mitochondrial bioenergetics and glucose metabolism in human hepatocarcinoma HepG2 cells. *Molecules*, 23(3), 1-17.

29) Lima Mdos, S., Silani Ide, S., Toaldo, I.M., Corrêa, L.C., Biasoto, A.C., Pereira, G.E., Bordignon-Luiz, M.T., Ninow, J.L. (2014). Phenolic compounds, organic acids and antioxidant activity of grape juices produced from new Brazilian varieties planted in the Northeast Region of Brazil. *Food Chemistry*, 161, 94-103.

30) Kalkan, H., Kılınç, E., Özsöz, M. (2002). High-performance liquid chromatographic determination of some phenolic acids of Turkish commercialwines: An electrochemical approach (Şaraplarda Bazı Fenolik Asitlerinin Elektrokimyasal Dedektörlü HPLC Sistemi ile Belirlenmesi). Turkey 5th Viticulture and Wine Making Symposium, 5- 9 October, 559–565, Nevsehir, Turkey.

31) Revilla, E., Ryan, J.M. (2000). Analysis of several phenolic compounds with potential antioxidant properties in grape extracts and wines by high-performance liquid chromatography–photodiode array detection without sample preparation. *Journal of Chromatography A*, 881, 461–469.

32) FAOSTAT. Food and Agriculture Organization of the United Nations. http://www.fao.org/faostat/en/#home, 24.02. 2020.

33) Beres, C., Costa, G.N., Cabezudo, I., da Silva-James, N.K., Teles, A.S., Cruz, A.P., Mellinger-Silva, C., Tonon, R.V., Cabral, L.M., Freitas, S.P. (2017). Towards integral utilization of grape pomace from winemaking process: A review. *Journal Waste Management*, 68, 581–59.

34) Moldovan, M.L., Bogdan, C., Iurian, S., Roman, C., Oniga, I., Benedec, D. (2020). Phenolic content and antioxidant capacity of pomace and canes extracts of some *Vitis vinifera* varieties cultivated in Romania. *Farmacia*, 68, 1

35) Soto, M.L., Falqué, E., Domínguez, H. (2015). Relevance of natural phenolics from grape and derivative products in the formulation of cosmetics. *Cosmetics*, 2(3), 259-276.

36) Sousa, E.C. (2014). Chemical composition and bioactive compounds of grape pomace (*Vitis vinifera* L.), Benitaka variety, grown in the semiarid region of Northeast Brazil. *International Journal of Toxicology*, 33, 48S-83S.

37) Shirkande, A.J. (2000). Wine byproducts with health benefits. *Food Research International* 33, 469–474.

38) Ahmad, S.M., Ali, Siahsar, B. (2011). Analogy of physicochemical attributes of two grape seeds cultivar. *Ciencia e Investigación Agraria, 38*(2), 291-301.

39) Rockenbach, I.I., Silva, G.L., Rodrigues, E., Gonzaga, L.V., Fett, R. (2007). Atividade antioxidante de extratos de bagaço de uva das variedades Regente e Pinot Noir (*Vitis vinifera*). *Revista do Instituto Adolfo Lutz*, 66(2), 158-163.

40) Pontes, P.R.B., Santiago, S.S., Szabo, T. N., Toledo, L.P., Gollücke, A.P.B. (2010). Atributos sensoriais e aceitação de sucos de uva comerciais. *Ciência e Tecnologia de Alimentos,* 30(2), 313-318.

41) Burin, V. M., Falcão, L.D., Gonzaga, L. V., Fett, R., Rosier, J. P., Bordignon-Luiz, M. T. (2010). Colour, phenolic content and antioxidant activity of grape juice. *Ciência e Tecnologia de Alimentos, 30*(4), 1027-1032.

42) González-Paramás, A. M., Esteban-Ruano, S., Santos-Buelga, C., Pascual-Teresa, S., Rivas-Gonzalo, J. (2004). Flavanol content and antioxidant activity in winery byproducts. *Journal of Agricultural and Food Chemistry*, 52, 234–238.

43) Arvanitoyannis I.S., Ladas D., Mavromatis, A. (2006b). Wine waste treatment methodology. *International Journal of Food Science and Technology*, 41, 1117-1151.

44) Sarıçiçek, B.Z., Kılıç, U. (2002). A Study On Determining in situ Degradability of Grape Pomace (Üzüm Cibresinin in situ Rumen Parçalanabilirliğinin Belirlenmesi). *Atatürk University Faculty of Agriculture Journal*, 33 (3), 289-292.

45) Aydeniz, A., Brohi, A., 1991. Fertilizers and Fertilization (Gübreler ve Gübreleme). C.U. Tokat Agricultural Faculty Publications: 10, Textbook: 3, Tokat, Turkey.

46) Özenç, N. (2004). The Effects of Hazelnut Harvest Residues and Other Organic Materials on the Properties and Product Quality of Hazelnut Cultivated Soils (Fındık Zurufu ve Diğer Organik Materyallerin Fındık Tarımı Yapılan Toprakların Özellikleri ve Ürün Kalitesi Üzerine Etkileri). Ankara University Institute of Science, PhD Thesis, Turkey.

47) Benito, M., Masaguer, A., De Antonio, R., Moliner, A. (2005). Use of Pruning Waste Compost as a Component in Soilless Growing Media. *Bioresource Technology*, 96, 597–603.

48) Mumcu, S., Doymaz, İ., Akgün, N. (2003). Utilization of Winery Waste (Şarap Fabrikası Atıklarının Değerlendirilmesi). J*ournal of Chemical Technologies*, 32, 70-77., 32, 70-77.

49) Hayward, N. (2000). WINETECH. Environmental Management & Pollution Prevention Bulletin, 1, 3.

50) Akgün N.A., Özkara N. (2004). Biofuel Production From Various Biomass Wastes By Pyrolysis Method (Piroliz Yöntemiyle Değişik Biokütlesel Atıklardan Bioyakıt Eldesi). Bioenergy, İzmir, Turkey.

51) Akgün N.A., Doymaz İ., Özkara N. (2004). Utilization of Winery Wastes for Energy Purposes. (Şarap Fabrikası Atıklarının Enerji Amaçlı Değerlendirilmesi). II. National Aegean Energy Symposium and Exhibition, Kütahya, Turkey.

52) Sousa, E.C., Uchoa-Thomaz, A.M.A., Carioca, J.O.B., Morais, S.M., Lima, A., Martins, C.G., Alexandrino, C.D., Ferreria, P.A.T., Rodrigues, A.L.M., Rodrigues, S.P., Silva, J.N., Rodrigues, L.L. (2014). Chemical composition and bioactive compounds of grape pomace (*Vitis vinifera* L.), Benitaka variety, grown in the semiarid region of Northeast Brazil. *Food Sciences and Technology (Campinas)*, 34(1), 135-142.

53) Pasqualone, A., Bianco, A.M., Paradiso, V.M., Summo, C., Gambacorta, G., Caponio, F. (2014). Physico-Chemical, Sensory and Volatile Profiles of Biscuits Enriched With Grape Marc Extract. *Food Research International* 65, 385–393.

54) Tseng, A., Zhao, Y. (2013). Wine Grape Pomace as Antioxidant Dietary Fibre for Enhancing Nutritional Value and İmproving Storability of of yogurt and salad dressing. *Food Chemistry*, 138, 356-65**.**

55) Bail, S., Stuebiger, G., Krist, S., Untrwager, H., Buchbaner, G. (2008). Characterization of various grape seed oils by volatile compounds, triacylglycerol composition, total phenols and antioxidant capacity. *Food Chemistry*, 108**,** 1122.

56) Crews, C., Hough, P., Godward, J., Brereton, P., Lees, M., Guiet, S., Winkelmann, W. (2006). Quantitation of the main constituents of some authentic grape-seed oils of different origin. *Journal of Agricultural and Food Chemistry*, 54, 6261.

57) Lachman, J., Hejtmankova, A., Taborsky, J., Kotíkova, Z., Pivec, V., Stralkova, R., Vollmannova, A., Bojnanska, T., Dedina, M. (2015). Evaluation of oil content and fatty acid composition in the seed of grapevine varieties. *LWT-Food Sci Technol*, 63, 620.

58) Özvural, E.B., Vural, H. (2008). The Effect of Red Grape Seed Flour and Oil on Quality Criteria of Sausages (Kırmızı Üzüm Çekirdeği Unu ve Yağının Sosislerin Kalite Kriterleri Üzerine Etkisi).Turkey 10th Food Congress, Erzurum, Turkey.

59) Yılmaz, Y., Toledo, R.T. (2006). Radical absorbance capacities of grape/wine industry by products and effect of solvent type on extraction of grape seed polyphenols. *Journal of Food Composition and Analysis*, 19, 41-48.

60) Arvanitoyannis I.S., Ladas D., Mavromatis A. (2006a). Potential uses and applications of treated wine waste: a review. *International Journal of Food Science and Technology*, 41, 475–487.

61) Moldes, D., Gallego, P., Rodrıguez-Couto, S., Sanroman, A. (2003). Grape seeds: the best lignocellulosic waste to produce laccaseby solid statecultures of Tramete shirsuta. *Biotechnology Letters*, 25, 491–495.

62) Fernandez, C.M., Ramos, M.J., Perez, A., Rodriguez, J.F. (2010). Production of biodiesel from winery waste: Extraction, refining and transesterification of grape see doil. *Bioresource Technology*, 101, 7019–7024.

63) Öztürk, A. (2005). Characterization of Proanthocyanidins in Grape Seed (*Vitis vinifera*) and Leaf and Their Use in Cosmetic Field (Üzüm Çekirdeği (*Vitis vinifera*) ve yaprağındaki Proanthocyanidinlerin Karakterizasyonu ve Kozmetik alanda Kullanımı). Celal Bayar University, Institute of Science, Turkey.

64) Demiryürek, İ. (2006). *Vitis vinifera* L. Evaluation of Seed Oil in Phytotherapy. Ankara University, Institute of Health Sciences, Department of Pharmacognosy, Phytotherapy Drugs, Non-Thesis Master's Term Project, Ankara, Turkey.

65) Nishino, H., Yoshida, T. (2002). Antitumor activity of compounds isolated from leaves of *Eriobotrya japonica. Journal of Agricultural and Food Chemistry*, 50, 2400-2403.

66) Ito, H., Kobayashi, E., Li, S.H., Hatano T., Suita, D., Kubo, N., Shimura, S., Itoh, Y., Tokuda, H., Nishino, H., Yoshida, T. (2002). Antitumor activity of compounds isolated from leaves of *Eriobotrya japonica.* J*ournal Agricultural and Food Chemistry*, 50, 2400-2403.

67) Amakura, Y., Umino, Y., Tsuji, S., Ito, H., Hatano, T., Yoshida, T., Tonogai, Y. (2002). Constituents and their antioxidative effects in eucalyptus leaf extract used as a natural food additive. *Food Chemistry*, 77, 47-56.

68) Siddhuraju, P., Becker, K. (2003). Antioxidant properties of various solvent extracts of total phenolic constituents from three different agroclimatic origins of drumstick tree (*Moringa oleifera* Lam.) leaves. *Journal of Agricultural and Food Chemistry*, 51, 2144-2155.

69) Naczk, M., Amarowicz, R., Zadernowski, R., Pegg, R., Shahidi, F. (2003). Antioxidant capacity of crude phenolic extracts from wild blueberry leaves. *Polish Journal Food and Nutrition Sciences*, 53, 166- 169.

70) Amaral, J.S., Ferreres, F., Andrade, P.B., Valentao, P., Pinheiro, C., Santos, A., Seabra, R. (2005). Phenolic profile of hazelnuts (*Corylus avellena* L.) leaves cultivars grown in Portugal. *Natural Product Research*, 19, 157-163.

71) Pari, L., Karamać, M., Kosińska, A., Rybarczyk, A., Amarowicz, R. (2007). Antioxidant activity of the crude extracts of drumstick tree (*Moringa oleifera* Lam.) and sweet broomweed (*Scoparia dulcis* L.) leaves. *Polish Journal Food and Nutrition Sciences*, 57, 203-208.

72) Hallaç Türk, F. (2009). Determination of phenolic and mineral compounds in leaves of some table grapes at different time (Bazı Sofralık Üzüm Çeşitlerinde Farklı Dönemlerde Alınan Yapraklardaki Fenolik ve Mineral Madde Değişimlerinin Belirlenmesi). Süleyman Demirel University, Institute of Science, PhD Thesis.

73) Weidner, S., Karamać, M., Amarowicz, R., Szypulska, E., Gołgowska, A. (2007). Changes in composition of phenolic compounds and antioxidant properties of *Vitis amurensis* seeds germinated under osmotic stress. *Acta Physiologiae Plantarum*, 29, 283-290.

74) Chevallier, A. (1996). The Encyclopedia of Medicinal Plants. Dorling Kindersley, London, 336.

75) Kedage, V.V., Tilak, J.C., Dixit, G.B., Devasagayam, T.P., Mhatre, M. (2007). A studyof antioxidant properties of some varieties of grapes (*Vitis vinifera* Linn). *Critical Reviews in Food Science and Nutrition*, 47, 175–185.

76) Orhan, N., Aslan, M., Orhan, D.D., Ergun F., Yeşilada, E. (2006). *In-vivo* assessment of antidiabeticand antioxidant activities of grapevine leaves (*Vitis vinifera*) in diabeticrats. *Journal of Ethnopharmacology*, 108, 280–286

77) Bruneton, J. (2005). Pharmacognosie. Phytochimie. Plantes Médicinales, TEC&DOC Lavoisier, Paris, 365.

78) Dulundu, E., Ozel, Y., Topaloglu, U., Toklu H., Ercan, F., Gedik, N., Sener, G. (2007). Grape seed extract reduces oxida-tive stress and fibrosis in experimental biliary obstruction. *Journal of Gastroenterology and Hepatology*, 22, 885–892.

79) Orhan, D.D., Orhan, N., Ergun, E., Ergün F. (2007). Hepatoprotective effect of *Vitisvinifera* L leaves on carbon tetrachloride-induced acute liver damage inrats. *Journal of Ethnopharmacology*, 112, 145–151.

78) Bekar, T. (2016). Waste Technology in Viticulture. *Iğdır University Journal of the Institute Science and Technology.* 6(1), 17-24, 2016

81) Felicio, J.D., Santos, R.S., Goncalez, E. (2001). Chemical constituents from *Vitisvinifera* (Vitaceae). *Arquivos do Instituto Biologico*, 68, 47–50.

Chapter 9

$f(\mathcal{R},\mathcal{T})$ GRAVITY AND NON-STATIC PLANE SYMMETRIC DOMAIN WALLS

Doğukan TAŞER [1]
Melis ULU DOĞRU[2]

1 Assist. Prof. Dr., Çanakkale Onsekiz Mart University, Çan Vocational School, Department of Electricity and Energy. Çanakkale, TURKEY dogukantaser@comu.edu.tr
2 Assoc. Prof. Dr., Çanakkale Onsekiz Mart University, Art and Science Faculty, Department of Physics. Çanakkale, TURKEY melisulu@comu.edu.tr

1. INTRODUCTION

Foundations of gravitation theories begin with Newton's theory. Although Newton's theory is very successful in studying motions of earth and determining orbits of planets and other celestial bodies, it has failed to explain many issues. Some scientific developments such as the Michelson Morley experiment at the end of the 19th century and the beginning of the 20th century radically changed what is known about the nature of light. It has been understood that the propagation speed of the interactions has a finite value and this value is equal to the speed of light. The situation required the abandonment of the Galileo transformations, which are the transformation formulas used in Newtonian theory, and the realization of the relations between reference systems by Lorentz transformations. After all gravitation theories with Lorentz invariance have been produced. The most consistent of these theories is Einstein's General Relativity. General Relativity theory is the most valid gravitation theory, providing tests such as the progression of the planet's perihelia, the gravitational deflection of light, and the red-shift phenomenon. Lagrangian density of geometric part is defined via curvature scalar in theory. Beginning of the theory, Einstein thought the universe was static form. Hence, Einstein manually added an extra term, called as the cosmological constant, to field equations because of the universe would collapse into itself due to gravitational gravity. After Hubble stated that the universe is not static with his red-shift observation, Einstein abandoned the cosmological concept by changing his idea of the stationary model. After that, alternative theories were proposed to express cosmologically dynamic structure of universe.

In this study, we aim to introduce readers to one of the alternative gravitation theories, $\mathfrak{f}(\mathfrak{R},\mathfrak{T})$ theory, and to explain the nature of an original cosmological model we developed in this gravitation theory. With technological advances, observational experiments about high red-shift of huge galaxies (Perlmutter *et al.*, 1999), fluctuation of background radiation (Seprgel *et al.*, 2003), X-ray experiments (Allen *et al.*, 2004) and large scale structure (Tegmark *et al.*, 2004) indicates that current behavior of universe shows expansion with acceleration (Sahoo and Reddy, 2018). In the last decade, data from Plank collaboration (Ade *et al.,* 2016), Atacama Cosmology Telescope Polarimeter (ACTPol) (Naess *et al.*, 2014) and Baryon Oscillation Spectroscopic Survey (BOSS) (Alam *et al.*, 2017) are the other observational experiments refreshing evidences about action of current universe. In cosmology, the driving force behind mechanism of universe is still an unresolved topic in a satisfactory way, recently. There are two attitudes in order to explain these phenomania in

theoretical basement. First attitude is based on dark energy definition which has repulsive gravitational effect in General Relativity. Cosmic microwave background fluctuations and high red-shift Supernovae experiments indicate that dark energy has 76 percent dominance over the overall structure (Sharif and Kausar, 2011). To qualify construction of the dark energy and current behavior of universe, there are quite a bit suggested cosmological dark energy models (Martin, 2008; Nojiri *et al.*, 2006). Besides, the other descriptions to denote the dark energy in the field equations are equation of state (EoS) (Hu and Sawicki, 2007; Starobinsky, 2007) and cosmological constant (Shabani and Ziaie, 2018). Despite all these cosmological efforts, the working mechanism and root of this dominant character in the universe is still a puzzle. Second attitude are called as modified theories which are constructed via modifications of General Relativity. It is possible to explain current expansion of universe without needing any exotic matter distribution by way of modified theories (Buchdahl, 1970; Carroll *et al.*, 2004; Bertolami *et al.*, 2007; Bengochea and Ferraro, 2009; Harko *et al.*, 2011).

The well-known generalization of the General Relativity is the $\mathfrak{f}(\mathfrak{R})$ gravitation theory. The Einstein-Hilbert (EH) action in theory has been defined by favor of an arbitrary function, $\mathfrak{f}(\mathfrak{R})$, depending on Ricci scalar as distinct from General Relativity (Buchdahl, 1970). Many cosmological topics have been examined with viable $\mathfrak{f}(\mathfrak{R})$ models (Felice and Tsujikawa, 2010; Sotiriou *et al.*, 2010). Union of early and late time behaviors of universe has been theoretically demonstrated to be possible for $\mathfrak{f}(\mathfrak{R})$ gravitation theory because of different applicable $\mathfrak{f}(\mathfrak{R})$ models (Sharif and Kausar, 2011). Recently, $\mathfrak{f}(\mathfrak{R},\mathfrak{T})$ theory is adopted for an adequate theory to explain current accelerated expansion of universe (Sharif and Siddiqa, 2017). $\mathfrak{f}(\mathfrak{R},\mathfrak{T})$ theory has been suggested by Harko *et. al.* (2011). EH action is described via a function depending on Ricci curvature scalar and the trace of the energy-momentum tensor. Field equation for theory has been derived from a source term representing variation of the energy-momentum tensor according to metric (Zaregonbadi *et al.*, 2016). Test particles don't pursue geodesic and existence of the cosmic accelerated expansion is always available due to the coupling between matter and geometry (Zubair *et al.*, 2016). Dependence of cosmic matter is a one argued topic and, $\mathfrak{T}$, could spring from existence of imperfect fluid or some kinds of quantum effects (Deb *et al.*, 2018). Cosmological application of the $\mathfrak{f}(\mathfrak{R},\mathfrak{T})$ theory has been deeply examined by authors (Moraes, 2014; Singh and Kumar, 2014; Rudra, 2015).

It is widely considered that universe had been various phase transitions during its evolution in very early stage. Symmetry of universe during phase transitions is broken spontaneously which could originate existence of topological defects (Aditya *et al.*, 2019). Topological defects are gained more attention because General Relativity is justified existence of these structures even though there are no observational evidences of them. Hill *et al.* (1989) have offered that thickness domain walls could have been generated during the late time phase transition and discussed effect of a new scenario of galaxy formation. Vilenkin (1983) firstly considered that a static metric could not be useful in order to describe a gravitational field of thin domain wall which is planar symmetric. Subsequently, it was demonstrated by Widrow that a thick domain wall could be identified by a static metric. Non-static metrics could be more suitable for description for thick domain walls with this viewpoint. Domain walls could be considered two ways. First way is to describe with an energy momentum tensor including a scalar field with a potential. Second way is to consider it as perfect fluid-like energy momentum tensor. Many authors have examined various properties of domain walls in cosmological way.

Our motivation is to investigate non-static plane symmetric domain walls in the consideration of $\mathfrak{f}(\mathfrak{R},\mathfrak{T})$ theory. Universe has a smoothed-out picture during early stage of its evolution. So, we consider spatial homogenetic and anisotropic universe for domain walls via a non-static plane symmetric model in one of the most popular modified theory.

This study has been organized in the following form: Firstly, $\mathfrak{f}(\mathfrak{R},\mathfrak{T})$ theory is recollected. After, non-static plane symmetric domain walls in $\mathfrak{f}(\mathfrak{R},\mathfrak{T}) = \mathfrak{R} + 2h(\mathfrak{T})$ model are examined. Exact solutions of given model are attained in $\mathfrak{f}(\mathfrak{R},\mathfrak{T})$ theory. Finally, physical and geometrical particulars for solutions are discussed.

2. FIELD EQUATIONS IN $\mathfrak{f}(\mathfrak{R},\mathfrak{T})$ GRAVITY

$\mathfrak{f}(\mathfrak{R},\mathfrak{T})$ theory is formulated by Harko *et. al.* (2011). Lagrangian for the theory is motivated by depending on Ricci scalar and energy and matter of universe. The Einstein-Hilbert action of $\mathfrak{f}(\mathfrak{R},\mathfrak{T})$ theory is represented as:

$$S = \frac{1}{16\pi}\int[\mathfrak{f}(\mathfrak{R},\mathfrak{T}) + \mathcal{L}_{mat}]\sqrt{-g}\,d^4x \qquad (1)$$

Here $\mathfrak{f}(\mathfrak{R},\mathfrak{T})$ is an arbitrary function depending on the Ricci curvature scalar, $\mathfrak{R}$, and trace of energy-momentum tensor of the cosmic matter, $\mathfrak{T}_{\ell m}$. L_{mat} is the matter Lagrangian density. g is the determinant of

metric tensor. The energy-momentum tensor of matter is given in the following form (Landau and Lifshitz, 2002):

$$\mathfrak{T}_{lm} = -\frac{2}{\sqrt{-g}}\frac{\delta(\sqrt{-g}\mathcal{L}_{mat})}{\delta g^{lm}} \tag{2}$$

Energy-momentum tensor of matter is obtained as

$$\mathfrak{T}_{lm} = \mathcal{L}_{mat}g_{lm} - 2\frac{\delta\mathcal{L}_{mat}}{\delta g^{lm}} \tag{3}$$

The metric variation of EH action given by Eq. (1) generates equations as:

$$\frac{\partial \mathfrak{f}(\mathfrak{R},\mathfrak{T})}{\partial \mathfrak{R}}\mathfrak{R}_{lm} - \frac{1}{2}\mathfrak{f}(\mathfrak{R},\mathfrak{T})g_{lm} + (g_{lm}\Box - \nabla_l\nabla_m)\frac{\partial \mathfrak{f}(\mathfrak{R},\mathfrak{T})}{\partial \mathfrak{R}} = 8\pi\mathfrak{T}_{lm} - \frac{\partial \mathfrak{f}(\mathfrak{R},\mathfrak{T})}{\partial \mathfrak{T}}\mathfrak{T}_{lm} - \frac{\partial \mathfrak{f}(\mathfrak{R},\mathfrak{T})}{\partial \mathfrak{T}}\Theta_{lm} \tag{4}$$

Here ∇_m indicates the covariant derivative. $\Box = \nabla_\ell\nabla^m$ defines D'Alambertian operator which is determined in following manner:

$$\Box = \frac{1}{\sqrt{-g}}\partial_l\left(\sqrt{-g}g^{lm}\right)\partial_m \tag{5}$$

Also, $\Theta_{\ell m}$ is defined as:

$$\Theta_{lm} = \frac{g^{\alpha\beta}\delta\mathfrak{T}_{\alpha\beta}}{\delta g^{lm}} = -\mathcal{L}_{mat}g_{lm} + 2g_{lm}\mathcal{L}_{mat} - 2\mathfrak{T}_{lm} - 2g^{\alpha\beta}\frac{\partial^2\mathcal{L}_{mat}}{\partial g^{lm}\,\partial g^{\alpha\beta}}. \tag{6}$$

The contraction of Eq. (4) is an important method to construct relation between geometry and matter parts. So, trace of Eq. (4) is obtained

$$\frac{\partial \mathfrak{f}(\mathfrak{R},\mathfrak{T})}{\partial \mathfrak{R}}\mathfrak{R} + 3\Box\frac{\partial \mathfrak{f}(\mathfrak{R},\mathfrak{T})}{\partial \mathfrak{R}} - 2\mathfrak{f}(\mathfrak{R},\mathfrak{T}) = 8\pi\mathfrak{T} - \frac{\partial \mathfrak{f}(\mathfrak{R},\mathfrak{T})}{\partial \mathfrak{T}}\mathfrak{T} - \frac{\partial \mathfrak{f}(\mathfrak{R},\mathfrak{T})}{\partial \mathfrak{T}} \tag{7}$$

where $\Theta = \Theta_\ell^\ell$. The nature of $\Theta_{\ell m}$ and matter field play significant role to designate structure of field equations of $\mathfrak{f}(\mathfrak{R},\mathfrak{T})$ theory. In this context, Harko et. al. (2011) studied on some classification of $\mathfrak{f}(\mathfrak{R},\mathfrak{T})$ models. In this study, it is considered $\mathfrak{f}(\mathfrak{R},\mathfrak{T}) = \mathfrak{R} + 2h(\mathfrak{T})$ model. In the presence of the $\mathfrak{f}(\mathfrak{R},\mathfrak{T}) = \mathfrak{R} + 2h(\mathfrak{T})$ model, field equation of theory is

$$\mathfrak{R}_{lm} - \frac{1}{2}\mathfrak{R}g_{lm} = 8\pi\mathfrak{T}_{lm} + 2\frac{\partial \mathfrak{f}(\mathfrak{R},\mathfrak{T})}{\partial \mathfrak{T}}\mathfrak{T}_{lm} + [2p\frac{\partial \mathfrak{f}(\mathfrak{R},\mathfrak{T})}{\partial \mathfrak{T}} + \mathfrak{f}(\mathfrak{T})]g_{lm} \tag{8}$$

3. NON-STATIC PLANE SYMMETRIC DOMAIN WALLS IN $\mathfrak{f}(\mathfrak{R},\mathfrak{T})$ GRAVITY

Non-static plane symmetric space-time is defined as

$$ds^2 = e^{2h}(dt^2 - dr^2 - r^2 d\theta^2 - s^2 dz^2) \tag{9}$$

Here h and s are functions depending on cosmic-time. The curvature scalar for given space-time is obtained

$$\mathfrak{R} = 6e^{-2h}\left[\dot{h}^2 + \ddot{h} + \frac{\dot{h}\dot{s}}{s} + \frac{\ddot{s}}{3s}\right] \tag{10}$$

where dot represent ordinary derivative according to cosmic-time. Also, energy-momentum tensor for domain walls formed perfect fluid is given by

$$\mathfrak{T}_{\mathfrak{lm}} = (\rho + p)u_{\mathfrak{l}}u_m - pg_{\mathfrak{l}m} \tag{11}$$

Where ρ and p are density and pressure of domain walls. Nonvanishing components of cosmic matter are attained as

$$\mathfrak{T}_1^1 = \mathfrak{T}_2^2 = T_3^3 = -p, \quad \mathfrak{T}_4^4 = \rho, \quad \mathfrak{T}_{\mathfrak{m}}^{\mathfrak{l}} = 0 \ for\ \mathfrak{l} \neq m \tag{12}$$

Domain walls incorporates normal matter, ρ_m, p_m and the tension, σ (which are related with $p = p_m - \sigma$ and $\rho = \rho_m + \sigma$) (Aktaş *et al.,* 2007). Also, density and pressure of normal matter obey equation state:

$$p_m = (\gamma - 1)\rho_m \tag{13}$$

where $1 \leq \gamma \leq 2$ is a constant (Aktaş *et al.,* 2007). In $\mathfrak{f}(\mathfrak{R},\mathfrak{T}) = \mathfrak{R} + 2h(\mathfrak{T})$ model, $h(\mathfrak{T})$ function could be selected as $h(\mathfrak{T}) = \lambda\mathfrak{T}$. λ is an arbitrary constant (Harko *et. al.*, 2011). By using Eqs.(8), (9) and (9)-(11), the field equations of constructed model in $\mathfrak{f}(\mathfrak{R},\mathfrak{T})$ theory are attained as

$$e^{-2h}\left(\dot{h}^2 + 2\frac{\dot{h}\dot{s}}{s} + \ddot{h} + \frac{\ddot{s}}{s}\right) = \lambda\rho - (8\pi + 3\lambda)p = -8\pi p^{eff} \tag{14}$$

$$e^{-2h}\left(\dot{h}^2 + 2\ddot{h}\right) = \lambda\rho - (8\pi + 3\lambda)p = -8\pi p^{eff} \tag{15}$$

and

$$e^{-2h}\left(3\dot{h}^2 + 2\frac{\dot{h}\dot{s}}{s}\right) = (8\pi + 3\lambda)\rho - \lambda p = 8\pi\rho^{eff} \tag{16}$$

where p^{eff} and ρ^{eff} are effective pressure and density, respectively. Here, non-static plane symmetric domain walls in theory generates three differential equations with unknown four functions. The aim of this study is investigation of non-static plane symmetric domain walls in theory. So, we consider linear relationship between metric potentials because of there is a correlation between shear scalar and scalar expansion:

$$e^h = s^k \tag{17}$$

Here $k \neq 1$ is a real constant. Red-shift studies shows that there is a restriction about shear and Hubble parameter for nearby place our galaxy. Collins *et al.* (1980) have noticed that relation between Hubble parameter and shear becomes constant in homogeneous and anisotropic universe. Under this assumption field equations of constructed model could be rewrite in the following forms:

$$s^{-2k-1}\left(\frac{k^2\dot{s}^2}{s} + \ddot{s}(2k+1)\right) = \lambda\rho - (8\pi + 3\lambda)p \tag{18}$$

$$s^{-2k-1}\left(\frac{k^2\dot{s}^2}{s} + 2k\left(\ddot{s} - \frac{\dot{s}^2}{s}\right)\right) = \lambda\rho - (8\pi + 3\lambda)p \tag{19}$$

and

$$k\dot{s}^2 s^{-2k-2}(3k+2) = (8\pi + 3\lambda)\rho - \lambda p \tag{20}$$

By using Eqs. (18)-(20), metric potential, *s(t)*, is attained from exact solution of field equations as:

$$s(t) = [(2k+1)(c_1 t + c_2)]^{\frac{1}{2k+1}} \tag{21}$$

By using Eqs. (17) and (21), the metric potential, $e^{h(t)}$, is obtained as:

$$e^{h(t)} = [(2k+1)(c_1 t + c_2)]^{\frac{k}{2k+1}} \tag{22}$$

Pressure and density of domain walls are obtained in the following form

$$p(t) = \rho(t) = \frac{1}{2}\frac{c_1^2 k(3k+2)[(2k+1)(c_1 t+c_2)]^{-\frac{2k}{2k+1}}}{(c_1 t+c_2)^2(2k+1)^2(4\pi+\lambda)} \tag{23}$$

Evolution of pressure and density of domain walls are represented in Fig. 1. Domain walls behave like stiff matter for constructed space-time in $\mathfrak{f}(\mathfrak{R},\mathfrak{T})$ theory. Also, pressure and density decrease over time. So, it could be said that domain walls consist at the beginning of time.

Condition of $\rho > 0$ is suitable when $\lambda > -4\pi$. Also, ρ_m, p_m σ are obtained by considering $p = p_m - \sigma$ and $\rho = \rho_m + \sigma$ and Eqs. (13):

$$p_m(t) = \frac{(\gamma-1)c_1^2 k(3k+2)[(2k+1)(c_1 t+c_2)]^{-\frac{2k}{2k+1}}}{\gamma(c_1 t+c_2)^2(2k+1)^2(4\pi+\lambda)} \tag{24}$$

$$\rho_m(t) = \frac{c_1^2 k(3k+2)[(2k+1)(c_1 t+c_2)]^{-\frac{2k}{2k+1}}}{\gamma(c_1 t+c_2)^2(2k+1)^2(4\pi+\lambda)} \tag{25}$$

and

$$\sigma(t) = \frac{1}{2}\frac{c_1^2 k(3k\gamma-6k+2\gamma-4)[(2k+1)(c_1 t+c_2)]^{-\frac{2k}{2k+1}}}{\gamma(c_1 t+c_2)^2(2k+1)^2(4\pi+\lambda)} \tag{26}$$

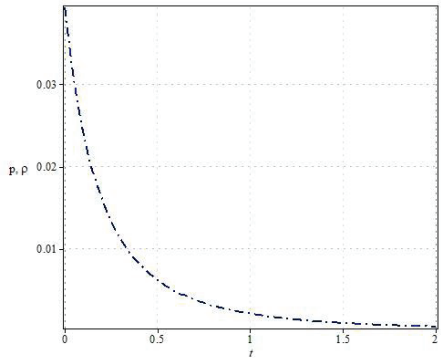

Figure 1. The change of density and pressure of domain wall. ($c_1 = 2, c_2 = 1, k = 1$ and $\lambda = 1$)

Evolution for pressure and density of normal matter are represented in Fig 2. and Fig 3. Pressure and density of normal matter are decreasing function with time, as well. Changing behavior of domain walls tension is represented in Fig. 4. The tension decreases over time. So, it is possible case that the domain walls could exist at beginning of time. Also, the tension approaches zero over time. As it is seen Fig. 4, it refers that the tension with increasing negative values over time is accordance with the argument of Zeldovich *et al.* (1975). The line element of non-static domain walls in $\mathfrak{f}(\mathfrak{R},\mathfrak{T})$ gravity could be rewritten as

$$ds^2 = [(2k+1)(c_1 t + c_2)]^{\frac{2k}{2k+1}}\Big(dt^2 - dr^2 - r^2 d\theta^2 - [(2k+1)(c_1 t + c_2)]^{\frac{2}{2k+1}} dz^2\Big) \tag{27}$$

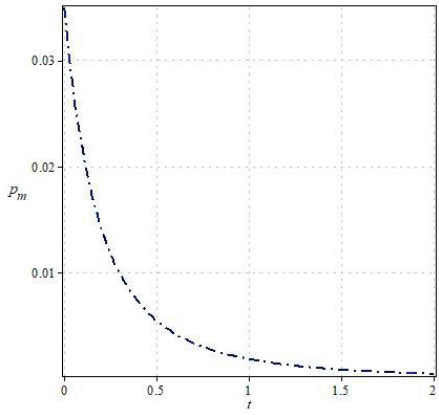

Figure 2. Changing of pressure of normal matter with time.
($c_1 = 2, c_2 = 1, k = 1, \lambda = 1$ and $\gamma = 1.8$)

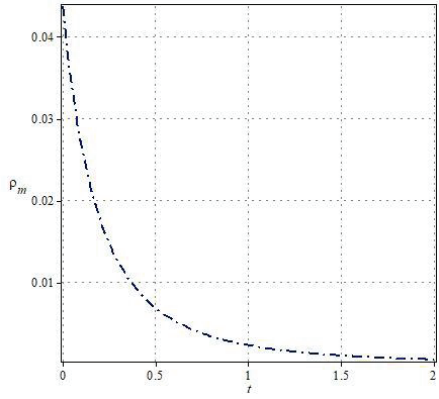

Figure 3. Changing of density of normal matter with time.
($c_1 = 2, c_2 = 1, k = 1, \lambda = 1$ and $\gamma = 1.8$)

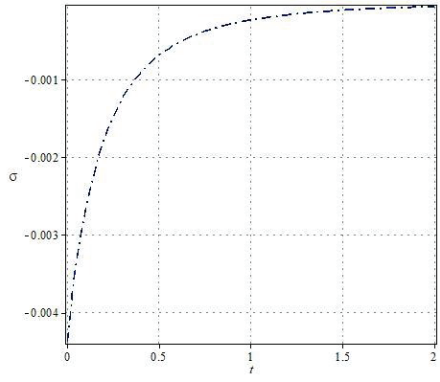

Figure 4. The change of tension of domain wall with time. ($c_1 = 2, c_2 = 1, k = 1, \lambda = 1$ and $\gamma = 1.8$)

Kinematic quantities such as Hubble parameter, expansion scalar, shear scalar, deceleration parameter and anisotropic parameter for average scale factor, $\mathcal{R}(t) = \left(Se^{4h}\right)^{1/3}$, are attained as:

$$H = \frac{\dot{\mathcal{R}}}{\mathcal{R}} = \frac{1}{3}(H_1 + H_2 + H_3) = \frac{1}{3}\frac{c_1(4k+1)}{(2k+1)(c_1 t + c_2)} \tag{28}$$

$$\Theta = 3H = \frac{c_1(4k+1)}{(2k+1)(c_1 t + c_2)} \tag{29}$$

$$\sigma^2 = \frac{1}{2}\left(\sum_{i=1}^{3} H_i^2 - \frac{1}{3}\Theta^2\right) = \frac{1}{3}\frac{c_1^2(2k-1)^2}{(2k+1)^2(c_1 t + c_2)^2} \tag{30}$$

$$q = -\frac{\mathcal{R}\ddot{\mathcal{R}}}{\dot{\mathcal{R}}^2} = \frac{2(k+1)}{4k+1} \tag{31}$$

$$\triangle = \frac{1}{3}\sum_{i=1}^{3}\left(\frac{H_i - H}{H}\right)^2 = \frac{2(2k-1)^2}{(4k+1)} \tag{32}$$

Evolution of Hubble parameter and expansion scalar is represented in Fig. 5. It is obvious that both functions are decreasing with time. They approach to zero at late time. Deceleration parameter is positive for constructed model because k is a positive constant. Non-static plane symmetric domain walls have deceleration in the standard way. Also, anisotropic parameter is constant. Thus, constructed space-time stayed as anisotropic during its evolution. In the case of $k > 1/2$, anisotropic parameter gets positive values.

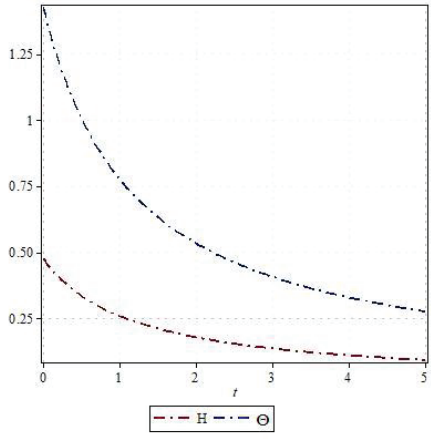

Figure 5. The change of Hubble parameter and expansion scalar with cosmic-time in the case of $c_1 = 0.92, c_2 = 1.1, k = 1.21$.

Also, Jerk (j), snap (s) and lerk (l) parameter give us to opportunity in order to get information about evolution of universe (Visser, 2004; Capozziello *et al.*, 2011). They are given by

$$j(t) = \frac{1}{\mathcal{R}}\frac{d^{3}\mathcal{R}}{dt^{3}}\left(\frac{1}{\mathcal{R}}\frac{d\mathcal{R}}{dt}\right)^{-3} \tag{33}$$

$$s(t) = \frac{1}{\mathcal{R}}\frac{d^{4}\mathcal{R}}{dt^{4}}\left(\frac{1}{\mathcal{R}}\frac{d\mathcal{R}}{dt}\right)^{-4} \tag{34}$$

$$l(t) = \frac{1}{\mathcal{R}}\frac{d^{5}\mathcal{R}}{dt^{5}}\left(\frac{1}{\mathcal{R}}\frac{d\mathcal{R}}{dt}\right)^{-5} \tag{35}$$

Jerk, snap and lerk parameters are obtained for constructed universe as:

$$j = \frac{2(8k^{2}+13k+5)}{(1+4k)^{2}} \tag{36}$$

$$s = -\frac{4(56k^{3}+123k^{2}+87k+20)}{(1+4k)^{3}} \tag{37}$$

$$l = \frac{4(1120k^{4}+3076k^{3}+3093k^{2}+1357k+220)}{(1+4k)^{4}} \tag{38}$$

It is clearly seen that all parameters are constants. All parameters depend on the k parameter. While jerk and lerk parameters are positive decreasing constants, snap parameter shows negative increasing constant behavior when k parameter is increasing. Value of snap parameter has values such as (-15) for radiation dominant area, (-7/2) for matter domination area and (1) for de-sitter domination area (Shabani and Farhoudi, 2014). For constructed model snap parameter could not be positive so the model cannot allow de-Sitter dominated area.

Energy conditions are available assumptions in order that investigate behavior of constructed model in $\mathfrak{f}(\mathfrak{R},\mathfrak{T})$ theory. Energy conditions are connected with Raychoudhuri equations. Energy conditions are classified as Strong Energy Condition (SEC), Dominant Energy Condition (DEC), Weak Energy Condition (WEC) and Null Energy Condition (NEC). Energy conditions are investigated via effective matter components. By using Eqs. (18)-(20) and (23), effective pressure and effective density are obtained as:

$$p^{eff} = \rho^{eff} = \frac{1}{8\pi}c_1^2 k(3k+2)[(2k+1)(c_1 t + c_2)]^{-\frac{2(3k+1)}{2k+1}} \tag{39}$$

Energy conditions are attained for constructed model in the following forms:

$$SEC: \rho^{eff} + 3p^{eff} = \frac{1}{2\pi} c_1^2 k(3k+2)[(2k+1)(c_1 t + c_2)]^{-\frac{2(3k+1)}{2k+1}} \geq 0 \quad (40)$$

$$DEC: \rho^{eff} - p^{eff} = 0 \geq 0 \quad (41)$$

$$WEC: \rho^{eff} = \frac{1}{8\pi} c_1^2 k(3k+2)[(2k+1)(c_1 t + c_2)]^{-\frac{2(3k+1)}{2k+1}} \geq 0 \quad (42)$$

$$NEC: \rho^{eff} + p^{eff} = \frac{1}{4\pi} c_1^2 k(3k+2)[(2k+1)(c_1 t + c_2)]^{-\frac{2(3k+1)}{2k+1}} \geq 0 \quad (43)$$

Chancing of energy conditions for constructed model are represented in Fig. 6. All energy conditions are satisfied for constructed model. SEC, WEC and NEC approaching to zero with time. Also, domain walls does not behave as exotic matter for constructed model in $\mathfrak{f}(\mathfrak{R}, \mathfrak{T})$ theory.

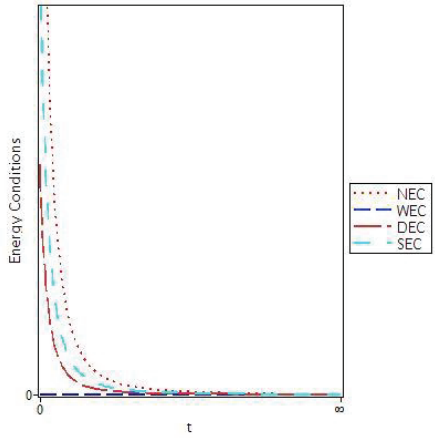

Figure 6. The change of Energy Conditions with cosmic-time. ($c_1 = 2$, $c_2 = 1, k = 1.1$)

4. CONCLUTION

In this study, main purpose is to investigate non-static plane symmetric domain walls in $\mathfrak{f}(\mathfrak{R}, \mathfrak{T})$ theory. Firstly, we set field equations of non-static plane symmetric domain walls by considering $\mathfrak{f}(\mathfrak{R}, \mathfrak{T}) = \mathfrak{R} + 2h(\mathfrak{T})$ model. Exact solutions of field equations are investigated. Constructed model indicates that pressure and density of domain walls are decreasing function with time and domain walls exist at the beginning of time. Also, tension of the domain walls could be positive or negative. Connection of between theory-related constant, λ and γ is change behavior of tension of domain wall. Also, domain walls behave like stiff

matter $(p = \rho)$. This condition supports stiff domain walls ideas in other gravitational theories (Aktaş *et al.*, 2007; Adhav *et al.*, 2011). Deceleration parameter is a positive constant for constructed model. Non-static plane symmetric domain walls have deceleration in the standard way. Also, anisotropic parameter is constant. Thus, constructed space-time stayed as anisotropic during its evolution. Also, Jerk, snap and lerk parameters are obtained for non-static plane symmetric domain walls. It is obtained that the model cannot allow de-Sitter dominated area. Also, energy conditions are satisfied for constructed model which is indicates stiff matter behavior. Also, SEC, WEC and NEC approach to zero with time. It is clearly seen from this study that domain walls cannot behave as dark energy in $\mathfrak{f}(\mathfrak{R},\mathfrak{T})$ theory for $\mathfrak{f}(\mathfrak{R},\mathfrak{T}) = \mathfrak{R} + 2h(\mathfrak{T})$ model. The study shows that given space-time does not allow expansion for selected $\mathfrak{f}(\mathfrak{R},\mathfrak{T})$ class.

References

Ade, P. A. R. et al. (2016), XIII. Cosmological parameters, A&A, 594, A13.

Adhav, K. S., Gadodia, P. S. and Bansod, A.S. (2011), Stiff domain walls in creation-field cosmology, Int. J. Theor. Phys., 50, 275-288.

Aditya, Y., Naidu, R. L. and Reddy, D. R. K. (2019), Non-vacuum plane symmetric universe in f (R) gravity, Result in Physics, 12, 339 - 343.

Allen, S. W. et al. (2004), Constraints on dark energy from Chandra observations of the largest relaxed galaxy clusters, Mon. Not. R. Astron. Soc., 353, 457.

Alam, S. et al. (2017), The clustering of galaxies in the completed SDSS-III Baryon Oscillation Spectroscopic Survey: cosmological analysis of the DR12 galaxy sample, Mon. Not. R. Astron. Soc., 470, 2617.

Aktaş, C., Yilmaz, İ., Aygün, M. and Demirel, C. (2007), Domain Wall Solutions With Quark Matter In Higher Dimensional Space-Times, AIP Conference Proceedings, 899, 137.

Buchdahl, H. A. (1970), Non-linear Lagrangians and cosmological theory, Mon. Not. Roy. Astr. Soc., 150, 1.

Bertolami, O., Bohmer, C. G., Harko, T. and Lobo, F. S. N. (2007), Extra force in f(R) modified theories of gravity, Phys. Rev. D, 75, 104016.

Bengochea, G. R. and Ferraro, R. (2009), Dark torsion as the cosmic speed-up, Phys. Rev. D, 79, 124019.

Capozziello, S., Cardone, V. F., Farajollahi, H. and Ravanpak, A. (2011), Cosmography in f(T) gravity, Phys. Rev. D, 84, 043527.

Carroll, S. M., Duvvuri, V., Trodden, M. and Turner, M. S. (2004), Is cosmic speed-up due to new gravitational physics?, Phys. Rev. D, 70, 043528.

Collins, C. B., Glass, E. N. and Wilkinson, D. A. (1980), Exact spatially homogeneous cosmologies, Gen. Relativ. Gravit., 12, 805-823.

Deb, D., Rahaman, F., Ray, S. and Guha, B. K. (2018), Strange stars in f(R, $\mathcal{T}$) gravity, JCAP, 03, 044.

Felice, A. D. and Tsujikawa, S. (2010), f(R) theories, Living Rev. Relativ., 13, 3.

Harko, T., Lobo, F.S.N., Nojiri, S. and Odintsov, S.D. (2011), *f(R,T)* gravity, Phys. Rev. D, 84, 024020.

Hill, C. T., Schramm D. N. and Fry, J. N. (1989), Comments, Nucl. Part. Phys., 19, 25.

Hu, W. and Sawicki, I. (2007), Models of f(R) cosmic acceleration that evade solar system tests. Phys. Rev. D 76, 064004.

Landau, L.D. and Lifshitz, E.M. (2002), The Classical Theory of Fields. Butterworth-Heinemann, Stoneham.

Martin, J. (2008), Quintessence: a mini-review, Mod. Phys. Lett. A, 23, 1252.

Moraes, P. H. R. S. (2014), Cosmology from induced matter model applied to 5D f(R, T) theory, Astrophys. Space Sci., 352, 273.

Naess, S. et al. (2014), The Atacama cosmology telescope: CMB polarization at 200< ℓ< 9000, JCAP, 1410 10.

Nojiri, S. Odintsov, S. D. and Sami M. (2006), Dark energy cosmology from higher-order, string-inspired gravity, and its reconstruction, Phys. Rev. D, 74, 046004.

Perlmutter, S. et al. (1999), Measurements of Ω and Λ from 42 High-Redshift Supernovae, Astrophys. J., 517, 565.

Rudra, P. (2015), Does f (R, T) gravity admit a stationary scenario between dark energy and dark matter in its framework?, Eur. Phys. J. Plus, 130, 66.

Sahoo P. and Reddy R. (2018), LRS Bianchi type-I bulk viscous cosmological models in f (R, T) gravity, Astrophysics, 61, 153-162.

Seprgel, D. N. et al. (2003), First Year Wilkinson Microwave Anisotropy Probe (WMAP) Observations: Determination of Cosmological Parameters, Astrophys. J. Suppl. Ser., 148, 175.

Shabani, H., Farhoudi, M. (2014), Cosmological and solar system consequences of f(R,T) gravity models, Phys. Rev. D 90, 044031.

Shabani, H. and Ziaie, A. H. (2018), nterpretation of f(R,T) gravity in terms of a conserved effective fluid, Int. J Mod. Phys. A, 33 1850050.

Sharif, M. and Kausar, H. R. (2011), Dust Static Spherically Symmetric Solution in f(R) Gravity, J. Phys. Soc. Jpn., 80, 044004.

Sharif, M. and Siddiqa, A. (2017), Study of charged stellar structures in f(R, T) gravity, Eur. Phys. J. Plus, 132, 529.

Singh, C. P. and Kumar, P. (2014), Friedmann model with viscous cosmology in modified f(R ,T) gravity theory, Eur. Phys. J. C, 74, 3070.

Sotiriou T.P. and V. Faraoni (2010), f(R) theories of gravity, Rev. Mod. Phys., 82, 451.

Starobinsky, A. A. (2007), Disappearing cosmological constant in f(R) gravity, J. Exp. Theor. Phys. Lett., 86, 157.

Tegmark, M. et al. (2004), Cosmological parameters from SDSS and WMAP, Phys. Rev. D, 69, 103501.

Vilenkin, A. (1983), Gravitational field of vacuum domain walls, Phys. Lett. B, 133, 177.

Visser, M. (2004), Jerk, snap and the cosmological equation of state, Class. Quant. Gravit., 21, 2603.

Zaregonbadi, R., Farhoudi, M. and Riazi, N. (2016), Dark matter from f(R,T) gravity, Phys. Rev. D, 94, 084052.

Zeldovich, Y. B., Kobzarev, I. Y. and Okun, L. B. (1975), Cosmological consequences of spontaneous violation of discrete symmetry, Sov. Phys. JETP., 40, 1.

Zubair, M., Abbas, G. and Noureen, I. (2016), Possible formation of compact stars in f(R, T) gravity, Astrophys. Space Sci., 361, 8.

Chapter 10

DEVELOPMENT OF DIAGNOSTICS FOR HUMAN-PATHOGENIC VIRUSES: ELECTROCHEMICAL BIOSENSOR APPLICATIONS

Gulsah CONGUR [1 2]

1 Bilecik Seyh Edebali University, Vocational School of Health Services, 11230 Bilecik, Turkey
2 Bilecik Seyh Edebali University, Biotechnology Application and Research Center, 11230, Bilecik, Turkey
* Corresponding author: gulsah.congur@bilecik.edu.tr, gulsah.congur@gmail.com, gulsah.congur@hotmail.com, Tel: +90 228 214 18 28, Fax: +90 228 214 13 72
ORCID: https://orcid.org/0000-0002-0599-0993

1. Introduction

Diseases caused by human-targeted viruses are one of the big problems of countries' health care systems. Humanity has been struggling with the viruses and tried to survive during all history. Most of the world lives in a high-tech environment, but we don't have the ability to fight and eradicate against most of these small beings-viruses. They caused several diseases, some of them like herpes labialis can be cured but viral diseases are mostly devastating and damaging for human health. When they find the host organism, they can spread and settle easily. Therefore, their fast and reliable diagnosis has high importance to prevent or to minimize their effects.

Electrochemical biosensors are sensitive, selective, quick and labor-friendly diagnostic platforms (Naresh et al. 2021:21; Imran et al. 2021:12; Yang et al., 2021:3). They have also miniaturizable structure. Thus, health care system has a big potential in terms of application of electrochemical biosensors for diagnosis of several vital diseases including viral diseases.

In this chapter, the principles of designing an electrochemical biosensor and new generation diagnostic tools developed by using electrochemical biosensors are presented. Different types of viruses and viral diseases and their electrochemical biosensor applications are also given.

1.1. The Principles of Designing An Electrochemical Biosensor

An electrochemical biosensor consists of a working electrode (WE), a counter electrode (CE) and a reference electrode (RE). This electrode system is called as three-electrode system. During the electrochemical measurements, this system is interconnected with a potentiostat. Electrical conductivity is achieved by performing the measurements into a buffer solution. The electrochemical reactions are performed on the WE and conductive, robust, having high surface area, cheap and easy-to-use WEs are always desirable. The RE provides a stable cell potential and all measurements are performed against the potential value determined by the RE and the electrical conductivity of the electrochemical cell is provided by the CE which has a high conductive structure without interruption. This is a basic electrochemical cell design. On the other hand, the modification of the WE determines that whether this design is a biosensor or a sensor. When a WE modified with a specific biological molecule such as a nucleic acid, enzyme, protein etc., the target analyte can be specifically detect using the biomolecular interaction occurred between the biomolecule (called as bioreceptor) and the target analyte. Then, this interaction is recognized by electrochemical measurements which is resulted the construction an electrochemical biosensor. There are several WE, CE and RE types such as carbon electrodes and metal electrodes as WE, Ag/AgCl electrode and

calomel electrode as RE, carbon electrode and platinum electrode as CE. Also, there are several electrochemical methods including voltammetric and impedimetric techniques (Erdem, 2007:74; Pohanka, 2020:15; Aamri et al., 2020:10).

Under the light of the information represented above, it is aimed to give an overview to the audience about what is an electrochemical biosensor and how can anyone who interested in this area design it. The details will be explained in sections and examples.

1.2. Viral diseases

Viruses are pathogenic beings and they have not metabolic activites without their host organisms. Thus, they do not replicate themself or encode their genetic information by themself. A virus contains genomic information into DNA or RNA surrounded by a protein-structured capsid and a virus (especially animal virus) is mostly surrounded a lipid-structured envelope. The encoding process of viruses depends on their entry into the host cell. After enty into the host cell, they can easily replicate themself or produce their proteins. Viral genome and the proteins are then packaged into virions and they are released from the cell by using different cellular processes such as lysis or exocytosis. The capsid and envelope contains many receptor proteins and they help to recognize and penetrate the host cell. When a viral infection occurs, the host organism produces an immune response and antibodies in order to recognize the antigen and destroy it. Vaccines and therapeutic agents are usually designed based on this immune response (Araf et al., 2021:18; Yuki et al., 2020:215; Yamauchi et al., 2013:126).

Most of the electrochemical biosensor designs for detection of viruses or viral diseases are rely on the specific interaction between the antigenic protein of viruses and the antibody produced from the host cell. The antibody is immobilized at the surface of the WE and the biointeraction between the antibody and the antigen is monitored by using electrochemical techniques. Most devastating viral diseases for humans and their electrochemical biosensor applications are presented in further sections.

1.1.2. Electrochemical Biosensors Developed For Detection of Human Immunodeficiency Virus (HIV)

HIV is a lentivirus and caused an incurable disease for humans, acquired immunodeficiency syndrome (AIDS) (Farzin et al., 2020:206). HIV was identified at the beginning of 80s and the following years AIDS was diagnosed (Emini, 2002; Montagnier, 2002:298). AIDS is global threaten factor for humanity, almost 1 million people died by AIDS related symptoms till 2018 (Farzin et al., 2020:206). The most appropriate

treatment of this disease is early diagnosis and then to start to apply suitable agents such as antiviral drugs (Wang et al., 2015:7). The analysis platforms designed by using electrochemical biosensors are able to detect the disease in a sensitive and selective way and help to early diagnose. Therefore, different electrochemical biosensor designs have been introduced in the literature for fast and reliable diagnosis of HIV. HIV protein 24 (p24) is one of the target molecule for these designs. Kheiri and coworkers developed an amperometric immunosensor for detection of p24 antigen (Kheiri et al., 2011:26). They used gold electrode (GE) as the WE and formed a nanostructure film for sensitive detection of p24. First, GE was polished using an alumina powder and rinsed in double distilled water. Then, GE was sonicated into acetone and double distilled water to complete cleaning step and GE was ready to use. Gold nanoparticle (GNP)/ amino functionalized carbon nanotube (CNT)/ acetone extracted propolis (AEP) film was prepared and immobilized at the surface of GE. After nanofilm was constructed onto the surface of GE, modified GE was immersed into biotinylated polyclonal p24 antibody solution during 12 h. After washing, streptavidin–horseradish peroxidase (HRP) conjugate was immobilized at the surface of GE. GE was incubated with bovine serum albumin (BSA) during 1 h to block unspecific bindings. Finally, HRP–streptavidin–biotin–anti-p24 Ab/GNP/CNT/AEP could be fabricated. The interaction between hydrogen peroxide and HRP was occuured and there was a detectable oxidation signal measured by amperometry. This signal was obtained in the absence and presence of p24 molecule, and the differences between the signals indicated the specific detection of p24. The electrochemical characterization of the nanostructured GE was performed using cyclic voltammetry (CV) and electrochemical impedance spectroscopy (EIS) technique. Selectivity of the biosensor was tested against glycine, glucose, α-fetoprotein, BSA, hepatitis B surface antigen (HBs Ag) and prostate specific antigen (PSA). The detection was also investigated in human serum samples.

Giannetto et al. (2017:7) carbon nanotube/chitosan based electrochemical immunosensor for detection of p24. Carboxyl-functionalized single-walled carbon nanotubes modified screen printed electrode (SPE) was used as the biosensor platform and modified with chitosan (CS). After then, glutaraldehyde was coated onto the surface of the biosensor to provide activation of amine groups of CS. p24 was immobilized at the surface of the biosensor during 1 h and overnight and blocking treatment was done by using α-casein. Immunocompetition was performed by interaction of immobilized p24 and a solution containing p24 and p24 specific antibody. When p24 concentration increased, antibody bound with the biosensor surface decreased. Then, secondary enzyme conjugated antibody was

immobilized at the surface of the biosensor and finally, the enzymatic reaction was performed in the presence of hydroquinone diphosphate which had an electroactive structure. Amperometric measurements were performed and the selective determination of p24 was achieved against BSA, carcinoembryonic antigen and carbohydrate antigen 125. The detection limit (DL) of p24 was found to be 2 pM in human serum.

In another study reported by Gan et al. (2013:6) electrochemical p24 detection was performed. For this purpose, HRP enzyme–antibody copolymer was firstly synthesized, then the incubation was done in the presence of the secondary antibody of p24. Gold nanocolloids were immobilized at the surface of the biosensor platform and the immunoreaction occurred between the capture probe constituted of silicon dioxide-coated magnetic Fe_3O_4 nanoparticles and p24. After then, a magnet was placed under the electrode to immobilize the immunocomplex and o-hydroxyl phenol (HQ) and H_2O_2. DL was estimated as 0.5 pg/mL by using this biosensor design and selectivity of the biosensor was studied in the presence of several interference factors as HIV gp 36 protein, HIV gp 160 protein, HIV antibody and human IgG. The detection of p24 using this biosensor was investigated in different human serum samples.

HIV p17 protein was also detected using electrochemical immunosensors (Cerrutti et al., 2015:71). Although they have a potential to detect the target analyte in sensitive and selective behavior, the fabrication of them depends on implementing exhaustive experimental procedures and using intensive chemical agents. In addition, antibody production requires to do animal experiments.

The detection of HIV is also possible by performing direct determination of HIV genome (Shamsipur et al., 2019:1055; Gong et al., 2017:89; Wang et al., 2015:7). As an example, Gong et al. (2017:89) used glassy carbon electrode (GCE) for fabrication of a DNA biosensor to monitor biomonitoring of HIV. To improve the sensitivity and selectivity of the biosensor, they modified GCE by using graphene-nafion composite film. They immobilized single stranded DNA which was specific for the target DNA of HIV and named as capture probe. In the presence of the full-matched DNA target, unique double stranded DNA could form whereas double stranded form could not be observed in the presence of one-base, two-base or three-base mismatched DNA. Before/after each modification/immobilization step, EIS measurements were performed to monitor changes at the charge transfer resistance value (R_{ct}) occurred electrode/electrolyte interface. DL was calculated as $2.3x10^{-14}$ M. An another impedimetric detection platform was introduced by the same group for detection of HIV gene (Gong et al., 2015:7). Wang et al. (2015:7) also used GCE to construct a DNA biosensor for detection of HIV DNA. They firstly synthesized

graphene stabilized gold nanoclusters (GR/AuNCs) and modified GCE using GR/AuNCs. In following experiments, they immobilized a capture probe to capture the target DNA molecule. The hybridization between DNA target and its capture probe was performed in the presence of exonuclease III. The measurements were done in methylene blue solution which is an electrochemical indicator for detection of full-match hybridization. The selectivity of the biosensor was tested against single-base mismatched and four-base mismatched DNA sequences.

1.1.3. Electrochemical Monitoring of Influenza Virus

Influenza A and B viruses (IAV and IBV, respectively) have the potential of causing pandemic diseases. H1N1, H2N2, H3N2, H5N1 and H7N9 are the pandemic diseases caused by IAVs. In addition, seasonal influenza can also be a threaten factor for human health (Li et al., 2020). Therefore, sensitive and selective detection of influenza virus has been an attractive topic for the researchers.

Park et al. (Park et al., 2021:14) developed an electrochemical biosensor which was composed of multifunctional DNA four-way junction (4WJ) and carboxyl molybdenum disulfide (carboxyl-MoS_2) for detection of H1N1 virus. The DNA 4WJ contained a recognition part, signal amplification part and tail group and constructed onto a silicon substrate. The recognition part was a DNA aptamer for specific detection of hemagglutinin which is the biomarker for H1N1 disease. The sensitivity of the biosensor increased by using carboxyl-MoS_2 hybrid material. The electrochemical and microscopic characterization of the biosensor surface was performed. The DL was found to be 10 pM and the selectivity of the biosensor was tested against H5N1, hemoglobin, myobglobin and CRP. It was concluded that the developed biosensor could be detected H1N1 in a sensitive and selective way.

In another study reported by Ravina and coworkers (Ravina et al., 2020:98), cysteine coated screen-printed gold electrode was used for fabrication of an electrochemical genosensor for H1N1 swine flu) in human respiratory nasal swabs. A DNA probe specific for haemagglutinin (HA) gene was immobilized at the surface of the electrode and the probe was labelled with amine group at 5′ end. Nucleic acid hybridization was done at the electrode surface, and the hybridization was detected using an electroactive indicator, methylene blue (MB). Differential pulse voltammetry (DPV) measurements were performed to monitor the oxidation signal of MB. Based on this strategy, the target DNA sequence was selectively and sensitively detected. The DL was estimated as 0.002 ng/6 µL and the selectivity of the biosensor was tested against *S. typhi, S. pyogenes* and *N. meningitidis*.

Bhardwaj et al. developed an electrochemical paper biosensor for rapid detection of air borne influenza virus (Bhardwaj et al., 2020:54). They developed two detection strategies. First, they used monoclonal hemagglutinin specific antibodies. They treated the virus samples with Triton X to prepare virus lysate and sent this lysate on the horseradish peroxidase tagged monoclonal antibody immobilized conjugate pad using a flow injection system. Then, this complex were bound onto the gold electrode as working electrode. In the second strategy, monoclonal and polyclonal antibodies were used together and immobilized at the surface of conjugate pad. The virus sample was prepared as aerosol and concentrated with an electrostatic particle concentrator (EPC). The interaction was performed using virus samples without lysate preparation. The specific biointeraction between hemagglutinin and the antibodies was detected using EIS technique. The DL value was found to be 2.13 PFU/mL and the detection methodology was implemented in the presence of different interference factors as adenovirus, MS2 and *P. fluorescens*.

An impedimetric immunosensor was reported by Dunajova et al. for detection of influenza A (Dunajová et al., 2020:858). Screen printed carbon electrode (SPE) was used as the biosensor platform. The SPEs were chemically cleaned before to use. Then, chemical activation of the SPEs was done using N-hydroxysuccinimide (NHS) and N-3-(dimethylaminopropyl)-N′-ethylcarbodiimide hydrochloride (EDC). Then human serum albumin (HSA) or bovine serum albumin (BSA) was immobilized at the electrode surface and virus nucleoprotein specific antibody was then immobilized. The biointeraction between the antibody and nucleoprotein was monitored using EIS technique. The changes at the R_{ct} value was evaluated in terms of the specific detection. The DL value was estimated as 0.79 fM.

1.1.3. Electrochemical Biosensor Applications for Detection of Hepatitis Viruses

Hepatitis virus infections related diseases have a huge mortality potential and threat global public health. The reported number of deaths per year is frightening. Every year about 1.5 million people died of hepatitis virus infections. There are A, B, C, D and E types of hepatitis virus and researches about investigation of other types of hepatitis virus have been continued (Shi et al., 2021:56). Considering the mortality of the infections, the specific and sensitive detection of the target hepatitis virus is crucial for our modern life.

Srisomwat and coworkers fabricate a paper-based electrochemical biosensor for detection of Hepatitis B virus (HBV) (Srisomwata et al., 2020:316). They printed the three-electrode system onto paper sample using wax printing technique. They synthesized a pyrrolidinyl peptide nucleic acid

(acpcPNA) as the capture probe and immobilized at the paper surface. The nucleic acid hybridization between the capture probe and target HBV DNA was monitored using DPV technique in the presence of hexacyanoferrate (III)/(II) couple. The selectivity of the biosensor was tested in the presence of one-mismatched, two-mismatched DNA sequences and non-complementary DNA sequences. The DL was reported as 1.45 pM.

Hepatitis E virus genotype 3 (HEV3) was detected using an electrochemical genosensor developed by Ngo et al. (Ngo et al., 2021:413). Streptavidin coated magnetic beads were used for immobilization of capture DNA probe which was designed for specific recognition of target HEV3 DNA. After nucleic acid hybridization between capture probe and target DNA at the surface of magnetic beads, separation was done using a magnetic field. Then, a reporter probe tagged with a quantum dot was added and again nucleic acid hybridization was performed. The hybridized form was chemically separated and square wave anodic stripping voltammetry measurements were performed. 1.23 fM concentration level was reported as the DL value and the biosensor had a good selectivity against non-complementary and mismatched DNA sequences and IBV and IAV DNA sequences. The applicability of the biosensor was shown by performing the detection route in spiked sample.

Rahmati et al. reported an impedimetric aptasensor for sensitive detection of core antigen of hepatitis C virus (Rahmati et al., 2021:22). They prepared 3D-$NiCo_2O_4$ nanowires to improve the selectivity of the biosensor and immobilized these nanowires at GCE surface. Then, they immobilized HCV antigen specific DNA aptamer at the biosensor surface and monitored the biointeraction between the aptamer and the target molecule by EIS technique. They found DL as 0.16 fg/mL and investigated the selectivity against human chorionic gonadotropin, progesterone, trypsin, histidine and hepatitis B virus core antigen.

1.1.4. Electrochemical Coronavirus Biosensors

Coronaviruses (CoVs) are the most well-known viruses in today's world since the global SARS-CoV-2 epidemic emerged. They have single stranded RNA molecule which contains the genome and a membrane envelope encapsulates this genomic material. CoVs have glycoproteins on the membrane and they have crownlike shape. The subfamily, *Coronavirinae* is divided into four genera as alpha, beta, gamma, and delta. Alpha and beta type CoVs infect humans and SARS-CoV-2 is a beta type coronavirus. CoVs have a big potential to cause epidemic/pandemic diseases including MERS-CoV, SARS-CoV and SARS-CoV-2 (Liu et al., 2020:6; Paul et al., 2021:4). Therefore, countless detection platforms have been reported for CoVs, including electrochemical biosensors.

Abad-Valle and coworkers (2005:20) were reported a design for an electrochemical biosensor platform for detection of SARS-CoV. They used a gold sputtering film as the working electrode and immobilized thiol labelled capture DNA probe at the working electrode surface. Nucleic acid hybridization was performed in the presence of the biotinylated SARS-CoV related target DNA sequence. Streptavidin alkaline phosphatase enzyme was then immobilized at biosensor surface and enzymatic reaction was done in the presence of α-naphthol or indigo carmine (IC). The DL values were estimated as 10^{-6} M and 7×10^{-6} M by using IC and α-naphthol substrates and SWV and CV techniques, respectively.

Molecularly imprinted polymers (MIPs) are new generation polymers which have a great potential for specific recognition of the target molecules (Karimi et al., 2016:27; Ji et al., 2015:66). Therefore, an MIP based electrochemical biosensors for detection of CoVs was reported by Raziq and coworkers (Raziq et al., 2021:178). They were studied for development of MIP based electrochemical biosensor for detection of SARS-CoV-2 antigen. First, they developed an MIP film which was specific for SARS-CoV-2 nucleoprotein (ncovNP). Then, they immobilized this film at the surface of a disposable sensor chip. The interaction between MIP film and ncovNP was determined using DPV technique in the presence of a redox couple. The DL was found to be 27 fM and the selectivity of the sensor was tested against S1, E2 HCV, BSA and CD48 proteins.

An electrochemical biosensor using a paper (ePAD) was reported by Yakoh et al. (Yakoh et al., 2021a:176) for detection of SARS-CoV-2. This ePAD was modified with graphene oxide to obtain enhanced biosensor response and to provide carboxyl groups at the surface of the ePAD. Then, spike protein receptor-binding domainof SARS-CoV-2 was immobilized at the surface of the ePAD and specific interaction between spike protein receptor-binding domainand SARS-CoV-2 antigen occurred. This specific interaction was detected using voltammetric and impedimetric techniques and a redox couple was used as the electrochemical indicator. 1 ng/mL DL for SARS-CoV-2 was achieved using this assay.

The detection of SARS-CoV-2 spike protein was performed using Cu_2O nanocube coated SPE (Yakoh et al., 2021b:188). The antibody of SARS-CoV-2 spike protein was immobilized at the electrode surface, then the biointeraction between the antibody and the antigen was monitored. The detection was achieved using EIS and CV techniques. The detection method was tested in artificial nasal, saliva and universal transport medium samples and the DL was found to be 0.04 fg/mL.

In another electrochemical biosensor design, rolling circle amplification (RCA) technique was applied for detection of SARS-CoV-2 S and N

genes (Chaibun et al., 2021:12). First samples were collected and RNA was extracted. Then, RCA was applied. RCA products containing S gene and N gene were immobilized at the surface of magnetic beads coated with specific capture probe. Nucleic acid hybridization was done and the samples were separated and transferred onto SPEs. The detection of the targets was achieved using DPV technique. The DLs of the N and S genes was determined as 1 copy/μL.

In this chapter, applications of the electrochemical biosensors into viral diagnostics area are explained by giving different biosensor designs for several viral diseases. The applications are not limited with this scope, it is expected the number of designed electrochemical biosensor for viruses or viral diseases will increase as new nanomaterials/biomaterials are used or innovative electrodes are developed.

REFERENCES

AAMRI M.E., YAMMOURI G., MOHAMMADI H., AMINE A., KORRI-YOUSSOUFI H. (2020) Electrochemical Biosensors for Detection of MicroRNA as a Cancer Biomarker: Pros and Cons, *Biosensors*, 10, 0186.

ABAD-VALLE P., FERNANDEZ-ABEDUL M.T., COSTA-GARCIA A. (2005) Genosensor on gold films with enzymatic electrochemical detection of a SARS virus sequence, Biosensors and Bioelectronics 20 2251–2260.

ARAF Y., ULLAH A., FARUQUI N.A., MOWNA S.A., PRIUM D.H., SARKAR B. (2021) Dengue Outbreak is a Global Recurrent Crisis: Review of the Literature, *Electronic Journal of General Medicine*, 18, em267.

BHARDWAJ J., KIM M.W., JANG J., (2020) Rapid Airborne Influenza Virus Quantification Using an Antibody Based Electrochemical Paper Sensor and Electrostatic Particle Concentrator, *Environmental Science and Technology*, 54, 17, 10700–10712.

CERRUTTI B.M., MORAES M.L., PULCINELLI S.H., SANTILLI C.V. (2015) Lignin as immobilization matrix for HIV p17 peptide used in immunosensing, *Biosensors and Bioelectronics*, 71, 420–426.

CHAIBUN T., PUENPA J., NGAMDEE T., BOONAPATCHAROEN N., ATHAMANOLAP P., O'MULLANE A.P., VONGPUNSAWAD S., POOVORAWAN Y., LEE S.Y. (2021) Lertanantawong B., Rapid electrochemical detection of coronavirus SARS-CoV-2, *Nature Communications*, 12, 802.

DUNAJOVÁ A.A., GÁL M., TOMČÍKOVÁ K., SOKOLOVÁ R., KOLIVOŠKA V., VANĚČKOVÁ E., KIELAR F., KOSTOLANSKÝ F., VAREČKOVÁ E., NAUMOWICZ M. (2020) Ultrasensitive impedimetric imunosensor for influenza A detection, Journal of Electroanalytical Chemistry, 858, 113813.

EMINI E.A., (2002) The Human Immunodeficiency Virus: Biology, Immunology, and Therapy, Princeton University Press., Princeton.

ERDEM A. (2007) Nanomaterial based electrochemical DNA sensing strategies, *Talanta*, 74, 318–325.

FARZIN L., SHAMSIPUR M., SAMANDARI L., SHEIBANI S. (2020) HIV biosensors for early diagnosis of infection: The intertwine of nanotechnology with sensing strategies, *Talanta*, 206, 120201.

GAN N., DU X., CAO Y., HU F., LI T., JIANG Q. (2013) An Ultrasensitive Electrochemical Immunosensor for HIV p24 Based on Fe_3O_4@SiO_2 Nanomagnetic Probes and Nanogold Colloid-Labeled Enzyme–Antibody Copolymer as Signal Tag, *Materials*, 6, 1255-1269.

GIANNETTO M., COSTANTINI M., MATTAROZZI M., CARERI M., (2017) Innovative gold-free carbon nanotube/chitosan based competitive immunosensor for determination of HIV-related p24 capsid protein in serum, *RSC Advances*, 7, 39970.

GONG Q., WANG Y., YANG H. (2017) A sensitive impedimetric DNA biosensor for the determination of the HIV gene based on graphene-Nafion composite film, *Biosensors and Bioelectronics*, 89, 565–569.

GONG Q., YANG H., DONG Y., ZHANG W. (2015) A sensitive impedimetric DNA biosensor for the determination of the HIV gene based on electrochemically reduced graphene oxide, *Analytical Methods*, 7, 2554–2562.

GONG, Q., WANG, Y., YANG, H. (2017) A sensitive impedimetric DNA biosensor for the determination of the HIV gene based on graphene-Nafion composite film, *Biosensors and Bioelectronics*, 89, 565–569.

IMRAN S., AHMADİ S., KERMAN K., (2021) Electrochemical Biosensors for the Detection of SARS-CoV-2 and Other Viruses, *Micromachines*, 12, 174.

JI J., ZHOU Z., ZHAO X., SUN J., SUN X. (2015) Electrochemical sensor based on molecularly imprinted film at Au nanoparticles-carbon nanotubes modified electrode for determination of cholesterol, *Biosensors and Bioelectronics*, 66, 590-595.

KARIMI M.A., RANJBAR M., AKBARPOOR M. (2016) Preparation of Magnetic Molecularly Imprinted Polymer Nanoparticles for Selective Adsorptionand Separation of b-Estradiol, *Journal of Cluster Science*, 27, 1067–1080.

KHEIRI F., SABZI R.E., JANNATDOUST E., SHOJAEEFAR E., SEDGHI H. (2011) A novel amperometric immunosensor based on acetone-extracted propolis for the detection of the HIV-1 p24 antigen, *Biosensors and Bioelectronics*, 26, 4457– 4463 2017.

LI Y., WANG L., SI H., YU Z., TIAN S., XIANG R., DENG X., LIANG R., JIANG S., YU F. (2020) Influenza virus glycoprotein-reactive human monoclonal antibodies, *Microbes and Infection*, 22, 263-271.

LIU C., ZHOU Q., LI Y., GARNER L.V., WATKINS S.P., CARTER L.P., SMOOT J., GREGG A.C., DANIELS A.D., JERVEY S., ALBAIU D. (2020) Research and Development on Therapeutic Agents and Vaccines for COVID-19 and Related Human Coronavirus Diseases, *ACS Central Science*, 6, 315−331.

MONTAGNIER L. (2002) A History of HIV Discovery, *Science*, 298, 1727–1728.

NARESH V., LEE N. (2021) A Review on Biosensors and Recent Development of Nanostructured Materials-Enabled Biosensors, *Sensors*, 21, 736.

NGO D.B., CHAIBUN T., YIN L.S., LERTANANTAWONG B., SURAREUNGCHAI W. (2021) Electrochemical DNA detection of hepatitis E virus genotype 3 using PbS quantum dot labelling, *Analytical and Bioanalytical Chemistry*, 413, 1027–1037.

PARK J.H., KIM J., KIM S.M., SOHN H., PARK C., KIM T., LEE J.H., LEE M.H., LEE T., (2021) Fabrication of Electrochemical Influenza Virus (H1N1) Biosensor Composed of Multifunctional DNA Four-Way Junction and Molybdenum Disulfide Hybrid Material, *Materials*, 14, 343.

PAUL D., KOLAR P., HALL S.G. (2021) A review of the impact of environmental factors on the fate and transport of coronaviruses in aqueous environments, *npj Clean Water*, 4, 7.

POHANKA M. (2020) Screen Printed Electrodes in Biosensors and Bioassays, A Review, *International Journal of Electrochemical Science,* 15, 11024–11035.

RAHMATI Z., ROUSHANI M., HOSSEINI H., (2021) Three-dimensional NiCo2O4 nanowires encapsulated in nitrogen-doped carbon networks as a high-performance aptamer stabilizer for impedimetric ultrasensitive detection of hepatitis C virus core antigen, *Surfaces and Interfaces*, 22, 100813.

RAVINA, DALAL A., GILL P.S., NARANG J., PRASAD M., MOHAN H., (2020) Genosensor for rapid, sensitive, specific point-of-care detection of H1N1 influenza (swine flu), Process Biochemistry, 98, 262–268.

RAZIQ A., KIDAKOVA A., BOROZNJAK R., REUT R., OPIK A., SYRITSKI V. (2021) Development of a portable MIP-based electrochemical sensor for detection of SARS-CoV-2 antigen, *Biosensors and Bioelectronics*, 178, 113029.

SHAMSIPUR M., SAMANDARI L., TAHERPOUR A., PASHABADI A. (2019) Sub-femtomolar detection of HIV-1 gene using DNA immobilized on composite platform reinforced by a conductive polymer sandwiched between two nanostructured layers: A solid signal amplification strategy, *Analytica Chimica Acta*, 1055, 7–16.

SHI Y., DU L., LV D., LI Y., ZHANG Z., HUANG X., TANG H. (2021) Emerging role and therapeutic application of exosome in hepatitis virus infection and associated diseases, *Journal of Gastroenterology*, 56, 336–349.

SRISOMWATA C., TEENGAMA P., CHUAYPEN N., TANGKIJVANİCH P., VILAIVAN T. (2020) Orawon Chailapakula, Pop-up paper electrochemical device for label-free hepatitis B virus DNA detection, *Sensors and Actuators: B. Chemical*, 316, 128077.

WANG Y., BAI X., WEN W., ZHANG X., WANG S. (2015) Ultrasensitive electrochemical biosensor for HIV gene detection based on graphene stabilized gold nanoclusters with exonuclease amplification, *ACS Applied Materials and Interfaces*, 7, 18872–18879.

YAKOH A., PIMPITAK U., RENGPIPAT S., HIRANKARN N., CHAILAPAKUL O., CHAIYO S. (2021a) Paper-based electrochemical biosensor for diagnosing COVID-19: Detection of SARS-CoV-2 antibodies and antigen, *Biosensors and Bioelectronics*, 176, 112912.

YAKOH A., PIMPITAK U., RENGPIPAT S., HIRANKARN N., CHAILAPAKUL O., CHAIYO S. (2021b) Electrochemical immunosensor with Cu2O nanocube coating for detection of SARS-CoV-2 spike protein, *Microchimica Acta*, 188, 105.

YAMAUCHI Y., HELENIUS A. (2013) Virus entry at a glance, *Journal of Cell Science*, 126, 1289–1295

YANG A., YAN F. (2021) Flexible Electrochemical Biosensors for Health Monitoring, *ACS Applied Electronic Materials,* 3, 53–56.

YUKI K., FUJIOGI M., KOUTSOGIANNAKI S. (2020) COVID-19 pathophysiology: A review, *Clinical Immunology*, 215, 108427.

Chapter 11

IN SILICO ANALYSIS OF BIOSEQUENCE SIMILARITIES

Nergiz SOYUPAK[1]

Çağın KANDEMİR-ÇAVAŞ[2]

1 Bilgisayar Bilimleri, Dokuz Eylül Üniversitesi Fen Bilimleri Enstitüsü 35400 Buca/İZMİR, nrgzsypk@gmail.com

2 Bilgisayar Bilimleri, Dokuz Eylül Üniversitesi Fen Fakültesi 35400 Buca/İZMİR, cagin.kandemir@deu.edu.tr

ABSTRACT

Bioinformatics has emerged as a strategic field on the border between biology and computer science, affecting medicine, biotechnology and society in many ways. In other words, it is the science of compiling and analyzing complex biological data. Sequence similarity analysis that plays an significant role in the improvement of biology studies and bioinformatics is used in the prediction of protein structure and in the researches of similarity between species. This study explains the method of performing image texture analysis using gray level co-occurrence matrix (GLCM). The sequences we use can calculate a matrix of similarity distance and computed some features. These features such as entropy, energy, correlation, contrast and homogeneity can help us see differences and similarities to species. This method can compute all of these features in each order. According to the results obtained, comments can be made about the similarity between species and new discoveries can be enabled by combining biology and computer science.

Keywords: Bioinformatics, Computer science, GLCM, Sequence similarity

INTRODUCTION

DNA (deoxyribonucleic acid) is the genetic substance which isa extremely powerful statement to molecular biologists. The organization of lifeless molecules into functioning, living cells, growth and reproduction allows by DNA. To give an example the person's curly hair of her/him mother and blue eyes of her /him father will be inherit which is a direct result. The varied units that control those characteristics at the genetic level which is be chemical compound are named genes. Genes contain their information as a specific sequence of nucleotides found in DNA molecules on their own. Guanine, Adenine, Thymine and Cytosine (G, A, T and C) are only four distinct bases which are used by DNA molecules. Their similarity may depend on how these letters are characterized. The traditional algorithm for similarity analysis of DNA sequences is alignment-based measurement. [5].

The attempt to use computer applications in biology, which began in the 1960s, has progressed rapidly in parallel with technological developments in both fields, and thus the emerging Bioinformatics branch has become one of the most popular academic and industrial sectors today.

The field of bioinformatics is the synthesis of the fields of mathematics, statistics, computer science, molecular biology and genetics in order to make sense, storage, visualization of biological data and make the most of this enormous knowledge. Another definition is the science of compiling and analyzing complex biological data.

A computer-based method for finding similarities in the amino acid sequences of two proteins has been improved. From these findings it is possible to decide whether substantial homology exists among the proteins. This knowledge is used to track their possible evolutionary improvement of proteins [8].

One of the most well-known texture analysis implements in the computation of image features is Gray Level Co-Occurence Matrices (GLCM). These texture properties are known for their use in image classification and segmentation. [9].

Texture analysis methods are widely used in the analysis and interpretation of medical images. Texture is a composition of statistical attributes of pixel density which is compares gray level differences between two different pixels at different locations. Texture features can be calculated using co-occurance matrices.

Gray Level Co-Occurrence Matrix (GLCM)

M. Haralick proposed to GLCM extraction method which is used to extract the property of a grayscale image. GLCM defines the relationship between two adjacent pixels. First pixel is known as the reference pixel and the second is named the adjacent pixel. The distribution in the matrix is set according to the distance and angle between pixels. This matrix is a square matrix, where each element of the matrix d represents the number of occurrences of the i and j pixel-valued pairs. In addition to the distance between pixels, it is necessary to know the orientation of the pairs of pixels. The most common known aspects are ϑ = 0, 45, 90, 135 (horizontal: 0°, diagonal: 45°, vertical: 90°, and antidiagonal: 135°) and their symmetric analogs. [4-5]

GLCM is known as a popular method in order to use in texture image segmentation. [5] Some texture features are calculated from a GLCM [3].This features called as the Haralick properties which is calculated from the GLCM were used for both supervised and unsupervised segmentation. These properties were calculated for 5 characteristics including contrast, correlation, energy, homogeneity and entropy. [7] Entropy is one of the few commonly used GLCM properties for unchecked partitioning.[5] GLCM is normalized before calculation and then the DNA sequence is calculated based on the digital vector and the co-occurence matrix. These properties were also used to analyze DNA sequences.

MATERIALS AND METHODS

GLCM has been used in many studies to differentiate and classify different images. We applied this mentioned theory to DNA sequence similarity analysis in this study. This method is different from sequence alignment where a realignment is needed when a sequence is compared to each different sequence. It must calculate these properties only once. The properties in each sequence are calculated independently of the other sequences. No further sequences are needed when processing sequences and calculating properties.

There are three steps in our method:

1. Definition and calculation of the co-occurrence matrix of the DNA sequence,

2. Converting the DNA sequence into a digital vector,
3. Calculation of a matching matrix of DNA sequence and calculation and formation of tissue features for each sequence

In this method, the integers 1, 2, 3 and 4 are used first to refer to nucleotides A, C, G and T respectively. Secondly, the numbers referring these nucleotides are added to the sequence number in which they are located. Because the character makes the same digital vector distinct in different places and it assigns a unique digital vector for each DNA sequence. Finally, the co-occurrence matrix for each DNA sequence is calculated based on the digital vector. For instance, the transformed digital code of the CGACTCGAT sequence is (3, 5, 4, 6, 9, 8, 10, 9, 13). Then the GLCM is (1 x n) in size on this digital vector and is calculated as follows. (***Figure 1)*** This co-occurrence matrix is use to calculate the Haralick features of each sequence. The mathematical equations of these features are as follows. Gray level co-occurrence matrix are in a certain direction and a pair of gray level pixel matrix that expresses the frequency of occurrence relative to each other a certain distance between them.

Formulas we use to describe the features such as entropy, contrast, energy and homogeneity of the DNA sequence is as follows;

$$Entropy = -\sum_{i=1}^{L}\sum_{j=1}^{L} p(i,j)\ln\big(p(i,j)\big),$$

$$Contrast = \sum_{i=1}^{L}\sum_{j=1}^{L} (i-j^2)\, p(i,j),$$

$$Energy = \sum_{i=1}^{L}\sum_{j=1}^{L} p(i,j^2)\,,$$

$$Homogeneity = \sum_{i=1}^{L}\sum_{j=1}^{L}, \left(\frac{p(i,j)}{1+|i-j|}\right),$$

where *L* is the number of gray levels in the image, *p(i,j)* is the *(i,j)* th element in the normalized GLCM; it is the combined probability occurrence that a pixel with value *i* is adjacent to a pixel with value *j* .

The formula we use to describe the correlation of the DNA sequence is as follows;

$$Correlation = \sum_{i=1}^{L}\sum_{j=1}^{L}, \left(\frac{(i-\mu_i)(j-\mu_j)p(i,j)}{\sigma_i\sigma_j}\right),$$

where μi , μj , σi , and σj are the means and standard deviations of *p i* and *p j* , the partial probability density functions.

Since the sequences used in this study are in .txt format, they are converted to 2D grayscale image format with the help of MATLAB program. The sequences used in the application consist of DNA nucleotides containing adenine, guanine, cytosine and thymine of each species. These sequences are first extracted from the file with the help of MATLAB and converted into digital vector. The GLCM matrix is then converted from the character format to the numerical format. Contrast, correlation, energy, homogeneity and entropy can be calculated from the grayscale matrix to see the similarity between the species. (***Figure 2-3***)

SJ =

[1 3 2 4 7 6 8 7 10]

glcm1

	1	2	3	4	5	6	7	8	9	10
1	0	0	1	0	0	0	0	0	0	0
2	0	0	0	1	0	0	0	0	0	0
3	0	1	0	0	0	0	0	0	0	0
4	0	0	0	0	0	0	1	0	0	0
5	0	0	0	0	0	0	0	0	0	0
6	0	0	0	0	0	0	0	1	0	0
7	0	0	0	0	0	1	0	0	0	1
8	0	0	0	0	0	0	1	0	0	0
9	0	0	0	0	0	0	0	0	0	0
10	0	0	0	0	0	0	0	0	0	0

Figure 1

```
A=[3 2 5 7 4 2 8 9 12 14 17 21 22 25 28]
B=[5 2 3 4 4 2 6 9 12 14 15 20]
C=[1 4 5 6 6 1 3 8 12 15 18]


[glcm1,SA] = graycomatrix(A,'NumLevels', 10, 'GrayLimits',[])
[glcm2,SB] = graycomatrix(B,'NumLevels', 10, 'GrayLimits',[])
[glcm1,SC] = graycomatrix(C,'NumLevels', 10, 'GrayLimits',[])


stats=graycoprops(glcm1)
stats=graycoprops(glcm2)
stats=graycoprops(glcm3)
J=entropy(glcm1)
P=entropy(glcm2)
S=entropy(glcm3)
```

Figure 2

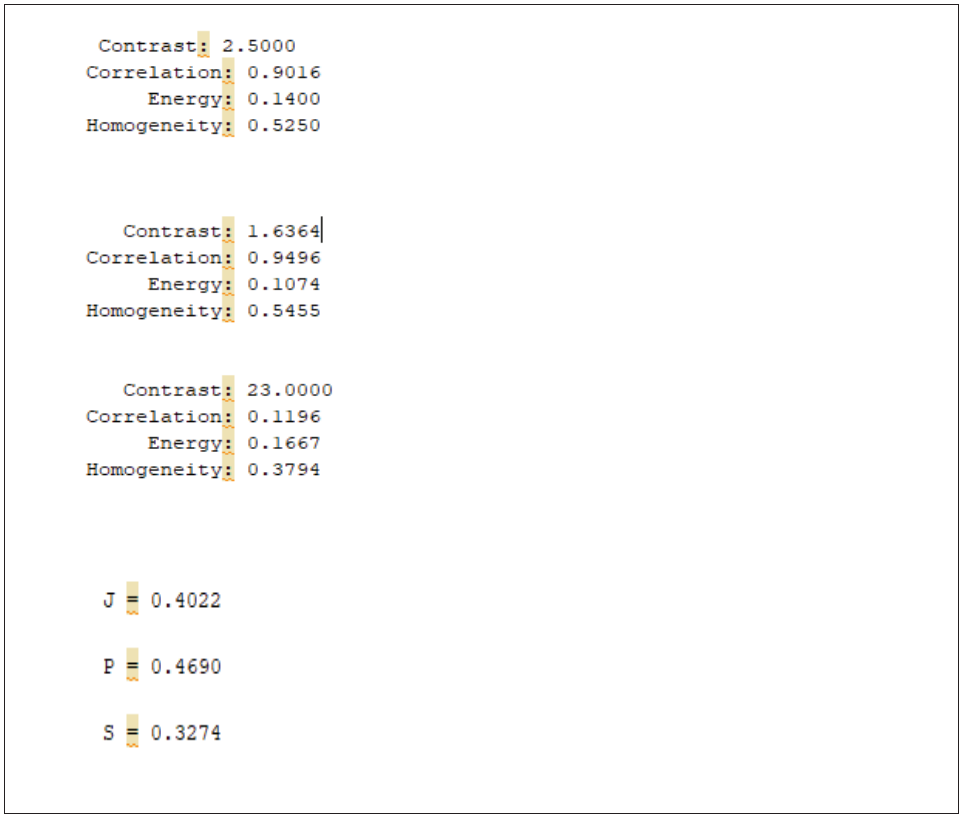

Figure 3

APPLICATION

We tested our method with three species and using DNA sequences of them . The co-occurrence matrix was calculated after transforming the DNA sequence to digital vectors for each DNA sequence. Each value in this matrix is the gray level of each pixel. SJ Matrix is the figure out gray-level co-occurrence matrix for the digital vector. The values in the GLCM are the number of horizontally adjacent pixels with a specified gray level. For example, in the application of *Mus musculus superoxide dismutase* has the first value (1 x 1) is 5 in the GLCM; it means that five pixel with a gray level of 1 consists in SJ Matrix horizontally adjacent elements another pixel with a gray level of 1.

Accordingly, the previously defined five properties were computed for each sequence depend on the co-occurrence matrix of each sequence.

***Mus musculus* superoxide dismutase 1:**
CAGACTCAGGCCTATAAAAGCTCCGTGGCGCCAGGGCCTCGTTTTTTTGCGCGGT
CCTTT

Digital vector:

[3 3 6 5 7 10 9 9 12 13 13 14 17 15 19 17 18 19 20 23
23 26 25 26 28 30 30 31 31 33 33 34 34 37 38 39 39 40 43 42
44 46 47 48 49 50 51 52 52 52 54 54 56 57 59 58 59 62 63 64]

SJ Matrix:

[1 1 1 1 1 2 1 1 2 2 2 2 3 2 3 3 3 3 3 4
4 4 4 4 5 5 5 5 5 5 5 6 6 6 6 6 6 7 7 7
7 8 8 8 8 8 8 9 9 9 9 9 9 9 10 10 10 10 10 10]

GLCM:

5 2 0 0 0 0 0 0 0 0
1 3 2 0 0 0 0 0 0 0
0 1 4 1 0 0 0 0 0 0
0 0 0 4 1 0 0 0 0 0
0 0 0 0 6 1 0 0 0 0
0 0 0 0 0 5 1 0 0 0
0 0 0 0 0 0 3 1 0 0
0 0 0 0 0 0 0 5 1 0
0 0 0 0 0 0 0 0 6 1
0 0 0 0 0 0 0 0 0 5

Contrast: 0.2203

Correlation: 0.9884

Energy: 0.0687

Homogeneity: 0.8898

Entropy: 0.7415

Human superoxide dismutase 1:

GCGCGGAGGTCTGGCCTATAAAGTAGTCGCGGAGACGGGGTGCTGGTTTGCGTCG
TAGTC

Digital Vector:

[4 4 6 6 8 9 8 11 12 14 13 16 16 17 17 18 21 19 23 21
22 23 26 28 26 29 31 30 32 32 34 35 34 37 36 38 40 41 42
43 45 45 45 48 48 49 51 52 53 53 53 55 57 56 58 60 58 61
63 62]

SJ Matrix:

[1 1 1 1 1 2 2 2 2 3 3 3 4 4 4 5 4 5 5 6 5 6 6 6 7 7 7 7 7 8 8 9 9 9 9 10 9 10 10 10 11 11 11 11 12 12 12 13 13 13 13 13 14 14 15 14 15 15 15 15]

GLCM:

4	1	0	0	0	0	0	0	0	0	0	0	0	0	0
0	3	1	0	0	0	0	0	0	0	0	0	0	0	0
0	0	2	1	0	0	0	0	0	0	0	0	0	0	0
0	0	0	2	2	0	0	0	0	0	0	0	0	0	0
0	0	0	1	1	2	0	0	0	0	0	0	0	0	0
0	0	0	0	1	2	1	0	0	0	0	0	0	0	0
0	0	0	0	0	0	4	1	0	0	0	0	0	0	0
0	0	0	0	0	0	0	1	1	0	0	0	0	0	0
0	0	0	0	0	0	0	0	3	2	0	0	0	0	0
0	0	0	0	0	0	0	0	1	2	1	0	0	0	0
0	0	0	0	0	0	0	0	0	0	3	1	0	0	0
0	0	0	0	0	0	0	0	0	0	0	2	1	0	0
0	0	0	0	0	0	0	0	0	0	0	0	4	1	0
0	0	0	0	0	0	0	0	0	0	0	0	0	1	2
0	0	0	0	0	0	0	0	0	0	0	0	0	1	3

Contrast: 0.3729

Correlation: 0.9916

Energy: 0.0394

Homogeneity: 0.8136

Entropy: 0.6014

Gallus superoxide dismutase 1:

GGCGCTGACGGCGGCTCTATATAAGCCCCGCGGGAGAGGCGGGCCTGTTAGCCCTCGGGC

Digital Vector:

[4 5 5 7 7 10 10 9 11 13 14 14 16 17 17 20 19 22 20 24 22 26 24 25 28 28 29 30 31 33 33 35 36 37 36 39 38 41 42 42 44 45 46 46 47 50 50 52 53 51 54 54 55 56 59 58 60 61 62 62]

SJ Matrix:

[1 1 1 1 1 2 2 1 2 2 2 2 3 3 3 3 3 4 3 4 4
4 4 5 5 5 5 5 6 6 6 6 6 6 7 6 7 7 7 7 8 8 8
8 8 8 9 9 9 9 9 9 9 10 10 10 10 10 10]

GLCM :

4	2	0	0	0	0	0	0	0	0
1	4	1	0	0	0	0	0	0	0
0	0	4	2	0	0	0	0	0	0
0	0	1	4	1	0	0	0	0	0
0	0	0	0	4	1	0	0	0	0
0	0	0	0	0	5	2	0	0	0
0	0	0	0	0	1	3	1	0	0
0	0	0	0	0	0	0	5	1	0
0	0	0	0	0	0	0	0	6	1
0	0	0	0	0	0	0	0	0	5

Contrast: 0.2542

Correlation: 0.9859

Energy: 0.0635

Homogeneity: 0.8729

Entropy: 0.1145

	ENERGY	HOMOGENEITY	CORRELATION	CONTRAST	ENTROPY
Mus musculus (superoxide dismutase 1)	0.0687	0.8898	0.9884	0.2203	0.7415
Human ***(superoxide dismutase 1)***	0.0394	0.8136	0.9916	0.3729	0.6014
Gallus ***(superoxide dismutase 1)***	0.0635	0.8729	0.9859	0.2542	0.7602

Figure 4

RESULTS

In conclusion, we define the co-occurrence matrix of the DNA sequence and calculated sequentially. We've transformed the DNA sequence into a digital vector. We have calculated and generate for each row of the matrix texture features by computing a match of the DNA sequence. Entropy, contrast, energy, correlation and homogeneity were calculated for each DNA sequence. In this study, we analyzed the similarity of sequences using MATLAB.(***Figure 4***) These results, we can see the next evolutionary relationships to measure the similarity of the DNA sequence along with the calculated feature.

Also in this applications represents that the sequence of Gallus has the utmost entropy. From Gallus to *mus musculus* and human the entropy decreases. Entropy is a measure of randomness and complexity; higher entropy denotes the higher randomness and the complexity. Here, previously defined sequence entropy gives a quantitative measurement of randomness and complexity. In contrast to entropy, energy is a measurement of uniformity. Figure 4 illustrates that the human DNA sequence has lower energy and lower entropy than the other species.

The importance of sequence similarity analysis is that there is research to predict the evolutionary relationship and protein structure between different species. The method we use can analyze for a DNA sequence and combine texture features. Using these properties, a matrix with similar distance can be calculated and phylogenetic trees can be extracted. Finally, it is very easy to see the similarity or difference between species. We were able to comment on the properties of the entropy and energy we calculated. The most important point in this method is that it is possible to calculate the multiple features that are natural in each sequence. Another important point is that these features should be calculated only once. Additionally, the properties of each array are calculated independently. It is a fact that using this method is very time-saving.

ACKNOWLEDGMENT

For the examination of different species, we retrieved the sequence of the gene fragment encoding the sod enzyme from https://epd.epfl.ch.

REFERENCES

[1] Baldi, P., Brunak, S., & Bach, F. (2001). *Bioinformatics: the machine learning approach*. MIT press.

[2] Canan KÜLAH, Meltem YALINAY ÇIRAK, (2010) "Ankara Bölgesindeki Hepatit B Virusu Genotiplerinin Dna Dizi Analizi Yöntemi İle Belirlenmesi", Gazi Üniversitesi Tıp Fakültesi

[3] Haralick, R. M., Shanmugam, K., & Dinstein, I. H. (1973). Textural features for image classification. *IEEE Transactions on systems, man, and cybernetics*, (6), 610-621.

[4] Horng, M. H., Huang, X. J., & Zhuang, J. H. (2003). Texture Feature Coding Method for Texture Analysis and It's Application. *Journal of Optical Engineering*, *42*(1), 228-238.

[5] Krane, D. E., & Raymer, M. L. Fundamental concepts of bioinformatics. 2003.

[6] Mapayi, T., Viriri, S., & Tapamo, J. R. (2015). Adaptive thresholding technique for retinal vessel segmentation based on GLCM-energy information. *Computational and mathematical methods in medicine*, *2015*.

[7] Mari Partio, Bogdan Cramariuc, Moncef Gabbouj, and Ari Visa. "Rock Texture Retrieval Using Gray Level Co-Occurrence Matrix", Tampere University of Technology

[8] Needleman, S. B., & Wunsch, C. D. (1970). A general method applicable to the search for similarities in the amino acid sequence of two proteins. Journal of molecular biology, 48(3), 443-453.

[9] Roumi, M. (2009). Implementing texture feature extraction algorithms on FPGA.

[10] Tahir, M. A. Bouridane, A. Kurugöllü, F. Amira, A.",Acceleratıng The Computatıon Of Glcm And Haralıck Texture Features On Reconfigurable Hardware", International Conference on Image Processing (ICIP),2004, 2857-2860

[11] Weiyang Chen, Bo Liao, Weiwei Li (2018) , " Use of image texture analysis to find DNA sequence similarities", College of Information, Qilu University of Technology

Chapter 12

REACTIVE OXYGEN SPECIES AND WOUND HEALING

Elif Naz ALVER[1]
Kaan KALTALIOGLU[2]
Sule COSKUN-CEVHER[3]

1 Biology Department, Science Faculty, Gazi University, 06500, Ankara, Turkey ORCID ID: 0000-0003-4946-1185
2 Espiye Vocational School, Giresun University, 28600, Giresun, Turkey Corresponding Author:Dr. Kaan Kaltalioglu kaan.kaltalioglu@gmail.com ORCID ID: 0000-0002-4995-2657
3 Biology Department, Science Faculty, Gazi University, 06500, Ankara, Turkey ORCID ID: 0000-0001-6204-2845

INTRODUCTION

The wound is a deterioration of the structural integrity and operation of tissues in the body for many reasons. Wound healing is all biological and physiological events in the process of making tissue functional immediately after the injury (Lee, Wysocki, Warburton, & Tuan, 2012). Healing process consists of sequential phases, including hemostasis, inflammatory, proliferation, and remodeling (Witte & Barbul, 1997).

The healing process has vital effects due to the decrease in quality of life and increase in health costs. Therefore, studies on the factors affecting wound healing and improving healing process are constantly being developed. In particular, the effects of redox signals on healing process form the basis of many wound healing studies (Sen & Roy, 2008). ROS, which form the basis of redox signals in healing process, are one of the major elements affecting wound healing.

ROS are very important regulators at many stages of healing processes (Schäfer & Werner, 2008; Sen & Roy, 2008) (Figure 1). ROS are involved in intracellular signaling during wound healing, proliferation and migration of cells, sterilization of wound area from pathogens and closure of scar tissue. Besides these positive effects of ROS, high ROS concentration in the wound area causes oxidative stress formation resulting in numerous cell damage, aging and neoplastic cell transformation. This affects the healing process and often leads to chronic wounds (Dunnill et al., 2015; Sen, 2009). In this chapter, it is aimed to explain the link between ROS and wound healing.

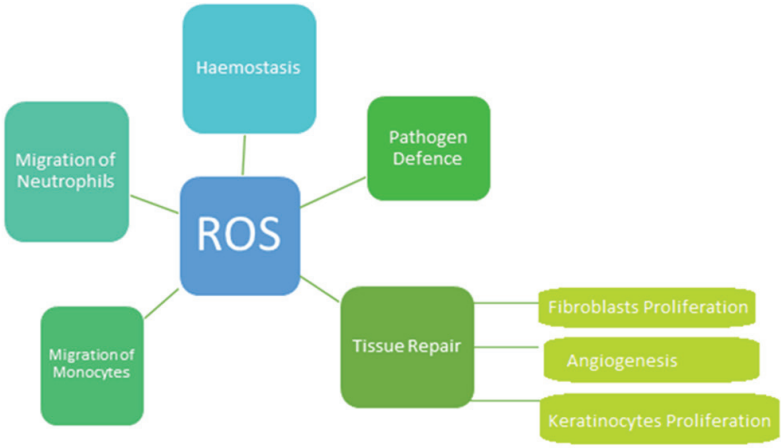

Figure 1. *Roles of reactive oxygen species in wound healing*

Reactive oxygen species

Oxygen is an indispensable element for the body and together with hydrogen, carbon, nitrogen and sulfur, it forms the basic building blocks of organic molecules. 90% of the oxygen required for metabolic reactions in cells is used during oxidative phosphorylation in mitochondria, 1-3% of the oxygen used causes the formation of ROS in mitochondria, and these molecules are called free radicals produced by mitochondria (Shinde, Ganu, & Naik, 2012). High energy atoms or molecules that has an unpaired electrons with independent existence are called free radicals (Halliwell & Gutteridge, 2015). Oxygen-derived free radicals are termed as ROS, beside nitrogen-derived free radicals are termed as reactive nitrogen species (RNS). Among the ROS are superoxide ($O_2^{\bullet-}$), hydroxyl ($OH^{\bullet}$), hydrogen peroxide (H_2O_2), peroxyl ($ROO^{\bullet}$), lipid peroxyl ($LOO^{\bullet}$), ozone (O_3) and lipid peroxide (LOOH) are commonly called as oxidants. These oxidant species are produced by living organisms under pathological and physiological conditions. Additionally, examples of RNS are nitric oxide (NO) and peroxynitrite ($ONOO^-$) (Bast, Haenen, & Doelman, 1991; Fang, Yang, & Wu, 2002).

Wound healing

The wound healing process is a delicate process that starts immediately after the damage. This process is controlled by a wide variety of detectors, such as hormones, cytokines, growth factors (Kunkemoeller & Kyriakides, 2017; Sen & Roy, 2008; Wlaschek & Scharffetter-Kochanek, 2005). In addition to these regulators, several studies show that there are numerous factors (local or systemic) that affect healing process. Local factors include infection in the wound area, poor blood circulation, hypoxia, tissue necrosis, and the presence of foreign particles. Systematic factors include diabetes, immunodeficiency, age, and the patient's genetic makeup (Guo & Dipietro, 2010; Robson, Steed, & Franz, 2001). These factors can increase the wound healing process or cause chronic non-healing wound formation.

ROS is essential for defense mechanism against microorganisms. Low reactive oxygen levels form the basis of intracellular signaling (Roy, Khanna, Nallu, Hunt, & Sen, 2006). Besides these useful effects of ROS, due to their high reactivity, high ROS concentration is quite harmful and negatively affects the healing process.

Wound healing can be splitted into 4 different phases; hemostasis, inflammatory, proliferation and remodeling.

Hemostasis Phase

The hemostatic process that initiates to stop bleeding immediately after the injury begins with the fibrin clot formation by platelet cells. In

hemostasis, the priority is to avoid blood loss by forming a blood clot to narrow the vessels and close the vein (Figure 2). The blood clot also acts as a temporary matrix for defense against microbial invasion and the collection of inflammatory cells (Roy et al., 2006; Sen & Roy, 2008).

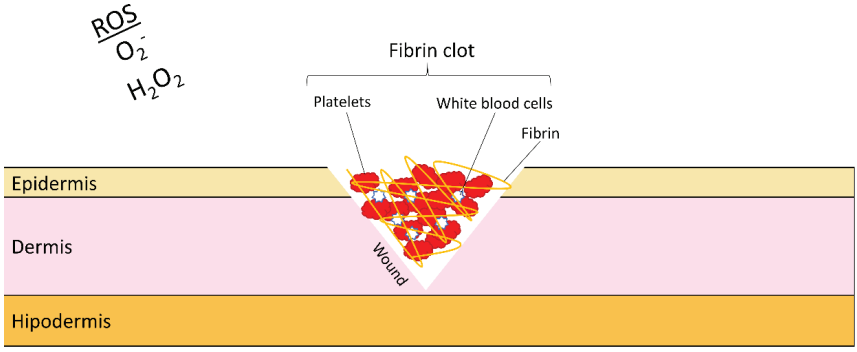

Figure 2. *Hemostasis phase of wound healing process*

The formation of the fibrin clot is associated with platelet aggregation and activation. There are many factors that affect platelet activation, and the most important of them is the oxidants found in the wound environment (Roy et al., 2006). The platelets themselves produce ROS and coexist with other ROS producing cells, such as white blood cells, in the wound area (Salvemini & Botting, 1993). Another factor affecting platelet activation is collagen activation. Platelet aggregation induced by collagen is associated with the production of hydrogen peroxide eliminated by catalase. Catalase decreases arachidonic acid, thromboxane A2 and inositol 1,4,5-trisphosphate (IP3). Platelet aggregation is associated with hydrogen peroxide, which acts as a secondary intracellular messenger by activating arachidonic acid metabolism and the phospholipase-C signal transduction pathway (Pignatelli, Pulcinelli, Lenti, Paolo Gazzaniga, & Violi, 1998). Additionally, activation of collagen triggers nicotinamide adenine dinucleotide phosphate (NADPH) oxidase-dependent superoxide release in platelets, which increases the presence of secreted adenosine diphosphate (ADP) (Krotz et al., 2002).

The first step in the establishment of the hemostatic plug is the establishment of the extrinsic coagulation (clotting) pathway, which causes the formation of thrombin secreted by platelets. The establishment of the coagulation pathway is due to the tissue factor (TF) and platelets increase tissue factor expression. Increased TF expression causes increased ROS and NADPH oxidase production (Essex & Li, 2003; Sen & Roy, 2008). The cell surface TF is activated by hydrogen peroxide (Penn, Patel, Cui, DiCorleto, & Chisolm, 1999). Activated TF improves thrombin formation by combining with Factor VIIa (FVIIa). The resulting thrombin stimulates

ROS formation with NADPH oxidases, then activates ROS-dependent signaling pathways that enhance a thrombogenic cycle through TF upregulation (Gorlach, 2005). Thus, thrombin accumulation occurs in the wound area and hemostatic plug is formed. It also prepares the wound site for the inflammatory phase by acting as a chemoattractive agent for thrombin, macrophages, leukocytes and fibroblasts that accumulate in the wound area.

Inflammatory Phase

The inflammatory phase is the second phase of healing process, in which neutrophils, macrophages and lymphocytes play an active role. Neutrophils are the first white blood cells in the wound area (Gillitzer & Goebeler, 2001; Lansdown, 2002) (Figure 3). Neutrophils produce promyelocytes in the bone marrow, pass through boneiness through circulation in response to calcium gradient, lipid mediators, hydrogen peroxide and chemokines released by damaged cells (Su & Richmond, 2015; van der Vliet & Janssen-Heininger, 2014). At this stage, thrombin and interleukin-8 (IL-8) adheres to endothelial cells and stimulates endothelial permeability. Thus, it facilitates the entry of circulating neutrophils into the wound area (Schäfer & Werner, 2008; Sen & Roy, 2008). Neutrophils coming into the wound site are responsible for the release of proteases and antimicrobial peptides, and the production of high amounts of ROS (Dunnill et al., 2015; Su & Richmond, 2015). After neutrophils, lymphocytes and monocytes arrive at the wound site and transform into active macrophages. Macrophages release proinflammatory cytokines and are also responsible for ROS secretion in the wound area. In addition, monocytes are responsible for the release of growth factors. Fibroblast growth factor-2 (FGF2), transforming growth factor beta (TGF-β), platelet-derived growth factor (PDGF) and vascular endothelial growth factor (VEGF) are responsible for the activation of endothelial cells, fibroblasts and keratinocytes (Novak & Koh, 2013). Kaltalioglu et al. (Kaan Kaltalioglu, Coskun-Cevher, Tugcu-Demiroz, & Celebi, 2013) reported that PDGF may have increased ROS production in the early stages of healing process. PDGF can also contribute to wound healing with this increase.

Neutrophils and macrophages generate a big amount of superoxide radical anions to protect the wound site from microbial contamination, and this phenomenon is response of the innate immune system and is called as respiratory burst (Cerutti, 1991). Fibroblasts stimulated by proinflammatory cytokines to remove pathogens by increasing ROS production also participate in ROS production. With the activation of NADPH oxidase in the plasma membrane of the cells, the cells produce a high degree of superoxide radical anion. The superoxide radical anions formed are rapidly broken into hydrogen peroxide and molecular oxygen by superoxide dismutase

(SOD). Although hydrogen peroxide is not included in the radical group, it plays a role in the production of hydroxyl radicals in the presence of iron or copper ions, which leads to serious cell damage. Hydroxyl radicals are destructive and result in oxidation of cellular macromolecules (Bedard & Krause, 2007). Therefore, hydrogen peroxide should be detoxified quickly. They are detoxified by ROS-sparing enzymes such as SOD, peroxidases, peroxydoxins, as well as small molecule antioxidants such as glutathione and vitamin E (Fitzmaurice, Sivamani, & Isseroff, 2011; Kunkemoeller & Kyriakides, 2017).

These reactions, which continue rapidly and regularly in the normal wound healing process, cannot occur due to local and systematic factors affecting the wound healing and cause chronic non-healing wounds (Cano Sanchez, Lancel, Boulanger, & Neviere, 2018). Hypoxia and type 2 diabetes are the most critical factors that can elicit the formation of chronic wounds (Guo & Dipietro, 2010; Sen & Roy, 2008). Chronic wound area may be characterized by excessive amounts of proinflammatory cytokines, increased matrix metalloproteinases (MMP) and increased ROS levels (Smith, Waypa, & Schumacker, 2017). The combination of these factors leads to disruption of ECM and growth factors, irregular inflammatory response, decreased cellular proliferation, increased bacterial colonization, thereby preventing wound healing and remaining in the inflammatory phase (Cano Sanchez et al., 2018).

When chronic inflammatory pathological conditions were examined, it was observed that NADPH oxidase activation increased, this situation triggered excessive ROS production and further increased inflammatory status and oxidative stress cellular damage (Cano Sanchez et al., 2018). Increased NADPH oxidase production causes more superoxide production (Schramm, Matusik, Osmenda, & Guzik, 2012; Zinkevich & Gutterman, 2011). Increased superoxide level converts the wound environment into a high oxidizing environment. This picture is often seen in cases of tissue hypoxia and hyperglycemia. This increase of ROS affects cellular hemostasis, creating redox imbalance, and due to the reduction in antioxidant defense, the amount of ROS in the tissue remains at high levels. High levels of ROS remain the primary factor causing healing to remain in the inflammatory phase. Therefore, recent studies have focused on antioxidant strategies to eliminate oxidative stress (Fitzmaurice et al., 2011; Kunkemoeller & Kyriakides, 2017).

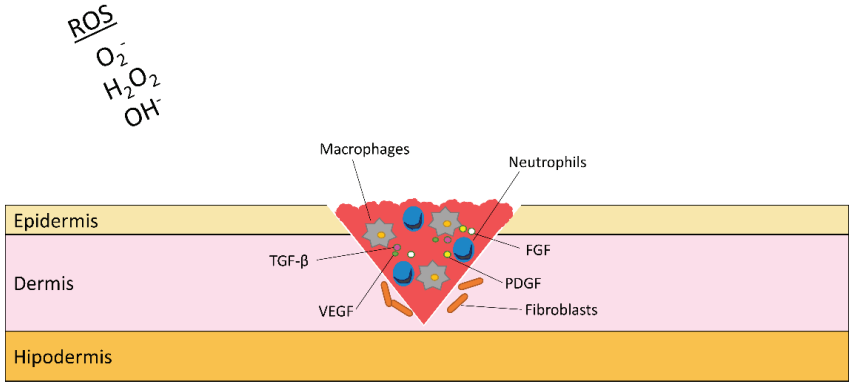

Figure 3. *Inflammatory phase of wound healing process*

Proliferation Phase

The proliferation phase can be expressed as the beginning of wound closure following the inflammatory phase. Intense cellular activities are necessary for the damaged tissue to restore its former integrity (Li, Chen, & Kirsner, 2007). The main events of this stage can be listed as fibroblast proliferation, ECM accumulation, angiogenesis and re-epithelialization (Brix, Dunkhorst, Mayer, & Jordans, 2008). Fibroblasts are the primary cell type in the proliferation phase. Fibroblasts are responsible for the production of ECM components and the stimulation of keratinocytes, which ensure reconstruction of epithelial integrity. Fibroblast activation is stimulated by PDGF, TGF-β and FGF secreted by macrophages in the wound area (K. Kaltalioglu & Coskun-Cevher, 2015). Another stimulator of fibroblast activation is ROS, which is also responsible for the secretion of growth factors. ROS mediates the production of ECM components such as fibronectin and collagen by promoting fibroblast proliferation and migration (Hoffmann & Griffiths, 2018).

Angiogenesis is a vital event for wound healing. It is described as the growth of new blood vessels from the existing vasculature (Folkman & Shing, 1992). New blood vessel formation is performed by stimulating endothelial cells located on the wound edge by growth factors (TGF-β and VEGF). ROS stimulates endothelial cell division in angiogenesis and is involved in new blood vessel formation by increasing VEGF expression (Hoffmann & Griffiths, 2018).

Fibroblast proliferation, accumulation of collagen and other ECM components, and newly formed blood vessels allow granulation tissue to cover the wound site (Thiruvoth, Mohapatra, Kumar, Chittoria, & Nandhagopal, 2015). Fibroblasts in granulation tissue differentiate into myofibroblasts through TGF-β induced by ROS. Myofibroblasts are

involved in wound contraction force, wound shrinkage and maturation of granulation tissue (Bainbridge, 2013).

Adequate migration, proliferation and stimulation of keratinocytes are very important in re-epithelialization. Epidermal growth factor (EGF) and TGF-β secreted by platelets stimulate keratinocytes in the early phase of injury. Keratinocytes are then triggered by growth factors and ROS to create a new epithelial barrier onto the wound (Li et al., 2007; Mendonca & Coutinho-Netto, 2009).

ROS, which acts at all key points of the proliferation phase, prevents wound healing by increasing the concentration in the wound tissue. In diabetic animals, oxidative stress causes severe damage to fibroblasts, which reduces the production of collagen fibrils in wound healing. Since fibroblasts are very sensitive to ROS, in environments with high concentrations of ROS, the number of fibroblasts decreases and collagen content decreases accordingly (Fujita et al., 2003). In other studies, nerve growth factor (NGF) and PDGF levels were found to be lower in diabetics than normal. Increased ROS products following injury cause damage to the cells that synthesize these growth factors. As a result, the synthesis and secretion of mediators in fibroblasts, macrophages and keratinocytes is reduced (Shetty, Udupa, & Udupa, 2008).

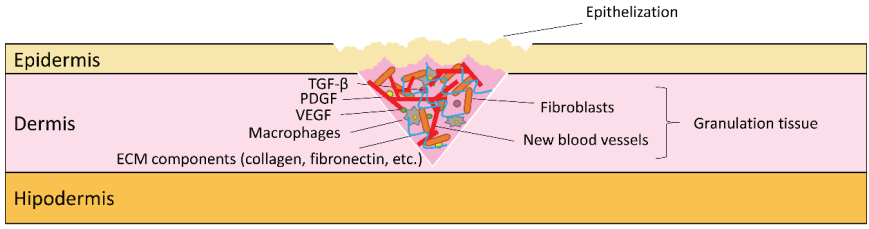

Figure 4. *Proliferation phase of wound healing process*

Remodeling Phase

The remodeling stage allows the wound repair to be terminated. In this process, the granulation tissue is replaced by scar tissue. Scar formation is the final result of healing process. The main point of this change is collagen balance. Collagen synthesis and degradation must be balanced (Toriseva & Kahari, 2009). Collagen type III in granulation tissue is replaced by collagen type I by activation of proteolytic enzymes and collagenases. MMPs, are proteolytic enzymes, and their inhibitors (metalloproteinase tissue inhibitors, TIMP) play a major role in the degradation and remodeling

of ECM (Witte et al., 1998). Control of zinc-induced endoproteinases synthesized by fibroblasts, keratinocytes, macrophages, and neutrophils takes place by cytokines, growth factors and chemokines (Behm, Babilas, Landthaler, & Schreml, 2012; Witte et al., 1998). In addition, it controls the production of these enzymes in NADPH oxidase mediated ROS in the wound environment (Hesketh, Sahin, West, & Murray, 2017).

Various protease production and activation varies in chronic wounds, including MMPs tightly regulated in acute wound healing, serine proteinases and neutrophil elastases (Mirastschijski et al., 2002). As a result of the increase in oxidative stress in chronic wounds and the increase in ROS concentration in the wound area, TIMP synthesis is inhibited, while the production of MMPs increases. Increased MMP level increases ECM destruction and prevents wound closure, resulting in non-healing wounds (Trengove et al., 1999).

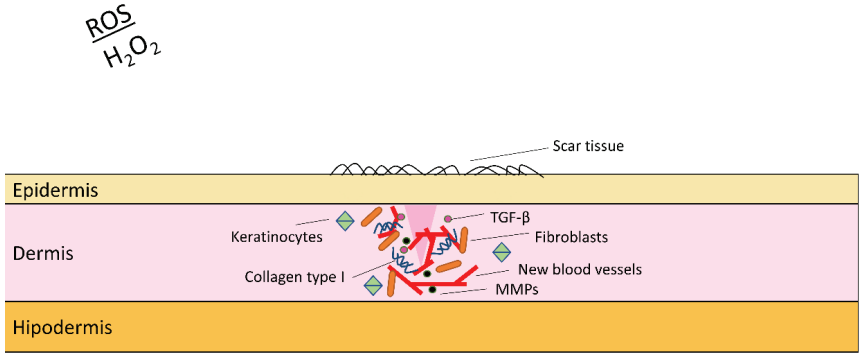

Figure 5. *Remodeling phase of wound healing process*

CONCLUSION

Wound healing is an important process that affects human life. Wound healing consists of four intertwined complex phases. ROS plays an important role in all of these phases. It is involved in establishing hemostasis, defending against invading pathogens, cell signaling, proliferation and migration of cells, angiogenesis and remodeling. In addition to these positive effects of ROS, the high ROS concentration in the wound area causes oxidative stress due to impaired detoxification. This increases the wound healing process, leading to the formation of non-healing wounds. The delay of wound healing time or the non-healing wounds negatively affect human life. In this regard, ROS production and detoxification must be strictly controlled for the normal repair process of wound healing. Identification of the basic regulators that will regulate this redox balance and the development of new antioxidant strategies will shed light on the elimination of the problems arising from ROS imbalance in the future.

REFERENCES

Bainbridge, P. (2013). Wound healing and the role of fibroblasts. *J Wound Care, 22*(8), 407-408, 410-412.

Bast, A., Haenen, G. R., & Doelman, C. J. (1991). Oxidants and antioxidants: state of the art. *Am J Med, 91*(3C), 2S-13S.

Bedard, K., & Krause, K. H. (2007). The NOX family of ROS-generating NADPH oxidases: physiology and pathophysiology. *Physiol Rev, 87*(1), 245-313.

Behm, B., Babilas, P., Landthaler, M., & Schreml, S. (2012). Cytokines, chemokines and growth factors in wound healing. *J Eur Acad Dermatol Venereol, 26*(7), 812-820.

Brix, K., Dunkhorst, A., Mayer, K., & Jordans, S. (2008). Cysteine cathepsins: cellular roadmap to different functions. *Biochimie, 90*(2), 194-207.

Cano Sanchez, M., Lancel, S., Boulanger, E., & Neviere, R. (2018). Targeting Oxidative Stress and Mitochondrial Dysfunction in the Treatment of Impaired Wound Healing: A Systematic Review. *Antioxidants (Basel), 7*(8), 98.

Cerutti, P. A. (1991). Oxidant stress and carcinogenesis. *Eur J Clin Invest, 21*(1), 1-5.

Dunnill, C., Patton, T., Brennan, J., Barrett, J., Dryden, M., Cooke, J., Leaper, D., Georgopoulos, N. T. (2015). Reactive oxygen species (ROS) and wound healing: the functional role of ROS and emerging ROS-modulating technologies for augmentation of the healing process. *International Wound Journal*, 1-8.

Essex, D. W., & Li, M. (2003). Redox control of platelet aggregation. *Biochemistry, 42*(1), 129-136.

Fang, Y. Z., Yang, S., & Wu, G. (2002). Free radicals, antioxidants, and nutrition. *Nutrition, 18*(10), 872-879.

Fitzmaurice, S. D., Sivamani, R. K., & Isseroff, R. R. (2011). Antioxidant Therapies for Wound Healing: A Clinical Guide to Currently Commercially Available Products. *Skin Pharmacology and Physiology, 24*, 113-126.

Folkman, J., & Shing, Y. (1992). Angiogenesis. *Journal of Biological Chemistry, 267*, 10931–10934.

Fujita, N., Sakaguchi, I., Kobayashi, H., Ikeda, N., Kato, Y., Minamino, M., & Ishii, M. (2003). An extract of the root of Lithospermun erythrorhison accelerates wound healing in diabetic mice. *Biol Pharm Bull, 26*(3), 329-335.

Gillitzer, R., & Goebeler, M. (2001). Chemokines in cutaneous wound healing. *J Leukoc Biol, 69*(4), 513-521.

Gorlach, A. (2005). Redox regulation of the coagulation cascade. *Antioxid Redox Signal, 7*(9-10), 1398-1404.

Guo, S., & Dipietro, L. A. (2010). Factors affecting wound healing. *J Dent Res, 89*, 219-229.

Halliwell, B., & Gutteridge, J. M. C. (2015). *Free Radicals in Biology and Medicine*: Oxford University Press.

Hesketh, M., Sahin, K. B., West, Z. E., & Murray, R. Z. (2017). Macrophage Phenotypes Regulate Scar Formation and Chronic Wound Healing. *Int J Mol Sci, 18*(7), 1545.

Hoffmann, M. H., & Griffiths, H. R. (2018). The dual role of Reactive Oxygen Species in autoimmune and inflammatory diseases: evidence from preclinical models. *Free Radic Biol Med, 125*, 62-71.

Kaltalioglu, K., & Coskun-Cevher, S. (2015). A bioactive molecule in a complex wound healing process: platelet-derived growth factor. *Int J Dermatol, 54*(8), 972-977.

Kaltalioglu, K., Coskun-Cevher, S., Tugcu-Demiroz, F., & Celebi, N. (2013). PDGF supplementation alters oxidative events in wound healing process: a time course study. *Archives of Dermatological Research, 305*(5), 415-422.

Krotz, F., Sohn, H. Y., Gloe, T., Zahler, S., Riexinger, T., Schiele, T. M., Becker, P. H., Theisen, K., Klauss, V., Pohl, U. (2002). NAD(P)H oxidase-dependent platelet superoxide anion release increases platelet recruitment. *Blood, 100*(3), 917-924.

Kunkemoeller, B., & Kyriakides, T. R. (2017). Redox Signaling in Diabetic Wound Healing Regulates Extracellular Matrix Deposition. *Antioxid Redox Signal, 27*(12), 823-838.

Lansdown, A. B. (2002). Calcium: a potential central regulator in wound healing in the skin. *Wound Repair Regen, 10*(5), 271-285.

Lee, Y. S., Wysocki, A., Warburton, D., & Tuan, T. L. (2012). Wound healing in development. *Birth Defects Res C Embryo Today, 96*(3), 213-222.

Li, J., Chen, J., & Kirsner, R. (2007). Pathophysiology of acute wound healing. *Clinics in Dermatology, 25*, 9-18.

Mendonca, R. J., & Coutinho-Netto, J. (2009). Cellular aspects of wound healing. *An Bras Dermatol, 84*(3), 257-262.

Mirastschijski, U., Impola, U., Jahkola, T., Karlsmark, T., MS, A. G., & Saarialho-Kere, U. (2002). Ectopic localization of matrix metalloproteinase-9 in chronic cutaneous wounds. *Hum Pathol, 33*(3), 355-364.

Novak, M. L., & Koh, T. J. (2013). Phenotypic transitions of macrophages orchestrate tissue repair. *Am J Pathol, 183*(5), 1352-1363.

Penn, M. S., Patel, C. V., Cui, M. Z., DiCorleto, P. E., & Chisolm, G. M. (1999). LDL increases inactive tissue factor on vascular smooth muscle cell surfaces: hydrogen peroxide activates latent cell surface tissue factor. *Circulation, 99*(13), 1753-1759.

Pignatelli, P., Pulcinelli, F. M., Lenti, L., Paolo Gazzaniga, P., & Violi, F. (1998). Hydrogen Peroxide Is Involved in Collagen-Induced Platelet Activation. *Blood, 91*(2), 484-490.

Robson, M. C., Steed, D. L., & Franz, M. G. (2001). Wound healing: biologic features and approaches to maximize healing trajectories. *Curr Probl Surg, 38*(2), 72-140.

Roy, S., Khanna, S., Nallu, K., Hunt, T. K., & Sen, C. K. (2006). Dermal wound healing is subject to redox control. *Molecular Therapy, 13*, 211-220.

Salvemini, D., & Botting, R. (1993). Modulation of platelet function by free radicals and free-radical scavengers. *Trends Pharmacol Sci, 14*(2), 36-42.

Schäfer, M., & Werner, S. (2008). Oxidative stress in normal and impaired wound repair. *Pharmacological Research, 58*, 165-171.

Schramm, A., Matusik, P., Osmenda, G., & Guzik, T. J. (2012). Targeting NADPH oxidases in vascular pharmacology. *Vascul Pharmacol, 56*(5-6), 216-231.

Sen, C. K. (2009). Wound healing essentials: let there be oxygen. *Wound Repair Regen, 17*(1), 1-18.

Sen, C. K., & Roy, S. (2008). Redox signals in wound healing. *Biochim Biophys Acta, 1780*(11), 1348-1361.

Shetty, S., Udupa, S., & Udupa, L. (2008). Evaluation of Antioxidant and Wound Healing Effects of Alcoholic and Aqueous Extract of Ocimum sanctum Linn in Rats. *Evid Based Complement Alternat Med, 5*(1), 95-101.

Shinde, A., Ganu, J., & Naik, P. (2012). Effect of Free Radicals & Antioxidants on Oxidative Stress: A Review. *Journal of Dental and Allied Sciences, 1*(2), 63.

Smith, K. A., Waypa, G. B., & Schumacker, P. T. (2017). Redox signaling during hypoxia in mammalian cells. *Redox Biol, 13*, 228-234.

Su, Y., & Richmond, A. (2015). Chemokine Regulation of Neutrophil Infiltration of Skin Wounds. *Adv Wound Care (New Rochelle), 4*(11), 631-640.

Thiruvoth, F., Mohapatra, D., Kumar, D., Chittoria, S., & Nandhagopal, V. (2015). Current concepts in the physiology of adult wound healing. *Plast Aesthet Res, 2*, 250-256.

Toriseva, M., & Kahari, V. M. (2009). Proteinases in cutaneous wound healing. *Cell Mol Life Sci, 66*(2), 203-224.

Trengove, N. J., Stacey, M. C., MacAuley, S., Bennett, N., Gibson, J., Burslem, F., Murphy, G, Schultz, G. (1999). Analysis of the acute and chronic wound environments: the role of proteases and their inhibitors. *Wound Repair Regen, 7*(6), 442-452.

van der Vliet, A., & Janssen-Heininger, Y. M. (2014). Hydrogen peroxide as a damage signal in tissue injury and inflammation: murderer, mediator, or messenger? *J Cell Biochem, 115*(3), 427-435.

Witte, M. B., & Barbul, A. (1997). General principles of wound healing. *Surg Clin North Am, 77*(3), 509-528.

Witte, M. B., Thornton, F. J., Kiyama, T., Efron, D. T., Schulz, G. S., Moldawer, L. L., & Barbul, A. (1998). Metalloproteinase inhibitors and wound healing: a novel enhancer of wound strength. *Surgery, 124*(2), 464-470.

Wlaschek, M., & Scharffetter-Kochanek, K. (2005). Oxidative stress in chronic venous leg ulcers. *Wound Repair Regen, 13*(5), 452-461.

Zinkevich, N. S., & Gutterman, D. D. (2011). ROS-induced ROS release in vascular biology: redox-redox signaling. *Am J Physiol Heart Circ Physiol, 301*(3), H647-653.

Chapter 13

INTERVAL ESTIMATION FOR ORDER STATISTICS BY CHEBYSHEV INEQUALITY

Erhan USTAOĞLU[1]

1 Marmara University, Faculty of Administrative Sciences, Business Informatics,
ORCID ID: 0000-0002-9077-4370

1. Introduction

Though it has appeared more often in various areas of applications recently, theoretical works on order statistics began early in 20^{th} century when Pearson provided an ordered statistical solution to Galton's difference problem [1]. Since then, order statistics from various discrete and continuous distributions have been widely studied both theoretically and computationally. Tippett calculated the extreme order statistics and ranges of normal distribution [2]. Davis tabulated the moments of order statistics for the logistic function [3]. Sukhatme derived the equation for the distribution of the order statistics of the standard exponential distribution [4]. Moments and ranges of order statistics from the normal distribution were also studied and computed by various authors [5], [6]. Gupta and Panchapakesan computed means and variances of extreme order statistics for binomial distribution [7].

Since the order statistics give the distribution of ordered samples from any population they are frequently applied in areas where the smallest or highest, median or the range of the statistics is of importance. For example, the distribution of highest of the samples is needed for determining the probability of a big earthquake or a destructive flood or a record high from any set data. On the hand the distribution of the smallest is useful where the minimum plays a significant role as in the analysis of strength of materials. In many applications the median is a better choice against the mean as the mean is more sensitive to extreme sample values. Range distribution between ordered samples is crucial if we need to identify the whole or a certain part of a process. In this respect order statistics is useful for reliability theory and allocation problems. Some examples of order statistic applications amongst many others are in areas of communications, finance, genetics and reliability theory [8], [9], [10], [11].

For a vast variety of applications determining the intervals between order statistics of a sample is important. When the underlying distribution is well known it is possible to compute the intervals by analytical or numerical methods. This paper investigates considering Chebyshev inequality as an option for determining the intervals when this is not the case. If the mean and the variances of the distribution known or estimated intervals can be calculated by using Chebyshev inequality. In this paper, first a general introduction of order statistics and calculation of moments are given. Then approximate mean and variances are derived for standard exponential and standard normal distributions. With these mean and variance values Chebyshev intervals are then calculated and compared to

those of obtained by exact calculation in order to shed light on how accurate it would be if the underlying distribution were unknown.

2. Order Statistics

Given that n random samples $X_1, \ldots, X_n$ from a continuous distribution function, order statistics are, as the name indicates, the corresponding ordered statistics as $X_{(1)} < X_{(2)} < \cdots < X_{(n)}$, $X_{(1)}$ being the smallest of these random variables and $X_{(n)}$ the largest. The condition that the underlying distribution be continuous ensures the uniqueness of the statistics, which means none of the random variables are equal in magnitude.

For finding the cumulative distribution of any r^{th} order statistic one can consider the probability of the event that the r^{th} order statistics is smaller than any given real value x as

$$F_{X_{(r)}} = P(X_{(n)} < x) \tag{1}$$

The above event is a success in binomial sense if r or more than r number of random samples are greater than x, then one can write the cumulative distribution function for the r^{th} order statistic as

$$F_{X_{(r)}} = \sum_{i=r}^{n} \binom{n}{i} [F_x(x)]^i [1 - F_x(x)]^{n-r} \tag{2}$$

By differentiation and some algebraic equations one can write the probability density function of r^{th} order statistic as

$$f_{X_{(r)}} = \frac{n!}{(r-1)!\,(n-r)!} [F_x(x)]^{r-1} [1 - F_x(x)]^{n-r} f_X \tag{3}$$

where $F_x(x)' = f_X$.

If the underlying cumulative distribution function is uniform from an interval (0,1) with $F_x(x) = x$, thus the probability density function of simply equals

$$f_{X_{(r)}} = \frac{n!}{(r-1)!\,(n-r)!} (x)^{r-1} (1-x)^{n-r}. \tag{4}$$

The equation implies a beta distribution having parameters $(r,\ n - r + 1)$ [12]. This result is important when one wants to derive the moments of order statistics using quantile functions.

The probability integral transformation states that if a random variable X has a continuous distribution $F(X)$ then the random variable defined as

$$U = F(X) \tag{5}$$

has a uniform distribution. If $U_1, \ldots, U_n$ are random samples from a uniform distribution on the interval (0,1) and $X_1, \ldots, X_n$ are random samples from any continuous distribution $F_x(x)$ then the ordered statistics $U_{(1)} < U_{(2)} < \cdots < U_{(n)}$ and $X_{(1)} < X_{(2)} < \cdots < X_{(n)}$ obtained from these distributions are identically distributed;

$$U_{(r)} = F(X_{(r)}) \tag{6}$$

Further it can be showed that any r^{th} order statistic is related to its inverse cumulative distribution through

$$X_{(r)} = F^{-1}(U_{(r)}) \tag{7}$$

2.1 Moments of Order Statistics

In this section approximates moments of order statistics for some continuous distributions are derived explicitly. Moments of any continuous order statistic can be calculated by employing moment definition and the underlying probability distribution function. As it could be difficult to deal with the integral involved for some distributions it is helpful to make use the quantile function. Any k^{th} moment of any order statistic is given as follows;

$$E\left(X_{(r)}^k\right) = \frac{n!}{(r-1)!\,(n-r)!}\int_{-\infty}^{\infty} y^k [F_x(y)]^{r-1}[1 - F_x(y)]^{n-r} f_X(y)\, dy \tag{8}$$

$$E\left(X_{(r)}^k\right) = \frac{n!}{(r-1)!\,(n-r)!}\int_{-\infty}^{\infty} y^k [F_x(y)]^{r-1}[1 - F_x(y)]^{n-r}\, dF_x(y) \tag{9}$$

$$E\left(X_{(r)}^k\right) = \frac{n!}{(r-1)!\,(n-r)!}\int_{-\infty}^{\infty} [Q_x(y)]^k [u]^{r-1}[1-u]^{n-r} du \tag{10}$$

$$E\left(X_{(r)}^k\right) = E[Q_x(U)]^k \tag{11}$$

In the above equation U has a beta distribution with parameters $(r,\ n-r+1)$. As special case when the random variable U has uniform distribution on interval (0,1), namely $Q_x(U)=u$, the integral in equation (11) becomes a beta integral with parameters $r+k$ and $n-r+1$.

$$E\left(X_{(r)}^{k}\right)=\frac{n!}{(r-1)!\,(n-r)!}\,B(r+k,n-r+1) \tag{12}$$

$$E\left(X_{(r)}^{k}\right)=\frac{n!}{(r-1)!\,(n-r)!}\,\frac{(r+k-1)!\,(n-r)!}{(n+k)!} \tag{13}$$

$$E\left(X_{(r)}^{k}\right)=\frac{n!\,(r+k-1)!}{(n+k)!\,(r-1)!} \tag{14}$$

From equation (14) the mean and the variance of order statistic for uniform distribution on (0,1) can be found to be [13];

$$E\left(X_{(r)}\right)=\frac{r}{n+1} \tag{15}$$

and

$$Var\left(X_{(r)}\right)=\frac{r(n-r+1)}{(n+1)^2(n+2)} \tag{16}$$

Having the relationship between quantile function and uniform distribution order statistics in hand we can proceed to derivation of moments of some continuous order statistics. Let's first consider the standard exponential distribution with cumulative distribution function

$$F(x)=1-e^{-x} \qquad 0<x<\infty \tag{17}$$

Using the relation with uniform distribution order statistics, r^{th} order statistic of the standard exponential distribution can be written as;

$$X_{(r)}=F^{-1}\left(U_{(r)}\right)=-\ln(1-U_{(r)}) \tag{18}$$

Since the inverse cumulative distribution function is also continuous, we can expand it around $E\left(U_{(r)}\right)=\mu$ using Taylor series;

$$F^{-1}\left(U_{(r)}\right) = -\ln(1-\mu) + \sum_{i=1}^{\infty} \frac{\left(U_{(r)}-\mu\right)^{i}}{i!}\left[-\ln(1-\mu)\right]^{(i)} \tag{19}$$

If we take expectation of both sides keeping the first two terms and letting $Var\left(U_{(r)}\right) = \sigma^2$ we get

$$E\left[F^{-1}\left(U_{(r)}\right)\right] = -\ln(1-\mu) + \frac{\sigma^2}{2}\,\frac{1}{(1-\mu^2)} \tag{20}$$

Similarly, the variance can be found by keeping the first two terms of Taylor series expansion and taking the expectation as

$$E\left\{F^{-1}\left(U_{(r)}\right) - E\left[F^{-1}\left(U_{(r)}\right)\right]\right\}^2 = \frac{\sigma^2}{(1-\mu^2)^2} - \frac{\sigma^4}{4}\,\frac{1}{(1-\mu^2)^4} \tag{21}$$

Since we have defined $E\left(U_{(r)}\right) = \mu$ and $Var\left(U_{(r)}\right) = \sigma^2$, replacing them in equations (20) and (21) and using equation (18), we get the mean and the variance of r^{th} order statistic of the standard exponential distribution as;

$$E\left[X_{(r)}\right] = -\ln\left(1-\frac{r}{n+1}\right) + \frac{r^2\,(n-r+1)^2}{2\,(n+1)^2\,(n+2)^2}\;\;\frac{1}{(n+1)^2-r^2} \tag{22}$$

$$Var\left[X_{(r)}\right] = \frac{r^2\,(n-r+1)^2}{(n+2)^2}\,\frac{1}{\{(n+1)^2-r^2\}^2} - \frac{r^4\,(n-r+1)^4}{\{(n+1)^2-r^2\}^4} \tag{23}$$

Similarly, the mean and the variance of the standard normal distribution with cumulative distribution function

$$\Phi(x) = \frac{1}{\sqrt{2\pi}}\int_{-\infty}^{x} e^{-t^2/2}\,dt \tag{24}$$

can be derived approximately by Taylor series expansion. First remembering equation (18) we can write

$$X_{(r)} = \Phi^{-1}\left(U_{(r)}\right) \tag{25}$$

Then the inverse cumulative distribution function can be expanded around $E\left(U_{(r)}\right) = \mu$ using Taylor series as;

$$\Phi^{-1}\left(U_{(r)}\right) = \Phi^{-1}(\mu) + \sum_{i=1}^{\infty} \frac{\left(U_{(r)} - \mu\right)^{i}}{i!} \left[\Phi^{-1}(\mu)\right]^{(i)} \tag{26}$$

where $\left[\Phi^{-1}\left(U_{(r)}\right)\right]^{(i)} = d^{i}\Phi^{-1}\left(U_{(r)}\right)/dU_{(r)}^{i}\,|_{U_{(r)}=\mu}$. Taking the expectation of both sides and letting $Var\left(U_{(r)}\right) = \sigma^2$ we can write

$$E\left[\Phi^{-1}\left(U_{(r)}\right)\right] = \Phi^{-1}(\mu) + \frac{\sigma^2}{2}\,\Phi^{-1^{(2)}}(\mu) \tag{27}$$

The variance can be found similarly with two term Taylor series expansions as;

$$E\left\{\Phi^{-1}\left(U_{(r)}\right) - E\left[\Phi^{-1}\left(U_{(r)}\right)\right]\right\}^2 = \sigma^2\left[\Phi^{-1^{(1)}}(\mu)\right]^2 - \frac{\sigma^4}{4}\left[\Phi^{-1^{(2)}}(\mu)\right]^2 \tag{28}$$

where $\Phi^{-1^{(1)}}$ and $\Phi^{-1^{(2)}}$ are first and second derivatives of quantile or inverse cumulative distribution function of standard normal distribution. Noting that $\Phi\left(\Phi^{-1}(x)\right) = x$ and using chain and product rules of derivation, the first and second derivatives of quantile distribution can be found to be

$$\Phi^{-1^{(1)}}(\mu) = \frac{1}{f\left(\Phi^{-1}(\mu)\right)} \tag{29}$$

$$\Phi^{-1^{(2)}}(\mu) = -\frac{f^{(1)}\left(\Phi^{-1}(\mu)\right)}{\left[f\left(\Phi^{-1}(\mu)\right)\right]^3} \tag{30}$$

where f and $f^{(1)}$ are standard normal density function and its derivative respectively. Replacing the results from equations (29) and (30) into the equations (27) and (28) and using equations (15), (16), $E\left(U_{(r)}\right) = \mu$,

$Var(U_{(r)}) = \sigma^2$, $X_{(r)} = \Phi^{-1}(U_{(r)})$, we can write the mean and the variance of r^{th} order statistic of the standard normal distribution as;

$$E[X_{(r)}] = \Phi^{-1}\left(\frac{r}{n+1}\right) - \frac{r(n-r+1)}{2(n+1)^2(n+2)} \frac{f^{(1)}\left(\Phi^{-1}\left(\frac{r}{n+1}\right)\right)}{\left[f\left(\Phi^{-1}\left(\frac{r}{n+1}\right)\right)\right]^3} \quad (31)$$

$$Var[X_{(r)}] = \frac{r(n-r+1)}{(n+1)^2(n+2)} \frac{1}{\left[f\left(\Phi^{-1}\left(\frac{r}{n+1}\right)\right)\right]^2} - \frac{r^2(n-r+1)^2}{4(n+1)^4(n+2)^2} \frac{\left[f^{(1)}\left(\Phi^{-1}\left(\frac{r}{n+1}\right)\right)\right]^2}{\left[f\left(\Phi^{-1}\left(\frac{r}{n+1}\right)\right)\right]^6} \quad (32)$$

where $f = d^1\Phi^{-1}(U_{(r)})/dU^1_{(r)}\,|_{U_{(r)}=\mu}$ and $f^{(1)} = d^2\Phi^{-1}(U_{(r)})/dU^2_{(r)}\,|_{U_{(r)}=\mu}$ are the standard normal probability density function and its derivative respectively.

As an example, the mean and variance of 10^{th} order statistic from the standard normal distribution of 24 samples can be found using standard normal table values and utilizing $f^{(1)}(x) = -xf(x)$

$$E[X_{(10)}] = -0.675 - \frac{(10)\,(15)}{2(25)^2(26)} \frac{(0.675)(0.3176)}{(0.3176)^3} = -0.2608 \quad (33)$$

$$Var[X_{(10)}] = \frac{(10)\,(15)}{(25)^2(26)} \frac{1}{(0.3176)^2} - \frac{(10)^2\,(15)^2}{4(25)^4(26)^2} \frac{(0.675)^2(0.3176)^2}{(0.3176)^6} = 0.0617\ \ (34) \quad (34)$$

2.2 Interval Estimation for Order Statistics

A confidence interval $100(1-\alpha)\%$ for a given value p, $0 < p < 1$, can be defined as

$$P\left(X_{(r)} < F^{-1}(p) < X_{(s)}\right) = 1 - \alpha \tag{35}$$

where $X_{(r)}$ and $X_{(s)}$, $r < s$, are two order statistics from a continuous distribution F. We can write using probability integral transform and equation (6)

$$\begin{aligned} P\left(X_{(r)} < F^{-1}(p)\right) &= P\left(F(X_{(r)}) < p\right) \\ &= P\left(U_{(r)} < p\right) \\ &= \sum_{i=r}^{n} \binom{n}{i} [p]^i [1-p]^{n-i} \end{aligned} \tag{36}$$

Since the event $P\left(X_{(r)} < F^{-1}(p)\right)$ occurs when the event $P\left(X_{(r)} < F^{-1}(p) < X_{(s)}\right)$ or the event $P\left(X_{(s)} > F^{-1}(p)\right)$ occurs, one can write [14]

$$\begin{aligned} P\left(X_{(r)} < F^{-1}(p)\right) &= P\left(X_{(r)} < F^{-1}(p) < X_{(s)}\right) \\ &+ P\left(X_{(s)} > F^{-1}(p)\right) \end{aligned} \tag{37}$$

Rearranging equation (37) and using the equation (36) this probability can be expressed as

$$\begin{aligned} P\left(X_{(r)} < F^{-1}(p) < X_{(s)}\right) \\ = P\left(X_{(r)} < F^{-1}(p)\right) - P\left(X_{(s)} > F^{-1}(p)\right) \end{aligned} \tag{38}$$

$$P\left(X_{(r)} < F^{-1}(p) < X_{(s)}\right) = \sum_{i=r}^{n} \binom{n}{i} [p]^i [1-p]^{n-i} - \sum_{i=s}^{n} \binom{n}{i} [p]^i [1-p]^{n-i} = \sum_{i=r}^{s-1} \binom{n}{i} [p]^i [1-p]^{n-i} \quad (39)$$

As the equation (39) reveals this confidence interval is not dependent on the cumulative distribution function and has a binomial distribution. It is not possible to find $X_{(r)}$ and $X_{(s)}$ uniquely from equation (39) for a given a α value. One way of determining these values uniquely is to use equal tail probabilities for the lower and the higher order statistics and write

$$\sum_{i=0}^{r-1} \binom{n}{i} [p]^i [1-p]^{n-i} \leq \frac{\alpha}{2}$$
$$\sum_{i=0}^{s-1} \binom{n}{i} [p]^i [1-p]^{n-i} \geq 1 - \frac{\alpha}{2} \quad (40)$$

Using these equations and binomial tables it is then possible to calculate the parameters r and s for the lower and upper bound order statistics which determines the confidence interval. As an example, if we take $n = 16$, $p = 0.40$ and $1 - \alpha = 0.95$ then we find from cumulative binomial tables $s - 1 = 10$ and $r - 1 = 2$ using equations in (40). Hence the exact confidence level for $p = 0.40$ becomes $0.9809 - 0.0183 = 0.9626$ with lower and upper order statistics $X_{(3)}$ and $X_{(11)}$ respectively.

3. Interval Estimation for Order Statistics by Chebyshev Inequality

Underlying cumulative probability distribution can be determined from the distribution of $X_{(n)}$ since $X_{(n)} = [F(x)]^n$ from equation (2). But the determination of $F(x)$ from other order statistics is not straightforward. Knowing some moments of one of the order statistics of is not sufficient for determining $F(x)$ completely. Instead, some moments of more than one order statistics are needed for that matter [15]. Although it is not possible to determine $F(x)$ completely from a few moments of an order statistic, it provides useful bounds for interval estimations. With the use

of mean and variance of any order statistics from a distribution with $F(x)$ and Chebyshev inequality, one can write

$$P\left(\left|X - E\left[X_{(r)}\right]\right| < kVar\left[X_{(r)}\right]\right) \geq 1 - \frac{1}{k^2} \tag{41}$$

Defining $kVar\left[X_{(r)}\right] = c$ and rearranging we get

$$P\left(X < E\left[X_{(r)}\right] + c\right) \geq 1 - \frac{Var\left[X_{(r)}\right]^2}{c^2} \tag{42}$$

Equation (42) provides a bound for the mean of any order statistics together with the knowledge of variance. For a confidence interval of 95%, means, variances and interval bounds for order statistics of sample $n = 15$ from standard normal distribution are given in Table 1.

Table 1. Mean, Variance and Intervals for Standard Normal Distribution

	$E\left[X_{(r)}\right]$	$Var\left[X_{(r)}\right]$	Lower Bound	Upper Bound
1	-1.70874	0.197287	-2.59103	-0.82644
2	-1.23726	0.144145	-1.8819	-0.59263
3	-0.94188	0.120739	-1.48184	-0.40192
4	-0.7108	0.107851	-1.19313	-0.22848
5	-0.51259	0.100186	-0.96064	-0.06455
6	-0.33324	0.095647	-0.76099	0.094502
7	-0.16432	0.093199	-0.58112	0.252477
8	0	0.092419	-0.41331	0.413312
9	0.16432	0.093199	-0.25248	0.581117
10	0.333245	0.095647	-0.0945	0.760992
11	0.512593	0.100186	0.064547	0.960639
12	0.710802	0.107851	0.228477	1.193127
13	0.941884	0.120739	0.401924	1.481843
14	1.237262	0.144145	0.592625	1.881898
15	1.708738	0.197287	0.826445	2.591031

Range distribution of order statistics will be employed in order to test the interval values obtained by Chebyshev inequality and given in Table 1. Range distribution of any order statistic is defined as $W_{(n)} = X_{(n)} - X_{(1)}$ and derived by using joint density functions of $W_{(n)}$ and $X_{(1)}$. The cumulative distribution function of the range is given as

$$P(W_{(n)} \leq w_0) = F_{W_{(n)}}(w_0) \tag{43}$$
$$= n \int_{-\infty}^{\infty} [F(x_1 + w_0) - F(x_1)]^{n-1} f(x_1)\ dx_1, \qquad 0 < w_0 < \infty$$

The above integral is not easy to handle for many of the cumulative distribution and requires tedious numerical calculation. Fortunately, the values for standard normal distribution are available up to sample sizes 20 [16]. Comparisons of ranges for sample sizes up to 19 are given in Table 2. Ranges obtained through Chebyshev inequality are calculated as the difference between the lower bound of the smallest order statistic and the upper bound of largest order statistic.

Table 2. Interval Comparison of Order Statistics

	Chebshev Intervals	**Exact Intervals**	**Difference**
19	5.27	4.97	0.30
17	5.23	4.90	0.33
15	5.18	4.80	0.38
13	5.13	4.69	0.44
11	5.08	4.55	0.53
9	5.02	4.39	0.63
7	4.95	4.17	0.78
5	4.88	3.86	1.02
3	4.78	3.32	1.46

As it can be seen from Table 2 Chebysev intervals are larger than those of exact calculation. Nevertheless, the difference between Chebyshev intervals and exact intervals gets smaller as the sample size increases.

4. Discussion

Since determining the intervals for order statistics is important for various applications, deployment of Chebyshev inequality for this purpose is investigated. The mean and the variances of standard normal distribution are derived and calculated. Using these values Chebyshev intervals for the range of the order statistics are calculated and compared to the exact values obtained by numerical calculations. In case of large enough sample sizes Chebyshev bounds can provide useful results when the underlying distribution of order statistics is unknown.

REFERENCES

[1] K. A. Pearson, Note on Francis Galton's difference problem, *Biometrika* 1 (1902), 390-399.

[2] L. H. C. Tippett, On the extreme individuals and the range of samples taken from a normal population, *Biometrika* 17 (1902), 364-387.

[3] P. V. Sukhatme, Tests of significance for samples of the $x^2 -$ population with two degrees of freedom, *Annals of Eugenics* 8 (1937), 52-56.

[4] H. RUBEN, On the moments of order statistics in samples from normal populations, *Biometrika* 41 (1954), 200-227.

[5] H. L. HARTER, Expected values of normal order statistics, *Biometrika* 48 (1961), 151-165.

[6] G. L. Tietjen, D. K. Kahaner, R. J. Beckman, Variances and covariances of the normal order statistics for sample sizes 2 to 50, *Selected Tables in Mathematical Statistics* 5 (1977), 1-73.

[7] S. S. Gupta, S. Panchapakesan, On moments of order statistics from independent binomial populations. *Ann. Inst. Statist. Math. Suppl*., 8 (1974), 95-113.

[8] A. C. Bovik, T. S. Huang, and D. C. Munson, A generalization of median filtering using linear combinations of order statistics, *IEEE Transactions on Acoustics, Speech, and Signal Processing*, 31-6 (1983),1342-1349.

[9] K. Dowd, Estimating VaR with Order Statistics, *The Journal of Derivatives*, 8 (2001), 23-30. [10] B. L. Browning, PRESTO: Rapid calculation of order statistic distributions and multiple-testing adjusted P-values via permutation for one and two-stage genetic association studies, *BMC Bioinformatics*, 9 (2008), 309.

[11] A. Katzur, U. Kamps, Order statistics with memory: a model with reliability applications, *Journal of applied probability,* 53 (2016), 974-988.

[12] H. A. David, H.N. Nagaraja, Order Statistics, John Wiley & Sons, New Jersey, USA, 2004, pp.9-10

[13] J.D. Gibbons, S. Chakraborti, Nonparametric Statistical Inference, Marcel Dekker, New York, USA, 2003, pp.53-54.

[14] B.C. Arnold, N. Balakrishnan, H. N. Nagaraja, A First Course in Order Statistics, Siam, Philadelphia, USA, 2008, pp.183-184.

[15] W. Hoeffding, On the distribution of the expected values of order statistics, *Ann. Math. Statist.*, 24 (1953), 93-100.

[16] H. O. Hartley, The probability integral of the range in samples of n observations from the normal population, Biometrika, 32 (1942), 301–308.

Chapter 14

BLACK HOLES

Nihal ERCAN[1]

1 Prof.Dr., Boğaziçi University,Physics Department

1. INTRODUCTION

From far away, stars are tiny points of light. But up close, stars are massive, seething, fiery balls of burning gas. This fierce display does not last forever. Eventually, the nuclear fusion which powers the star will burn all its fuel. Gravity then collapses the remaining matter together. For very large stars, what happens next is a display of extremes. First, the star explodes in a supernova, scattering much of its matter throughout the universe. For a brief moment, the dying star outshines its entire galaxy. But once the light fades and darkness returns, the remaining matter forms an object so dense that anything that gets too close will completely disappear from view which is a *black hole*.

Black holes are the strangest, extraordinary, finest formations in the universe that break all the laws of physics. It is the subject of the greatest and heated debates of the physics world and even the scientific world.

2. THEORETICAL ASPECTS OF BLACK HOLES

Starting from the past, everyone talked about it after Newton introduced the universal law of gravity. Different scientists who interpreted this law were coming to a conclusion at some point. The larger the mass of an object, the greater the gravitational effect had to increase. So anything that wanted to move away from a giant body, in this situation, had to move much faster. So what if the object had a mass that would stretch the limits of imagination, if it had tens of times more mass than the sun? In this case, even light cannot escape from this object. This is how the first assumption about black holes was 400 years ago: A dark star. It is not a very wrong conclusion according to that time. Because no matter what, a phenomenon that even light could not escape was not very acceptable. Something that even the light cannot escape. For a very long time, many physics and scientists were not dealed with this opinion that even the biggest names were unlikely. But the real debates started about 100 years ago with another revolution in the world of physics. The name behind this revolution was Albert Einstein. With the General Theory of Relativity, Einstein changed everything. He talked about Space-Time and said that the universe has a "fabric" and that is the larger an object, the more it bends. In fact, giant bodies would bend everything. Time also bends and time could stop at one point, this look like a crazy idea.

Starting off from this revolutionary theory, German physicist Karl Scwarzchild also made a very crazy conclusion. Keeping the mass constant, if you reduce the size of an object as much as possible, as much as the atoms allow, then its density will increase incredibly, and the curvature in space-time will also increase. For example, if we take the sun, this is what can happen when we reduce the sun to a diameter of 3 km, or reduce our

world to 9 mm in diameter, that is, to fit into a standard pistol bullet. So it's a big twist. Density would reach such a level at some point that space-time could bend "forever". So "forever" is just our deduction because of our inadequacy as human beings. In other words, when the earth is 9 mm, the object will bend the space-time so much that we cannot see it because even the light cannot escape. This is called as intensity limit, where light cannot escape, as the "event horizon". This is the starting point of the black hole phenomenon. However, despite all these assumptions, no one believed that "thing" exists in the universe. So it was something that completely broke the laws of physics.

But a 19-year-old Indian teenager, a very unknown name, a young genius named Subrahmanyan Chandrasekhar had idea about it. Thanks to his studies on the inner structure of stars, he was accepted to Cambridge University and his work on the White Dwarfs would shine a light here in the 1930s. White dwarfs are the creatures that emerge after the death of a star that consumes nuclear fuel. But there is a limit by which these stars can also shrink. It ejects some of its mass in a kind of explosion, and the remaining matter is compressed into a small star remnant with increased density. There is also a reason for this limit. Atoms allow a substance to shrink to a certain point so, a white dwarf can be as big as the earth but its mass as the sun. Imagine that a sugar cube can weigh several tons. At the time that Chandrasekhar was working in England, everyone thought that all stars were white dwarfs at the end of their lives, and that they completed their lives in this way. It was believed that there was a limit at which atoms could get stuck. But Chandrasekhar's calculations said very different things. It was concluded that these white dwarfs also continued to collapse and shrink into infinity after exceeding a certain mass limit. While it was previously believed that the limit at which a star could shrink was a maximum diameter of 10,000 km, Chandrasekhar found that if a star was about 1.4 times the size of our sun, it would not withstand its own gravitational effect and would continue to collapse into infinity.

This is the simplest definition of a black hole. But of course, these findings met with serious resistance in the scientific world. Another name, Sir Arthur Eddington, who was in Cambridge, where Chandrasekhar was located at that time, would have proved quite harsh. Eddington is one of the scientists who supported Einstein. He is the person who proved General Relativity with a solar eclipse, but the idea even sounded crazy to him. "Let's say a star has shrunk to a few kilometers. That's okay. But after that, it would simply say "absurd" in its simplest form to shrink to infinity as you say". After this, Chandrasekhar continued to work on this in America.

A new and very crazy finding that emerged in the scientific world during this period strengthen this claim again. It was known that atomic

nuclei consisted of protons and neutrons, and electrons were also in orbit. However, in 1932, it was discovered that in an extraordinary compression situation, electrons and protons could combine to form a structure consisting only of neutrons. And it has been theoretically proven that this neutron can become even more compressed and, in the case of a star 1.4 times bigger than the sun, transform into a "neutron star", one of the wildest structures in the universe, with a huge explosion like the neutron star in the Crab Nebula shown in the figure. The star surrounded by this nebula is a neutron star. It was mentioned before that 1 cube of sugar in a white dwarf can weigh several tons. In a neutron star, it is necessary to consider that a sugar cube can weigh hundreds of millions of tons. In other words, it is now known that a star does not remain in a white dwarf while it dies but there was more than that: Neutron stars but here again, there was resistance, and everyone said that the last point a star can reach is the Neutron Star, it cannot be beyond and that is impossible.

Here, the voice of a completely different scientist rose. J. Robert Oppenheimer, one of the smartest, most controversial, most loved, or most hated scientists in history. He reminds people of The Manhattan Project and Atomic Bombs. Anyway, Oppenheimer did his own calculations and calculated that if a star was 3 times the size of the sun, it would die while not staying in the neutron star. But of course the discussions do not end. Another famous name, John Wheeler, opposed Oppenheimer and said that after a star shrinks as the sun while losing its mass, the collapse will begin and eventually become either a neutron star or a white dwarf, beyond is meaningless. No one could admit that something so strange could exist. John Wheeler continued his studies to explain why the phenomena cannot happen. In fact, it is odd that it is John Wheeler himself who introduced the term "Black Hole" into the literature. But as Wheeler gets into it, he gets lost in it. He uses all the theories, general relativity, gravity, space-time and it did not happened. On their way to prove the impossibility of Black Holes, all the calculations showed one thing: there could be something called as Black Hole. It was supposed to be in line and had no other explanation. The dream of a 19-year-old, Chandrasekhar, who set off from India, came true. And after many years, all his efforts were finally appreciated and he received the Nobel Prize in Physics in 1983. So in the end, the existence of black holes became an indisputable fact. Moreover, it is now known how they came about. The complete recipe is achieved but something is missing, a black hole so the proof. There is not any image, or anything to prove its existence. Then, a new challenge began: finding the first black hole. It has become the dream of all scientists to find and prove a phenomenon that was initially thought to be improbable. The question that everyone is looking to answer right now is the gap between quantum

physics and the general theory of relativity. The theory that connects these two revolutionary phenomena is the theory of everything. Here, black holes can give the answer to that too. As much as Newton, as much as Einstein, thanks to a name that has barely mentioned before, Stephen Hawking carried out studies on this subject.

3. OBSERVATIONAL PROPERTIES OF BLACK HOLES

The idea of a black hole originated hundreds of years ago. In 1687, Isaac Newton published his landmark work known as The Principia. Here he detailed his laws of motion and the universal law of gravitation. Using a thought experiment involving a cannon placed on a very tall mountain, Newton derived the notion of escape velocity. This is the launch speed required to break free from the pull of gravity.

In 1783, the English clergyman John Michell found that a star 500 times larger than our sun would have an escape velocity greater than the speed of light. He called these giant objects "dark stars" because they could not emit starlight. This idea lay dormant for more than a century.

Then, in the early 20th century, Albert Einstein developed two theories of relativity that changed our view of space and time: the special theory and the general theory. The special theory is famous for the equation $E=mc^2$. The general theory painted a new and different picture of gravity. According to the general theory of relativity, matter and energy bend space and time. Because of this, objects which travel near a large mass will appear to move along a curved path because of the bending in spacetime. We call this effect gravity. One consequence of this idea is that light is also affected by gravity. After all, if spacetime is curved, then everything must follow along a curved path, including light.

Einstein published his general theory of relativity in 1915. And while Newton's theory of gravity could be expressed using a simple formula, Einstein's theory required a set of complex equations known as the "field equations." Only a few months after Einstein's publication, the German scientist Karl Schwarzschild found a surprising solution. According to the field equations, an extremely dense ball of matter creates a spherical region in space where nothing can escape, not even light. At first, the idea of a black sphere in space from which nothing could escape was considered purely a mathematical result, but one which would not really happen. However, as the decades passed, our understanding of the lifecycle of stars grew. It was observed that some dying stars became pulsars, another exotic object predicted by theory. This suggested that dark stars could actually be real as well. These strange spheres were named "black holes," and scientists began the hard work of finding them, describing them and understanding how they are created.

When it comes to finding black holes in universe, scientists had a hard time finding such an object in space that is completely black. Fortunately, since black holes have a large mass, they also have a large gravitational field. Thus, while we may not be able to see a black hole, we can observe its gravity pulling on its neighbors. With this in mind, astronomers looked for a place where a visible star and a black hole were in close proximity to one another. One such place is *binary stars*. A binary star is a system of two stars orbiting one another. We can spot them in several ways. You can look for stars that change position back and forth ever-so-slightly. Alternatively, if you observe a binary star from the side, the brightness will change when one star passes behind the other. So, it's possible that somewhere in space, there's a binary star consisting of a black hole and a visible star. In fact, such binary systems have been observed! Astronomers have found stars orbiting an invisible companion. From the size of the visible star and its orbit, astronomers calculated the mass of its invisible neighbor. It fit the profile of a black hole.

Since we can't see a black hole, is there a way to find its size? From Einstein's field equations, we know that given the mass of a black hole, we can determine the size of the sphere that separates the region of no escape from the rest of space. The radius of this sphere is called the Schwarzschild radius in honor of Karl Schwarzschild. The surface of the sphere is called the event horizon. If anything crosses the event horizon, it's gone forever — hidden from the rest of the universe. This means, once you know the mass of a black hole, you can compute its size using a simple formula. And it's actually quite easy to measure the mass of a black hole. Just take a standard issue space probe and shoot it into orbit around the black hole. Just like any other system of orbiting bodies — like the Earth orbiting the Sun, or the Moon orbiting the Earth — the size and period of the orbit will tell you the mass of the black hole. If you don't have a space probe handy, then compute the mass and orbit of a companion star and use that to find the Schwarzschild radius.

Black holes come in many sizes. If it was made from a dying star, then we call it a "stellar mass" black hole, because its mass is in the same range as stars. But we can go bigger - much bigger. And to do so, we are going to visit the center of a galaxy. Galaxies can contain billions and billions of stars, all orbiting a central point. Scientists now believe that in the center of most galaxies lives a black hole which we call a "supermassive black hole," because of its tremendous mass. The size can vary from hundreds of thousands to even billions of solar masses. For example, at the center of our own Milky Way galaxy is a supermassive black hole with a mass 4 million times that of our sun.

Black holes have another property we can measure - their spin. Just like the planets, stars rotate. And different stars spin at different speeds.

Imagine we can adjust the size of this star but keep the mass constant. If we increase the radius, the spinning slows down… If we decrease the size, the spinning speeds up. But while the rotational speed can vary, the angular momentum never changes - it remains constant. Even if the star were to collapse into a black hole, it would still have angular momentum. We could measure this by firing two probes into opposite orbits close to the black hole. Because of their angular momentum, black holes create a spinning current in space-time. The probe orbiting along with the current will travel faster than the one fighting it, and by measuring the difference in their orbital periods we can compute the black hole's angular momentum. This space-time current is so extreme it creates a region called the ergo-sphere where nothing, including light, can overcome it. Inside the ergo-sphere, nothing can stand still. Everything inside this region is dragged along by the spinning space-time. The event horizon fits inside the ergo-sphere, and they touch at the poles. So in one sense, black holes are like whirlpools of space-time. Once inside the ergo-sphere, you are caught by the current. And after you cross the event horizon, you disappear.

One final property of black holes we can measure is electric charge. While most of the matter we encounter in our day-to-day lives is uncharged, a black hole may have a net positive or negative charge. This can easily be measured by seeing how hard the black hole pulls on a magnet. But charged black holes are not expected to exist in nature. This is because the universe is teeming with charged particles, so a charged black hole would simply attract oppositely charged particles until the overall charge is neutralized. There are 3 fundamental properties of a black hole we can measure - mass, angular momentum, and electric charge. It is believed that once you know these three values, you can completely describe the black hole. This result is humorously known as the "no hair theorem," since other than these 3 properties, black holes have no distinguishing characteristics.

Although we have a good idea of a black hole from the outside, we do not have information about what it looks like on the inside. Unfortunately, we can't send a probe inside to take a look. Once any instrument crosses the event horizon, it's gone. However, if Einstein's field equations correctly describe space-time outside the black hole, then we can use them to predict what's going on inside as well. To solve the field equations, scientists considered two separate cases: rotating black holes, and non-rotating black holes. Non-rotating black holes are simpler and were the first to be understood. In this case, all the matter inside the black hole collapses to a single point in the center, called a singularity. At this point, space-time is infinitely warped. Rotating black holes have a different interior. In this case, the mass inside a black hole will continue to collapse, but because of the rotation it will coalesce into a circle, not a point. This circle has no thickness and is called a ring singularity.

Black hole research continues to this day. Scientists are actively investigating the possibility that black holes appeared right after the big bang, and the idea that black holes can create bridges called wormholes connecting distant points of our universe. The first-ever image of a black hole is released by the Event Horizon Telescope collaboration on April 10th, 2019. It shows plasma orbiting the supermassive black hole at the center of the galaxy M87. The bright region shows where plasma is coming towards us and since it's traveling near the speed of light it appears brighter when coming towards us and dimmer when going away. This is called relativistic beaming. From the images scientists can tell that the plasma is orbiting clockwise. It takes around 2 days for the plasma to complete one orbit. Here we are looking at the black hole using electromagnetic waves with a wavelength of 1.3 millimeters - radio waves.

3.1. Image of the Black Hole

Below is a photograph of a galaxy 55 million light-years away from us, a huge black hole at the center of the galaxy M87.

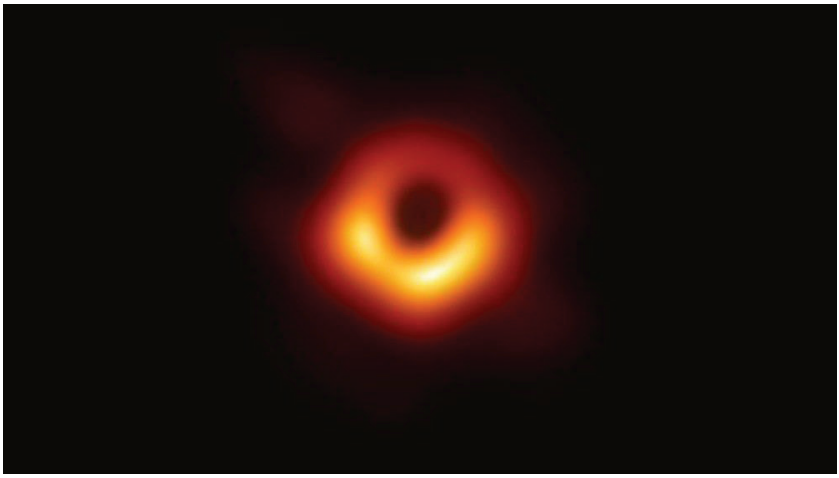

Figure 2.1*: Photograph of black hole at the center of the galaxy M87 (6)*

This is a real black hole photo so one of the greatest achievements in human history. Until photograph was taken, all the black hole pictures were models, drawings, illustrations. It was known black holes existed, but there was had no evidence. Turkey time on April 10, 2019 16: 00 scientists from across the world announced at a press conference conducted at the same time to share these photographs. The reason why this event is shared with the same excitement and happiness all over the world is that thousands of people struggled for years to create this photo and mobilized all their time and resources for a common purpose. There are several reasons why this photo is so important. Firstly, it is known that at the center of the Milky Way galaxy, 26000 light-years from us, there is a black hole in a chaotic nebula

called Saggitarius A, and for many years, scientists have tried to image this black hole, and the photo was not clear. There are several reasons for this. In fact, it is very difficult to view this black hole, although it is much closer than the M87 since this black hole is so small. In other words, it stays as much as a basketball ball next to the black hole in the M87. Due to its small size, its movement speed is much higher. Also, the black hole found in Sagittarius A is in a very chaotic group. In other words, it is covered with clouds and unfortunately there is no clear image. Therefore, scientists are turning their eyes to the galaxy M87. The black hole here is much bigger and moves much slower therefore a much clearer image can be obtained . The galaxy M87 is so far away that a telescope that can get there must be as big as our world. To solve this problem, different telescopes placed at 8 different points of the world were connected to each other, allowing it to work like a single telescope. Thanks to this, a picture of a black hole far away from world was taken. The regions where these telescopes are located on are 4 sides of the world, and the air must be clear at the same time. This alone is a very, very difficult situation. For this reason, scientists have been waiting for this opportunity for months. Apart from that, very reliable and error-free algorithm is needed to interpret, analyze, combine and turn the received data into a photograph.

The most important feature of this photo, is that this black hole is also a proof of the General Theory of Relativity developed by Einstein almost 100 years ago. Einstein said in his theory that a matter of sufficient mass and density can even absorb light into a gravitational field and trap it. Since nothing can move faster than light, according to the laws of physics, it can be said that there is no exit from black holes.

In the same theory, when defining black holes, Einstein mentions that there is an invisible part in a circle called the event horizon and he mentions that there is a point in the center of this invisible part that we can call singularity. This is where the laws of physics lose their validity since neither light, nor speed, nor mass exists at that point.

There are planets, stars, meteorites, asteroids in the red area in the photo that starts where the event horizon ends and it is around the black hole. The reason why it is red is that the black hole apparently rotates clockwise and begins to rotate at a speed close to the speed of light as all the matter around it is pulled towards it. In the meantime, they rub against each other. As a result, temperatures up to millions occur. As a result of this heat, they emit X rays. In the future, the goal is to follow this black hole and watch its movements, development and changes. Even by placing a telescope in space to photograph more clearly and maybe even shoot a video of the black hole.

4. DISCUSSION & CONCLUSION & RESULTS

The uncertainty of "quantum physics" is discussed in general. However, as in classical physics, there is a certain "determinism", or certainty, in quantum physics. It may not known exactly where a particle is, but it can said that it is in a "cloud of possibility". As time passes, the location of this probability cloud will also change, but it ca be predicted where this cloud will be. When all the information about the quantum state of an object is obtained such as momentum, spin etc., the future also can be predicted.

According to the "Law of Conservation of Energy", energy must remain constant in closed systems. In other words, the total amount of energy does not change unless it interacts with an outside system, it just changes shape. When the universe is considered as a closed system, the energy in it is fixed and unchangeable. When we adapt this to "knowledge", that is, the conservation of information, people can get a little confused. Because we can create information very comfortably and we can destroy that information with different methods. But. All information available in the quantum universe can neither be created nor destroyed. So when you produce information, you are actually just changing the form of existing information.

4.1. The Paradox of Black Hole

As no scientific discovery can be attributed to a single person, here too, when Stephen Hawking spoke with Soviet scientists Yakov Zel'dovich and Alexei Starobinsky in 1973 in Moscow, these scientists said that the rotating black holes formed particles and black holes also repel these particles in a way. When Hawking took this prediction and did the calculations, he saw that not only rotating but also fixed black holes produced a "radiation". In other words, black holes had a certain temperature and with this phenomenon that is called as "Hawking radiation" today, in fact, black holes were evaporating like boiling water in the furnace and losing their energy and thus their mass. Black holes were not really dark or anything. After a certain time the black hole would evaporate and disappear at some point. It is worth highlighting here. It takes billions of years for a black hole to disappear in this way, but that's the theory so, black holes are also dying. The trouble comes across exactly at this point. Hawking Radiation, Hawking Radiation is a thermal radiation and it does not carry information. It is a completely random glow and all black holes evaporate in a similar glow, regardless of what is contained in it. In other words, the phenomenon that we call Hawking Radiation is entirely related to the mass, rotation and charge of the black hole. It has no other features. So all black holes are exactly the same except for these features. The information about the particles contained in it is not found in Hawking Radiation. As the radiaiton and evaporation continues, one day the black hole will die.

There are different theories. Let's look at the possible explanations that sound the most. The existence of black holes is known long before. According to Einstein's Theory of General Relativity guesses are made. However, Quantum Mechanics is used while trying to explain Hawking Radiation. It is known that general relativity and quantum physics in particular do not get along well. In order to explain Hawking Radiation, two revolutionary laws that best explain the universe must be united. Another great paradox for the scientific world emerges here. Black hole takes a material and never gives it back, let's imagine it died one day, throwing all his energy away with Hawking Radiation and all the information inside is disappearing as well which cannot be explained. It can be predicted as the information is not actually lost but maybe the radiation contains the information. However, any mathematical model did not solve this problem, no close explanation has been given, including Stephen Hawking himself. I t can be deduced either there is something that human eye cannot see or something is missing or maybe our mathematical models are not enough for now, they must be progressed.

More observations are in need to solve the puzzle; so most reliable and high technology satellites will provide us more and more results in the near future.

I would like to thank Aysun Cece, one of my undergraduate students for her hard work for this review.

REFERENCES

[1] https://www.nasa.gov/audience/forstudents/k-4/stories/nasa-knows/what-is-a-black-hole-k4.html (retrieved at January 2021).

[2] https://www.nationalgeographic.com/science/space/universe/black-holes/ (retrieved at January 2021).

[3]https://www.space.com/15421-black-holes-facts-formation-discovery-sdcmp.html (retrieved at January 2021).

[4] https://www.britannica.com/science/black-hole (retrieved at January 2021).

[5]https://www.sciencemag.org/news/2021/01/after-decades-effort-scientists-are-finally-seeing-black-holes-or-are-they (retrieved at January 2021).

[6] https://www.space.com/first-black-hole-photo-science-breakthrough-2019.html (retrieved at January 2021).

Chapter 15

THE STATUS OF MYCETOZOA STUDIES OF THE WORLD AND TURKEY

Hasan AKGÜL[1]
Celal BAL[2]
Emre Cem ERASLAN[1]
Ali İmran KORKMAZ[3]

1 Akdeniz University, Science Faculty, Department of Biology, Antalya, Turkey.
2 Gaziantep University, Oguzeli Vocational School, Gaziantep, Turkey.
3 Gaziantep Islam, Science and Technology University, Health Services Vocational School, Department of Medical Services and Techniques, Gaziantep, Turkey.
Orcid id : https://orcid.org/0000-0001-8514-9776, 0000-0001-6856-3254, 0000-0003-1773-1443, 0000-0002-5194-5528

INTRODUCTION

The myxomycetes (Mycetozoa) are a group of primitive phagotrophic eukaryotes, commonly associated with decaying plant material in terrestrial ecosystems (Stephenson and Stempen, 1994). Myxomycetes live predatory on other microorganisms such as bacteria, yeasts, algae, or true fungi, feed phagotrophically on bacteria, yeasts, spores of filamentous fungi, algae, and other protists the production of fruiting bodies and dispersal by spores, cause myxomycetes to appear similar to fungi (Baba, 2012; Sevindik and Akgül, 2019). The life cycle of a myxomycete includes two morphologically distinct trophic stages, one consisting of uninucleate amoebae (with or without flagella), and the other consisting of a distinctive multinucleate structure, the plasmodium. Under favorable condition, the plasmodium will give rise to fruiting bodies containing spores (Martin et al. 1983; Baba et al., 2016a).

Myxomycetes are classified in the kingdoms of Plantae (class Myxomycota) and Animalia (class Mycetozoa). Because, myxomycetes are typically found in the same habitats as fungi and presence of spores, they considered as Kingdom Mycota (class Myxomycetes). However, because of the lack of a mycelium (the diagnostic characteristic of true fungi) and absence of a rigid cell wall in the amoeboid and the plasmodium, plus ingestion of food by mean of phagocytosis, unlike fungi, myxomycetes do not excrete extracellular, digestive enzymes they cannot be considered fungi. More recently, phylogenetic analysis on highly conserved, elongation factor 1-alpha (EF-1α) gene sequences and demonstrated that myxomycetes are not fungi. Physiological, morphological, historical, and genetic analyses support the classification of myxomycetes in the kingdom Protoctista along with other eukaryotic microorganisms (Baldauf and Doolittle 1997; Baba, 2017; Baba et al., 2018).

The History of Mycetozoa

The first scientific treatment of fungi, including myxomycetes, was by the Italian Pier Antonio Micheli. Micheli appears to be the first person to have used a microscope in the study of fungi and to realize the role of spores. The first literature on myxomycetes dates back to 1654 with Pankow's figure and illustration of the species now known as *Lycogala epidendrum* (L.) Fr. Myxomycetes have a fossil past that dates back to stalked sporangia of *Stemonitis splendens, Arcyria sulcata* and *Protophysarum balticum* that are well preserved in Baltic amber from the Tertiary Period and Eocene Epoch approximately 35 to 40 million years ago (Keller and Everhart 2008). Although Linnaeus Species Plantarum, published in 1753, is the nomenclatural starting point for the Myxomycetes, his treatment of them was best summed up by Martin and Alexopoulos 1969. Fruiting

bodies of several species of myxomycetes are funguslike in appearance and the first species noted in the literature were classified within the fungi. A good example is the species now called *Lycogala epidendrum*. Linnaeus (1753) referred it to the genus *Lycoperdon*, apparently based on its gasteromycete-like habit.

For the first time, Persoon classified Myxomycetes as fungi in Gastromycetes in his work titled "Synopsis Methodica Fungorum" (1801). Fries (1829) regarded the myxomycetes as related to gasteromycetes but because of their possession of motile cells and a plasmodium in the life cycle they were accommodated in a distinct suborder, the Myxogastres, within the Order Gasteromycetes in his monumental work "Systema Mycologicum, Vol. III" (1829). The name, myxomycetes (in Greek, myxa – slime, myketes- fungi) was first used by Heinrich Link in 1883. As the name implied, Link (1883) considered myxomycetes as fungi. However, this view was not commonly supported by other biologists at that time. When the life cycle of Myxomycetes was studied in more detail after the middle of the 19th century, thanks to the availability and improved quality of microscopes, it became evident that they were closer to amoeboid protozoa than to fungi in structure and life cycle, and the name Mycetozoa was proposed by many researcher (Stephenson and Stempen, 1994). He world monograph, "The Myxomycetes" by Macbride and Martin was published in 1934 and recognized a total of 59 genera, 366 species, and 40 varieties.

In their study, Martin and Alexopoulos (1969) divided Mycota into two sub branches as Myxomycotina and Eumycotina and grouped myxomycetes class in Mycotina and other mushrooms in Eumycotina. Almost 50 years have passed since the publication of the world monograph The Myxomycetes by Martin and Alexopoulos (1969). The book represented a major taxonomic platform by stimulating interest in these organisms and encouraging further studies. A considerable number of myxomycete papers now appear every year and among them are several books. Many books published during the past 50 years are of a monographic nature but geographically restricted. Examples include Sluzowce Polski (Krzemieniewska, 1960), De Nederlandse Myxomyceten (Nannenga-Bremekamp, 1974), A Guide to Temperate Myxomycetes (Nannenga-Bremekamp, 1991), Flora Neotropica Monograph No. 16. Myxomycetes (Farr, 1976), The Myxomycetes of Japan (Emoto, 1977), Indian Myxomycetes (Lakhanpal and Mukerji, 1981), Definitorium Fungorum Rossiae. Divisio Myxomyctota (Novozhilov, 1993), the volume Myxomycetes I of the Flora Mycologica Iberica (Lado and Pando, 1997), The Myxomycete Biota of Japan (Yamamoto, 1998), The Myxomycetes of Britain and Ireland (Ing, 1999), Myxomycetes of New

Zealand (Stephenson, 2003), and Limasienet (Finnish myxomycetes) (Härkönen and Sivonen, 2011). The three-volume work Die Myxomyceten (Neubert et al., 1993; Neubert et al., 1995; Neubert et al., 2000) treats the myxomycetes of Germany and neighboring regions of the Alps. Les Myxomycètes (Poulain et al., 2011) essentially covers the species of central Europe but includes numerous species thus far found only in other parts of the world (Ing and Stephenson, 2017).

The moist chamber culture technique that was introduced by Gilbert and Martin (1933) has led to the discovery of many new tiny myxomycetes found on the bark of living trees. With moist chamber culture technique obtained more myxomycetes than natural (Baba et al., 2016b). North American Flora project as author of The Myxomycetes published by the New York Botanical Garden (Martin 1949). The subsequent world monograph, (Martin and Alexopoulos 1969) is still considered the most authoritative work on the subject. According to Alexopoulos et al. (1996), Mycetae divided 3 divisio Gymnomycota, Mastigomycota and Amastigomycota, Myxomycetes with Protosteliomycetes in subdivisio Plasmodiogymnomycotina and have 3 subclass and 6 ordo. The firs modern classification of Myxomycetes maded by de Bary's student Joseph Rostafinski and this classification is uses now. Phylum Myxomycota has one clasis Myxomycetes and in this class 3 subclass and 6 order. Martin et al. (1983), based on the type of development of the fruiting bodies and type of plasmodia, recognized, in this class, three subclasses, Ceratiomyxomycetidae, Myxogastromycetidae, and Stemonitomycetidae. This division has been largely accepted and serves as a basis for the general classification presented here. These orders are: Liceales, Echinosteliales, Trichiales, Physarales, Stemonitales and Ceratiomyxales. The basis of this distinction is based on the development of sporofor, the type of sporofor produced, the method of sporofor production, spor color, the presence or absence of capilium, the presence or absence of lime, and plasmodium types (Alexopoulos et al., 1996). In 2001, Lado published Nomenmyx, which involved the monumental task of searching the literature for names of myxomycete species. Of the 4000 names applied to various myxomycete taxa the uncovered, 900 are current names for accepted species. These names are now in a database that can be updated over time with the addition of new names and which has been developed into the online resource nomen.eumycetoza.com. Lately, based on small-subunit ribosomal-DNA (SSU rDNA) sequence phylogeny, myxomycetes are placed into the Protozoa. However, only one species of myxomycetes, *Physarum polycephalum* was included in the analysis. Gene analysis of the elongation factor EF-1 α revealed that the clade formed by Physarum (myxomycetes), Dictyostelium (Dictyostelids),

and Planoprotostelium (Protostelids) is the sister group of Animalia and Fungi. In general, literature on the origin and evolution of myxomycetes based on molecular methods is not well defined. However, nowadays, most of myxomycologists and mycologists agree with the classification of myxomycetes as a class in the Phylum Myxostelida that belongs in the Kingdom Protozoa (Baldauf, 1999; Lado, 2001).

The latest situation of Mycetozoa

Distribution Taxonomical and Ecological investigation

There have been several studies on the ecology and taxonomy of myxomycetes in various parts of the world. Northeastern America and India (Stephenson et al., 1993), Taiwan (Chung and Liu, 1996), Hong Kong (Chung, 1997), Israel (Nissan, 1997) Costa Rica (Schnittler and Stephenson, 2000), high latitude regions of the Northern Hemisphere (Stephenson et al., 2000), Austria (Singer et al., 2001), New Zealand (Stephenson, 2003), Puerto Rico (Novozhilov et al., 2001), Upper Egypt (Abdel- Raheem, 2002), and Mexico (Lado et al., 2003), Europe (Moreno et al., 2003), Japan (Takahashi and Hada, 2009); and Turkey (Baba et al, 2019). About 115 checklists for countries or larger regions are published, but many of them do not include studies with the moist chamber method. Remarkable local monographs were published by Nannenga-Bremekamp (1974, 1991) focusing on the Netherlands; or Neubert et al., 1993; Neubert et al., 1995; Neubert et al., 2000 for Germany and Austria. The latter monograph is especially noteworthy by the excellent drawings and colour photographs of myxomycete fructifications. Novozhilov (1993) published a monographic treatment for Russia, likewise Yamamoto (1998) for Japan. One of the most complete treatments is the myxomycete flora for Great Britain (Ing, 2000), followed by the Irish checklist (Ing and McHugh, 1988). Other countries with a very well studied myxomycete flora are Finland (Härkönen 1979a; Härkönen et al., 1999), Germany (Schnittler et al. 1996), India (Lakhanpal and Mukerji, 1981) and Spain (Lado, 1993) and Turkey (Baba and Sevindik, 2019). (Ing and Stephenson, 2017).

The first studies carried out in Turkey on Myxomycet are made by Lohwag (1957). *Lycogala epidendrum* (L.) Fr. from Bolu and Istanbul Belgrad Forests reported the type. Harkönen and Uotila (1983) made their first studies on myxomycetes in floristic sense. In the field studies carried out by the researchers in Marmara and Western Anatolia, they found 43 myxomycete species by using live tree bark, moist room culture technique. The first study of local scientists was presented by Gücin and Öner (1986) (Baba and Tamer, 2007). Also, different researchers have done many myxomycetes studies. (Ergül et al., 2005a; Ergül et al., 2005b;

Ergül and Akgül, 2011; Ergül et al., 2016; Baba et al., 2020a; Baba et al., 2020c; Baba et al., 2021a; Baba et al., 2021b; Baba et al., 2021c).

Later in the checklists; 102 taxa from Ergül and Dülger (2000c),177 taxa from Sesli and Denchev (2005), 202 taxa from Dülger (2007), 232 taxa from Sesli and Danchev (2014), 252 taxa from Sesli et al (2016) and 286 taxa from Baba and Sevindik (2019) have published in the lists. Today, the number is still 286 Myxomycet known in Turkey. The Mycetozoa are considered to represent a taxonomic divisio Protosteliida, Echinostellida, Liceida, Trichiida, Physarida and Stemonitida. Mycetozoa are 6 orders, 15 families, 63 genera and 1041 species in world. In Turkey 6 orders, 13 families, 45 genera and 291 species (Lado, 2020; Baba ve Sevindik, 2020b; Baba et al., 2021a; Baba et al., 2021b).

Moleculer investigations

Even though the morphological identification of myxomycetes is relatively constant, and readily observable, inherent genetic and environmental variations may sometimes create difficulties in preparing precise morphological descriptions. In addition, Clark (1995) indicated that myxomycetes have a relatively limited number of morphological traits; moreover, geological distribution and frequent asexuality can make species definitions especially difficult. Therefore, when using morphological characteristics only, it may be difficult to avoid making overlap in species identifications. On the basis of evidence from molecular studies, some workers suggested that myxomycetes would have a significant evolutionary history with other eukaryotes. However, due to the fragile nature of the fruiting body, fossil records of the group are exceedingly rare. Consequently, there is little known concerning the genetic diversity of myxomycetes (Cavalier-Smith, 1993).

A few studies have attempted to quantify plasmodia in the soil by using a simple enumeration technique in order to evaluate the abundance of myxomycetes, however, there is still a need to develop more effective methods to characterize myxomycete biodiversity and ecology in the environment. Stephenson et al. (2008) suggested that direct environmantal sampling with the use of molecular techniques had considerable potential value for revealing the hidden taxa or population such as myxoamoebae and plasmodia of myxomycetes (Feest and Madelin, 1985a).

However, the literature available on most aspects of the molecular biology of myxomycetes is not very extensive. Virtually all early studies were directed towards the model species Physarum polycephalum. Recently, a number of studies have demonstrated that it is possible to design myxomycete-specific primers. A couple of studies have provided

some data relating to phylogenetic analysis among the higher orders and within the dark-spored members of myxomycetes. There have been only two previous instances in which molecular fingerprinting has been applied to the study of diversity in myxomycetes. The first involved the detection of myxomycetes from soil and the second represented an effort to detect these organisms from airborne spores. However, data from molecular studies of these organisms are still rather limited (Fiore-Donno et al., 2008).

Cavalier-Smith (1993) suggested placing the myxomycetes into the Kingdom Protozoa according to the molecular phylogeny results on small-subunit ribosomal-DNA sequence analyses. Gene analysis of the elongation factor EF-1A revealed that the clade formed by Physarum (myxomycetes), Dictyostelium (dictyostelids), and Planoprotostelium (protostelids) is the sister group of Animalia and Fungi. According to DNA and RNA analyses, myxomycetes should be placed within the "crown" clade of eukaryotes.

Baba et al. (2015), 7 different PCR primers targeting 18 different myxomycetes genera were designed and ribosomal DNA ITS1-5.8SrDNAITS2 regions of 52 morphologically characterized species from Turkey were amplified and sequenced.

Significances of Mycetozoa

Although myxomycetes have no direct economic value, they play very important roles in the ecosystem and in some aspects of human life (Baba and Sevindik, 2018). Myxomycetes possess the mobile, giant cell with multi – nuclei existing independently, and especially non-enclosed by a cell wall. In many cytological, molecular, biochemical, and biophysical laboratories to investigate fundamental biological problems such as cell differentiation (cancer-cell development), cell movement, nuclear division (Monnat, 1999). Myxomycetes have been used as biological resources in laboratory studies of various aspects of cellular physiology and biochemistry. For example, the vigorous protoplasmic streaming exhibited by some types of plasmodia represents an ideal situation for studying cellular motility. The majör transformation in the life cycle of a myxomycete from uninucleate amoeboflagellate cells to a multinucleate plasmodia and then to fruiting bodies makes these organisms suitable for use as experimental organisms for studies of cell growth and differentiation. Wormington and Weaver (1976) reported that myxomycetes have been used in cell differentiation studies connected with cancer research since the biochemical changes that take place during the process of the plasmodium differentiating into fruiting bodies are suggestive of the changes that take place when a normal cell becomes cancerous. In experiments designed to

determine aging and lifespan, Didymium iridis and Physarum cinereum plasmodiums have shown that longevity and aging are not due to genetic nuclear factors, but to stoplasmic factors (Clark and Lott, 1989).

The most remarkable feature of cancer treatment myxomycetes is that Polycefin is capable of breaking down the non-toxic immunogenic substance called Polycefin in the drug delivery system. And this compound is synthesized by *Physarum polycephalum*. As with immunoflourescent or immunoperoxidase staining methods, the fluorescently labeled antibody molecule for the detection of antigen was injected into the vein in the mouse and its tail and observed to accumulate inside the breast and brain tumor cells. (Ljubimova et al. 2008).

Both of the two trophic stages of myxomycetes are known to feed upon bacteria; and myxomycetes have a significant role in maintaining the natural balance that exists between bacteria and other micro-organisms in the soil environment. In soil microbial communities, the amoeboid stages of dictyostelids (cellular slime molds) and myxomycetes (plasmodial slime molds), and the plasmodial stage of myxomycetes make up a substantial proportion of the bacterivores present in most soils and this fact seem to suggest that myxomycetes play a key role in the detritus food chain. Recently, extraction of the bioactive chemicals from some species of myxomycetes has received attention, and these have produced some certainly prospective results. An anti–inflammatory substance, which can affect mucous membranes, has been isolated from fruiting bodies of *Lycogala epidendrum* and can be used as external application. Two unusual new triacylglycerols, two new diacylglycerols, and lycogalic acid dimethylesterns were also harvested from *Lycogala epidendrum* (Buchanan, 1996).

In a molecular study on myxomycetes, the reproductive structures of *Cribraria purpurea* were collected from the Kochi Region in Japan, and Cribrarione A was obtained. Cribrarione A (1), isolated from *Cribraria purpurea*, was found to be a new dihydrofuranonaftoquinone pigment with antimicrobial activity against *Bacillus subtilis* (Naoe et al. 2003).

Chemical studies on the secondary metabolites of the myxomycetes demonstrated that myxomycetes have developed rather unique secondary metabolites. Almost 100 natural compounds including their chemical structures and biological activities are described; Lipids, Fatty acid amides and derivatives, Alkaloids, Amino acids and peptides, Naphthoquinone pigments, Aromatic compounds, Carbohydrate compounds, Terpenoid compounds. These compounds include; inhibitory effect against cancer cells, having antimicrobial activity against fungi and bacteria, has an

antibiotic effect, cytotoxic effect, used to develop of medicines (Dembitsky et al. 2005).

Myxomycetes have been used as biological resources in laboratory studies of various aspects of cellular physiology and biochemistry. For example, the vigorous protoplasmic streaming exhibited by some types of plasmodia represents an ideal situation for studying cellular motility (Stephenson and Stempen, 1994). The majör transformation in the life cycle of a myxomycete from uninucleate amoeboflagellate cells to a multinucleate plasmodia and then to fruiting bodies makes these organisms suitable for use as experimental organisms for studies of cell growth and differentiation. An anti-inflammatory substance, which can affect mucous membranes, has been isolated from fruiting bodies of Lycogala epidendrum and can be used as external application. The fruiting bodies of Tubifera dimorphotheca have produced two triterpenoid lactones (Tubiferal-A and B) and one of these (Tubiferal-A) possesses a new compound that exhibited a reversal effect of vincristine resistance against VCRresistant KB cell lines (Kamata et al., 2004). Recently, bisindole alkaloids isolated from myxomycetes have received considerable attention because they have potential for biological activity as small-molecule Wnt signal inhibitors. Kamata et al. (2005) reported that bisindole alkaloid compounds were successfully isolated from the naturally occurring fruiting bodies of Arcyria cinerea and Lycogala epidendrum. Among these compounds, one bisindol alkaloid compound (named bisindoles A12) showed cytotoxicity against cultured tumor cell lines. Kaniwa et al. (2007) successfully isolated bisindole alkaloids from the sporocarps of *Arcyria ferruginea*.

Dülger and Ergül in Turkey (2001) investigated the antimicrobial activity of Enteridi miksomiset I splendens species. In the study, Enteridium splendens extracts determined that they showed quite high antimicrobial activity against some Gram (-) bacteria, especially *Escherichia coli* and *Enterobacter aerogenes*. In addition, it has been found that it has no antimicrobial activity against Gram (+) bacteria, yeast cultures and acid-fast *Mycobacterium smegmatis*. Another antimicrobial study was done with myxomycet *Lycogala epidendrum*. The chloroform and ethanol extracts from *L. epidendrum* did not show antimicrobial activity against Gram (+) bacteria, but showed an antimicrobial activity on Gram (-) bacteria (Dülger et al., 2007).

Furthermore, some species of myxomycetes could be used as a human food source. Examples include young aethalia of Enteridium lycoperdon and the plasmodium of *Fuligo septica*, which are collected, fried, and eaten by some indigenous peoples in the state of Veracruz in Mexico. Moreover, plasmodia and fruiting bodies of some myxomycetes are very beautiful and intriguing such that myxomycetes have become

"irresistible models" for photographers and other people encountering them in nature. Myxomycetes feed on bacteria, fungal spores and the other minute organisms, but they also provide favorable substrates and shelters for various species of fungi and insects (Stephenson and Stempen, 1994). *Physarum album* could be consumed as a natural antioxidant and antimicrobial source (Sevindik et al. 2018).

Plasmodia of some myxomycetes, such as *Fuligo septica* and *Physarum cinereum* are very large, colonising ornamental plants, and lawns, rendering them unsightly, even though they are harmless organisms. Plasmodia and fruiting bodies of some myxomycetes are very beautiful and intriguing such that myxomycetes have become "irresistible models" for photographers, and people encountering them (Stephenson and Stempen, 1994).

Future study

As biology science advanced in the second half of the 20th century, the physiology, biochemistry and genetics of myxomycetes began to attract the attention of experimental biologists. A valuable glance was provided by Myxomycetes Biology by Gray and Alexopoulos (1968). Another useful introduction is Ashworth and Dee (1975), with some emphasis on genetics. The complex life cycle of these relatively simple organisms provides distinct stages where developmental transitions can be studied. Descriptions of these stages have been reviewed and include the following transitions: myxamoebae to cysts, myxamoebae to flagellated cells, myxamoebae to plasmodia, plasmodia to spherules (sclerotia), and plasmodia to fruiting bodies.

Preservation of myxomycete collections in the past usually involved exposure to para-dichlorobenzene (PDB) and/or naphthalene (organic chemical compounds present in mothballs) used to protect against insects, mites, and fungal contaminants. This was standard practice for many herbaria of the mid-twentieth century. However, combination of age and treatment with organic agents appears to fragment DNA in older type myxomycete specimens, which impedes DNA amplification for taxonomic molecular studies. PDB adversely affects life cycle stages, myxamoebae died, plasmodia stopped protoplasmic streaming within 40 seconds and caused death after 20 minutes. Additional experiments showed that spores from sporangia of Comatricha nigra, Trichia varia and T. favoginea collected on decaying wood showed a consistent reduction in the percentage of germinated spores when exposed to vapor from PDB crystals. Furthermore, after exposure to PDB, spores were abnormally wrinkled and distorted in shape. These experiments also showed that

the percentage of spore germination decreased markedly after only three months (Keller, 2012).

The United States National Fungus Collections (USNFC)— The USNFC has a herbarium, a library and extensive databases and web resources that serve as a national and international resource. It is managed under the Systematic Mycology and Microbiology Laboratory (SMML), a federal laboratory of the US Department of Agriculture. There is a good overview of the resources with links to each.

It is very important to develop new and easier methods on alternative production methods of myxomycetes in the future (Baba, 2018). In addition, it is important to conduct new research on ecological demands of myxomycetes on production parameters. (Zümre et al. 2019). The importance of spore to-spore culture of myxomycetes and the deposit of living cultures with the United States American Type Culture Collection (ATCC) provides future source materials for scientific experimentation, genetic discovery, and species validation. The mission of ATCC (www.atcc.org), a private nonprofit biological resource center and research organization, is to acquire, authenticate, preserve, develop, standardize, and distribute biological materials and information for the advancement and application of scientific knowledge (Keller, 2012).

Future directions using DNA sequencing techniques will surely unlock many phylogenetic mysteries among the five myxomycete orders (Echinosteliales, Liceales, Trichiales, Stemonitales, Physarales) plus a number of genera difficult to classify. DNA analysis of some taxa is performed due to their uncertain taxonomic positions. The further increase of these analyzes will allow the diagnosis of species with suspected or undiagnosed morphological diagnosis.

Myxomycetes are known to produce various metabolites, and the bioactivities of these metabolites have been subjected to study, especially over the past couple of decades. Some of those metabolites have been demonstrated to possess antibacterial, cytotoxic, and antioxidant activities.

Conclusion

Myxomycetes have been thought to represent a potential source of natural active products that have unique chemical structures, and studies carried out to date have proved this to be the case. However, additional investigations are still required because the number of species examined thus far is still relatively small. Nevertheless, myxomycetes have a unique life cycle and are expected to produce many useful metabolites.

REFERENCES

1. A .M .Fiore-Donno, M. Meyer, S. L . Baldauf, J. Pawlowski, ‘’ Evolution of dark-spored myxomycetes (slime-molds): molecules versus morphology.’’ *Mol. Phylogenet. Evol.,* 46: 878–889, 2008.
2. A. Feest, M. F. Madelin, ‘’A method for the enumeration of myxomycetes in soils and its application to a wide range of soils. ‘’FEMS Microbiology Ecology, 31: 103 – 109, 1985a.
3. A. M. Abdel-Raheem, ‘’Myxomycetes from upper Egypt.’’ *Microbiological research*, 157(1), 47-67,2002.
4. A. Naoe, M. Ishibashi, Y. Yamamoto, ‘’ Cribrarione A, a new antimicrobial Naphthoquinone pigment from a myxomycete *Cribraria purpurea*.’’ *Tetrahedron*, 59: 3433–3435, 2003.
5. B. Dülger, C. Ergül, ‘’Miksomiset *Enteridium splendens* (Morgan) Macbr.’in antimikrobiyal aktivitesi.’’ *Ot Botanik Dergisi,* 8 (1): 133-140, 2001.
6. B. Dülger, T. B. Süerdem, M. Hacıoğlu, ‘’*Lycogala epidendrum* (J.C.Buxb. Ex L.) Fr’un (Miksomiset) Antimikrobiyal Aktivitesi.’’ *Afyon Kocatepe Üniversitesi,* 7 (1): 259-266, 2007.
7. B. Ing, ‘’Microsphaera azaleae, the perfect state of the Rhododendron mildew in England.’’ *Mycologist*, 14(4), 165, 2000.
8. B. Ing, ‘’The myxomycetes of Britain and Ireland: an identification handbook.’’ *Richmond Pub. Co.,* 1999.
9. B. Ing, R. McHugh, ‘’A revision of Irish Myxomycetes. In Proceedings of the Royal Irish Academy. Section B: Biological, Geological, and Chemical Science’’ *Royal Irish Academy*, 99-117, 1988.
10. B. Ing, S.L. Stephenson, ‘’The History of the Study of Myxomycetes, Chapter 2: in Myxomycetes: Biology, Systematics, Biogeography, and Ecology, Edited by Stephenson S.L. and Rojas,’’ *C. Academic Press is an imprint of Elsevier*, ISBN: 978-0-12-805089-7, 2017.
11. B. Nissan, ‘’Myxomycetes from Israel IV.’’ *Mycoscience*, 38(1), 87-89, 1997.
12. C. H. Chung, C. H. Liu, ‘’More fimicolous myxomycetes from Taiwan.’’ *Taiwania-Taipei*, 41, 259-264, 1996.
13. C. Lado, ‘’A checklist of myxomycetes in Mediterranean countries.’’ *Mycotaxon,* 52: 117–185, 1994.
14. C. Lado, ‘’ Bases corológicas de flora micológica ibérica’’ *Editorial CSIC-CSIC Press.* 376(692), 1993
15. C. Lado, ‘’An on line nomenclatural information system of Eumycetozoa’’. *Real Jardín Botánico, CSIC*. Madrid, Spain. http://www.nomen.eumycetozoa.com. Last updated June 09, 2020.

16. C. Lado, ‘’Nomenmyx. a nomenclatural taxabase of myxomycetes.’’ *Cuadernos de Trabajo de Flora Micológica* Ibérica, 16: 1–221, 2001.

17. C. Lado, A. Estrada-Torres, S. L. Stephenson, D. Wrigley de Basanta, M. Schnittler, ‘’Biodiversity assessment of myxomycetes from two tropical forest reserves in Mexico.’’ *Fungal Diversity,* 12(1), 67-110, 2003.

18. C. Lado, F. Pando, ‘’Flora Mycologica Iberica, Vol. 2. Myxomycetes, I. Ceratiomyxales, Echinosteliales,Liceales, Trichales’’ *Madrid, Berlin, Stuttgart, J.Cramer:* 323 pp. 1997.

19. C.C. Ergül, B. Dülger, ‘’A new myxomycetes genus record for Turkey (Stemonitopsis (Nann.-Brem.) Nann.-Brem.).’’ *Turkish Journal of Botany,* 24: 355–357, 2000c.

20. C.C. Ergül, B. Dülger, R.B. Oran, H. Akgul “Myxomycetes of the western Black Sea region of Turkey.” *Mycotaxon*, 93: 269-272, 2005a.

21. C.C. Ergül, B. Dülger, H. Akgul “Myxomycetes of Mezit stream valley of Turkey.” *Mycotaxon*, 92: 269-272, 2005b.

22. C.C. Ergül, H. Akgul “Myxomycete diversity of Uludağ national park, Turkey.” *Mycotaxon*, 116(479): 1-16, 2011.

23. C.C. Ergül, H. Akgul, R.B. Oran “New records of Mycetozoa taxa from Turkey. *Oxidation Communications*, 39(2): 1615-1623, 2016.

24. C.J. Alexopoulos, C.W. Mims, M. Blackwell, ‘’Introductory Mycology.’’ *John Wiley & Sons, Inc*, pp 808,1996.

25. E. Sesli, I. Akata, T. T. Denchev, C. M. Denchev, ‘’Myxomycetes in Turkey a checklist.’’ *Mycobiota,* 6: 1–20, 2016.

26. E. Sesli, C. M. Denchev, ‘’Checklist of the myxomycetes and macromycetes in Turkey.’’ *Mycologia Balcanica,* 2: 119-160, 2005.

27. E. Sesli, C. M. Denchev, ‘’ Checklists of the myxomycetes, larger ascomycetes, and larger basidiomycetes in Turkey. 6th edn. ‘’*Mycotaxon Checklists Online*, 1–136, 2014.

28. F. Gücin, M. Öner, ‘’Taxonomic observations on some Turkish Myxomycetes species.’’ *Journal of Fırat University,* 1 (1): 19–28, 1986.

29. G. Moreno, H. Singer, C. Illana, A. Sanchez, ‘’SEM-studies on nivicolous Myxomycetes. The Diderma niveum complex in Europe.’’ *Cryptogamie. Mycologie*, 24(1), 39-58, 2003.

30. G. W. Martin C. J. Alexopoulos , ‘’The Myxomycetes.’’ *Iowa City: University of Iowa Press.,* 560 p, 1969.

31. G. W. Martin, ‘’North American Flora. Vol. 1: Fungi. Myxomycetes. Ceratiomyxales, Liceales, Trichiales, Stemonitales, Physarales: Bibliography: Index: Fungi.’’ *New York Botanical Garden*. 1949.

32. G. W. Martin, C. J. Alexopoulos, M. L. Farr, ‘’The Genera of Myxomycetes.’’ *University of Iowa Press, Iowa City,* USA, 1983.

33. H. Baba, A.Ü. Tamer, '' A study on the Myxomycetes in Manisa. ''*The Herb Journal of Systematic Botany*, 14 (2): 179–196, 2007.

34. H. Baba, '' Miksomisetlerin alternatif üretim yöntemleri üzerine bir çalışma''. *The Herb Journal of Systematic Botany*, 25: 1, 137-148, 2018.

35. H. Baba, ''Diversity and Ecology of Myxomycetes in Antakya-Hatay (Turkey).'' *The Journal of Fungus,* 3 (1-2): 5–11, 2012.

36. H. Baba, ''Some Mycetozoa (Myxomycetes) members from zorkun high plateau (Osmaniye).'' *Anatolian Journal of Botany*, 1 (2): 37−40, 2017.

37. H. Baba, E. Cennet, M. Sevindik, ''Investigation of Myxomycetes (Myxomycota) in Kırıkhan (Hatay Province).'' *Communications Faculty of Sciences University of Ankara Series C Biology*, 29 (2): 160-169, 2019.

38. H. Baba, M. Gelen, M. Sevindik, ''Taxonomic investigation of myxomycetes in Altınözü, Turkey.'' *Mycopath*, 16 (1): 23–31,2018.

39. H. Baba, M. Kolukırık, M. Zümre, '' Differentiation of some Myxomycetes species by ITS sequences.'' *Turk. J. Botany,* 39: 377–382, 2015.

40. H. Baba, M. Sevindik, ''Mycetozoa of Turkey (Checklist).'' *Mycopath* 17 (1): 1-14, 2019.

41. H. Baba, M. Sevindik, ''Myxomycetes of Eşmişek Plateau (Kırıkhan-Hatay).'' *KSU J. Agric Nat.,* 23 (4): 917-923, 2020a.

42. H. Baba, M. Sevindik, ''The roles of myxomycetes in ecosystems.'' *Journal of Bacteriology & Mycology: Open Access*, 6 (3): 165–166, 2018.

43. H. Baba, B. Altaş, M. Sevindik, "Myxomycetes Diversity of Batman Province and Hasankeyf district." *Kahramanmaraş Sütçü İmam Üniversitesi Tarım ve Doğa Dergisi*, 24(2): 435-441, 2021a.

44. H. Baba, M. Sevindik, A. Er, M. Atay, Y. Dogan, B. Altas, H. Akgul "New Four Mycetozoa Records From South East Anatolia-Turkey." *Fresenius Environmental Bulletin*, 30(4): 3565-3574, 2021b.

45. H. Baba, M. Sevindik, ''A New Myxomycetes record (Myxogastria) from Turkey: *Didymium listeri* Massee.'' *Kahramanmaraş Sütçü İmam Üniversitesi Tarım ve Doğa Dergisi*, 24(4): 820-823, 2021c.

46. Baba, H., Sevindik, M., Dogan, M., & Akgul, H. Antioxidant, Antimicrobial Activities and Heavy Metal Contents of Some Myxomycetes. *Fresenius Environmental Bulletin*, 29(9): 7840-7846, 2020b.

47. H. Baba, M. Zümre, İ. Özyiğit, ''A comparative biogeographical study of myxomycetes in four different habitats of eastern mediterranean part of Turkey.'' *Fresenius Environmental Bulletin*, 25 (5): 1448 -1459, 2016b.

48. H. Baba, A. Er, M. Sevindik, "Myxomycetes Diversity of Belen Region of Hatay Province (Turkey)." *Kastamonu Üniversitesi Orman Fakültesi Dergisi*, 20(2): 86-96, 2020c.

49. H. Baba, M. Zümre, M. Gelen, ‘’An Investigation on North Adana (Turkey) Myxomycetes.‘’ *Chiang Mai J. Sci.,* 43: 54-67, 2016a.

50. H. C. Gilbert, G. W. Martin, ‘’ Myxomycetes found on the bark of living trees.” *Univ. Iowa Stud. Nat. Hist.,* 15: 3-8, 1933.

51. H. Krzemieniewska, ‘’Sluzowce Polski,” *Warschau*, 27,315, 1960.

52. H. Neubert, W. Nowotny, K. Baumann, ‘’Die Myxomyceten. –Karlheinz Baumann Verlag,’’ *Gomaringen*. 1993-2000.

53. H. Singer, G. Moreno, C. Illana, M. Kirchmair, ’’Nivicolous Myxomycetes from Tyrol (Austria). I.” *Cryptogamie Mycologie,* 22(2), 79-94, 2001.

54. H. W. Keller, ‘’Myxomycete history and taxonomy: highlights from the past, present, and future.’’ *Mycotaxon*, 122: 369–387, 2012.

55. J. Clark, T. Lott, ‘’Age heterokaryon studies in *Didymium iridis*.’’ *Mycologia*, 81: 636–638, 1989.

56. J. Clark, ‘’Myxomycete reproductive systems: additional information.’’ *Mycologia,* 87(6), 779-786, 1995.

57. J. M. Ashworth, J. Dee, ‘’The biology of slime moulds. studies in biology’’ No: 56. Edward Arnold, London, pp 67,1995.

58. J. Y. Ljubimova, M. Fujita, N. M. Khazenzon, B. S. Lee, S. Wachsmann-Hogiu, D. L. Farkas, K.L., Black, E. Holler, ‘’ Nanoconjugate based on polymalic acid for tumor targeting. ‘’*Chem. Biol. Interact.,* 171 (2): 195–203, 2008a.

59. K. Kamata, H. Onuki, H., Hirota, Y. Yamamoto, M. Hayashi, K. Komiyama, M. Sato, M. Ishibashi, ‘’ Tubiferal A, a backbone-rearranged triterpenoid lactone isolated from the myxomycete *Tubifera dimorphotheca*, possessing reversal of drug resistance activity.’’ *Tetrahedron,* 60: 9835–9839, 2004.

60. K. Kamata, M. Kiyota, A. Naoe, S. Nakatani, Y. Yamamoto, M. Hayashi, K. Komiyama, T. Yamori, M. Ishibashi, ‘’New bisindole alkaloids isolated from myxomycete *Arcyria cinerea* and *Lycogala epidendrum*.’’ *Chem. Pharm. Bull.,* 53 (5): 594–597, 2005.

61. K. Kaniwa, M. A. Arai, X. Li, M. Ishibashi, ‘’Synthesis, determination of stereochemistry, and evaluation of new bisindole alkaloids from the myxomycete *Arcyria ferruginea*: An approach for Wnt signal inhibitör.’’ *Bioorganic & Medicinal Chemistry Letters*, 17 (15): 4254-4257, 2007.

62. K. Lohwag, ‘’Research on Turkish mycoflora.’’ *İstanbul Üniversitesi Orman Fakültesi Dergisi*, 7 (1): 129–137, 1957.

63. K. Takahashi, Y. Hada, ‘’ Distribution of Myxomycetes on coarse woody debris of Pinus densiflora at different decay stages in secondary forests of western Japan.’’ *Mycoscience*, 50(4), 253-260, 2009.

64. M. G. Tairbekov, S. I. Beylina, D. B. Lairand, A. A. Budnitzky, V. V. Lednev, ‘’Plasmodium of myxomycetes as the object of the investigation

in gravitation biology.'' *Iswestiya Akademii Nauk USSR Seriya Biologitscheskaya*, 2: 198–209, 1984.

65. M. Härkönen, ''A check-list of Finnish Myxomycetes.'' *Karstenia*, 19, 8-18, 1979.

66. M. Härkönen, E. Sivonen, '' Limasienet''. *Finnish Museum of Natural History*, Helsinki, 2011.

67. M. Härkönen, P. Uotila, '' Turkish myxomycetes developed in moist chamber culture.'' *Karstenia*, 23: 1–9, 1983.

68. M. Härkönen, T. Ukkola, K. Pekkala, ''Additions and amendments to the myxomycetes in Finland,'' *Karstenia*, 39:49-57, 1999.

69. M. L. Farr, ''Myxomycetes.'' *Flora neotropica*, 16, 1-304,1976.

70. M. Poulain M. Meyer J. Bozonnet , ''Les Myxomycètes. T.1 : guide de détermina - tions. T. 2: planches.'' *Sévrier: Fédération Mycologique et Botanique DauphinéSavoie,* 544-568, 2011.

71. M. Schnittler, L. G. Krieglsteiner, H. Marx, L. Flatau, H. Neubert, W. Nowotny, K. Baumann, ''Vorläufige Rote Liste der Schleimpilze (Myxomyceten) Deutschlands.'' *Schriftenreihe für Vegetationskunde*, 28, 481-525, 1996.

72. M. Sevindik, H. Baba, C. Bal, O. F. Colak, H. Akgül, '' Antioxidant, Oxidant and Antimicrobial Capacities of *Physarum album*.'' *Journal of Bacteriology & Mycology: Open Access*, 6 (6): 317–320, 2018.

73. M. Sevindik, H. Akgül, "Fruiting bodies structures of myxomycetes." *J Bacteriol Mycol Open Access*, 7(6): 144-148, 2019.

74. M. Zümre, H. Baba, M. Sevindik, ''Investigation of myxomycetes in Selcen Mountain (Turkey) and its close environs.'' *Eurasian Journal of Forest Science*, 7(3): 284-292, 2019.

75. M.S. Buchanan, ''Acylglycerols from the slime mould, *Glycogala epidendrum*.'' *Phytochemistry*, 41: 791-794, 1996.

76. N. Dülger, ''Checklist of the myxomycetes in Turkey. ''*Mycologia Balcanica*, 4: 151–155, 2007.

77. N. E. Nannenga-Bremekamp, ''A guide to temperate Myxomycetes.'' *Biopress.* 1991.

78. N. E. Nannenga-Bremekamp, ''De nederlandse myxomyceten.'' *Koninklijke Koninklijke Nederlandse Naturhistorische Vereniging,* 1974.

79. R. J. Monnat, ''Generation of Highly site – specific DNA double – strand breaks in Human cells by the homing Endonulceases I – PpoI and I- Crel.'' *Biochemical and Biophysical Research Communication,* 255: 88-93, 1999.

80. S. E. Everhart, H.W. Keller, ''Life history strategies of corticolous myxomycetes: the life cycle, plasmodial types, fruiting bodies, and taxonomic orders.'' *Fungal Diversity,* 29, 1-16, 2008.

81. S. L . Stephenson, ‘’Myxomycetes of New Zealand.’’ *Manaaki Whenua Landcare Research*, 2003.

82. S. L . Stephenson, H. Stempen, ‘’Myxomycetes, a Handbook of Slime Molds.’’ *Timber Press*, Portland, Oregon, pp183 1994.

83. S. L . Stephenson, I. Kalyanasundaram, T. N. Lakhanpal, ‘’A comparative biogeographical study of myxomycetes in the mid-Appalachians of eastern North America and two regions of India. ‘’*Journal of Biogeography,* 645-657, 1993a.

84. S. L .Stephenson, M. Schnittler, Y. K . Novozhilov, ‘’ Myxomycete diversity and distribution from the fossil record to the present.’’ *Biodiversity and Conservation,* 17(2), 285-301, 2008.

85. S. L .Stephenson, Y. K . Novozhilov, M. Schnittler, ‘’ Distribution and ecology of myxomycetes in high-latitude regions of the Northern Hemisphere.’’ *Journal of Biogeography,* 27(3), 741-754, 2000.

86. S. Nakatani, M. Kiyota, J. Matsumoto, M. Ishibashi, ‘’Pyrroloiminoquinone pigments from *Didymium iridis*.’’ *Biochem. Syst. Ecol.,* 33: 323–325, 2005b.

87. S.L. Baldauf, W.F. Doolittle, ‘’ Origin and evolution of the slime molds (Mycetozoa).’’ *Proc. Natl. Acad. Sci*. USA, 94: 12007-12012, 1997.

88. S.L. Bauldaulf, ‘’ A research for the origins of animals and fungi: comparing and combining molecular data.’’ *American Nature,* 154: 178-181, 1999.

89. T. Cavalier- Smith, ‘’ Kingdom Protozoa and its 18 Phyla. ‘’*Microbiology Review,* 57: 953-994, 1993.

90. T. N. Lakhanpal, K. G. Mukerji, ‘’ Taxonomy of the Indian myxomycetes.’’ *J. Cramer,* 1981.

91. V. M. Dembitsky, R. Tomas, S. Jaroslav, L. O.Hanus, ‘’Secondary metabolites of slime molds (myxomycetes).’’ *Phytochemistry,* 66 (7): 747–769, 2005.

92. W. D. Gray, C. J. Alexopoulos, ‘’ Biology of the Myxomycetes.’’ *The Ronald Press Company*, New York, pp 560, 1968.

93. W. M. Wormington , R. F. Weaver , ‘’Photoreceptor pigment that induces differentiation in the slime mold *Physarum polycephalum*. ‘’ *Proc. Natl. Acad. Sci*. USA, 73 (11): 3896-3899 1976.

94. Y. Emoto, “Myxomycetes of Japan.” *Sangyo Tosho Publishing Co. Ltd. Japan*. (1977).

95. Y. Novozhilov, ‘’ Classis Myxomycetes (Definitorium Fungorum Rossiae. Divisio Myxomycota, Fasc. 1).’’ *Petropolis*.1993.

96. Y. Novozhilov, ‘’Myxomycetes from different forest types in Puerto Rico.’’ *Mycotaxon*, 52, 285-299, 2001.

97. Y. Yamamoto, ‘’ The myxomycete biota of Japan.’’ *Toyo Shorin Publ*..1998.